Università degli Studi di Milano

PhD Course in
Experimental Medicine

CYCLE XXXIV

PhD thesis

Tyrosine kinase inhibitors in neuroendocrine tumors: from *in vitro* to zebrafish model

---

Candidate: **Dr. Davide Saronni**
Matr. R12172

Tutor: **Prof. Giovanni Vitale**

Supervisor: **Dr. Germano Gaudenzi**

Director: **Prof. Nicoletta Landsberger**

Academic Year 2020-2021

Table of contents

Abstract 3

Disclosure for research integrity 5

Abbreviations 6

1. Introduction 8

1.1 Lung neuroendocrine tumors 9

1.2 Medullary thyroid carcinoma 10

1.3 Current strategies for lung NET and MTC treatment 11

1.4 Angiogenesis in NETs 14

1.5 Zebrafish model 17

2. Aim of the thesis 20

3. Materials and Methods 21

3.1 Reagents and cell culture 21

3.2 Proliferation assay 21

3.3 Cell cycle evaluation 22

3.4 Apoptosis assay 23

3.5 Wound-healing assay 23

3.6 *In vivo* zebrafish assay for tumor-induced angiogenesis 24

3.7 *In vivo* zebrafish assay for migration 25

3.8 Statistical analysis 25

4. Results 26

4.1 Effects of TKIs on cell viability 26

4.2 Effects of TKIs on cell cycle 29

4.3 Effects of TKIs on apoptosis/necrosis 31

4.4 Effects of TKIs on cell migration 34

4.5 Effects of TKIs on *in vivo* tumor-induced angiogenesis 38

4.6 Effects of TKIs on *in vivo* migration 42

5. Discussion 43

5.1 Lung neuroendocrine tumors 43

5.2 Medullary thyroid carcinoma 44

6. Conclusions 47

Acknowledgments 48

References 49

List of figures and tables 64

Dissemination of results 65

Appendix 67

Abstract

(1) Background: Neuroendocrine neoplasms (NENs) are a group of tumors that arise from neuroendocrine cells throughout the body, with the lungs and gastrointestinal tract being the most common sites of origin. In patients with NENs and distant metastases, surgery is generally not curative. Although well-differentiated and low-grade NENs, classified as neuroendocrine tumors (NETs), are usually less aggressive than poorly-differentiated NENs, they can develop distant metastases in about 15% of cases. These patients require chronic medical management. However, the clinical efficacy of these treatments is limited by the low objective response rate, due to the occurrence of tumor resistance and the high biological heterogeneity of these neoplasms.

(2) Research problem: We addressed this study on two rare NETs: lung neuroendocrine tumors (LNETs) and medullary thyroid carcinoma (MTC). LNETs represent about 2% of lung tumors, while MTCs are rare thyroid tumors caused by mutations in the RET proto-oncogene. Both NETs are well-differentiated neoplasms and are known to be highly vascularized. Therefore, they represent a potential target for tyrosine kinase inhibitors (TKIs) selective for receptors involved in angiogenesis. The aim of this project was to evaluate the antitumor activity of several new TKIs both *in vitro*, using LNETs (NCI-H727, UMC-11 and NCI-H835) and MTC (TT and MZ-CRC-1) cell lines, and *in vivo*, adopting a novel zebrafish xenograft model to study angiogenesis. In LNETs we tested: sulfatinib, a small molecule that inhibits the Vascular Endothelial Growth Factor Receptor (VEGFR) 1, 2, and 3, and the Fibroblast Growth Factor Receptor type 1 (FGFR1); cabozantinib, a multi-target inhibitor selective for VEGFR2, c-Met, Kit, Axl and Flt3; and axitinib, a multi-target TKI of VEGFR1, 2, 3 and Platelet-Derived Growth Factor Receptor-beta (PDGFRβ). In MTC we tested: sulfatinib; SPP86, a RET-specific inhibitor; and SU5402, an inhibitor of the FGFR1 and VEGFR2.

(3) Methodology: In LNETs and MTC cells the effects of selected TKIs have been evaluated *in vitro* through: MTT (3-(4,5-dimethylthiazol-2-yl)-2,5-diphenyltetrazolium bromide) and MTS (3-(4,5-dimethylthiazol-2-yl)-5-(3-carboxymethoxyphenyl)-2-(4-sulfophenyl)-2H-tetrazolium) assays, for assessing cell viability; flow-cytometer analysis, for the evaluation of cell cycle and apoptosis; and wound-healing assay, to

study cell migration. *In vivo* we took advantage of the transgenic zebrafish line of *Tg(fli1a:EGFP)^{y1}*. Through the xenotransplantation of NET cells in the subperidermal space near the subintestinal vein, we assessed the effects of TKIs on tumor-induced angiogenesis and cancer dissemination.

(4) Key Results: In LNET cell lines we observed a dose-dependent decrease in cell viability after incubation with all TKIs. This effect seems to be related to the perturbation of the cell cycle and induction in apoptosis. In NCI-H727 wound healing assay showed a significant reduction in cell migration only after incubation with cabozantinib. In the zebrafish model, we found a significant reduction of the tumor-induced angiogenesis in implanted LNET cell lines after treatment with all TKIs. Cabozantinib and axitinib were more potent than sulfatinib in inhibition of angiogenesis, while cabozantinib was the most efficient in reducing cell migration from the transplantation site to the tail. In MTC cell lines, sulfatinib, SU5402 and SPP86 showed a decrease in cell viability, confirmed by the significant reduction in S phase cell population. Moreover, sulfatinib and SPP86 showed for both cell lines a significant induction of apoptosis. Sulfatinib and SPP86 inhibited the migration of TT and MZCRC-1 cells, evaluated through the wound healing assay, while SU5402 was able to inhibit migration only in TT cells. *In vivo* we observed a significant reduction of TT cells-induced angiogenesis in zebrafish embryos after treatment with sulfatinib and SPP86.

(5) Conclusions: Despite sulfatinib resulted the most potent compound in terms of inhibition of LNET cell proliferation, cabozantinib showed *in vivo* the most effective impact in reducing tumor-induced angiogenesis. Cabozantinib was the only TKI able to inhibit *in vivo* the dissemination of implanted LNET cells. According to these data, cabozantinib could represent a potential candidate in the therapy of patients with highly vascularized LNET. In MTC cell lines, SPP86 and sulfatinib displayed a similar antitumor activity both *in vitro* and *in vivo*, suggesting a good efficacy of specific RET inhibitors (SPP86) with potentially less adverse effects than multitarget TKIs (sulfatinib). In addition, this study showed that the zebrafish model for NETs represents an innovative tool for drug screening with several advantages compared with rodent models: rapidity of procedure, animal immune suppression is not required, lower number of tumor cells for implant and the optical transparency provides a real-time monitoring of cell-stromal interactions and cancer progression in living animals.

Disclosure for research integrity

The following project has been conducted pursuing the values of reliability, honesty, respect and accountability stated by the **European Code of Conduct for Research Integrity**.

Abbreviations

AC = Atypical Carcinoid

bFGF = basic fibroblast growth factor

CCV = common cardinal vein

DMSO = dimethyl sulfoxide solution

EGF = epidermal growth factor

EGFR = epidermal growth factor receptor

FBS = fetal bovine serum

FGFR = fibroblast growth factor receptor

HIF = hypoxia inducible factor

LCNEC = Large Cell Neuroendocrine Carcinoma

LNET = Lung Neuroendocrine Tumor

MEN = multiple endocrine neoplasia

MTC = Medullary Thyroid Carcinoma

MTS = 3-(4,5-dimethylthiazol-2-yl)-5-(3-carboxymethoxyphenyl)-2-(4-sulfophenyl)-2H-tetrazolium

MTT = (3-(4,5-dimethylthiazol-2-yl)-2,5-diphenyltetrazolium bromide

NEC = Neuroendocrine Carcinoma

NEN = Neuroendocrine Neoplasm

NET = Neuroendocrine Tumor

PDGFR = platelet-derived growth factor receptor

PDX = patient-derived cancer cell xenotransplantation

PI = Propidium iodide

PRRT = peptide receptor radionuclide therapy

RET = Rearranged during Transfections

SCLC = Small Cell Lung Carcinoma

SIV = subintestinal vein

SSA = somatostatin analog

TC = Typical Carcinoids

TKI = Tyrosine Kinase Inhibitor

VEGF = vascular endothelial growth factor

VEGFR = vascular endothelial growth factor receptor

1. Introduction

Neuroendocrine neoplasms (NENs) are a heterogeneous group of neoplasms that originate from secretory cells of the neuroendocrine system. They represent about 0.5% of newly diagnosed malignancies with an incidence of around 5.86/100,000 and an increasing tendency over the last years (1, 2). NENs are classified according to various features based on their biological behaviour. NENs are mainly divided into poorly-differentiated (neuroendocrine carcinomas, NECs) and well-differentiated (neuroendocrine tumors, NETs). Morphology represents the first cornerstone for the differential diagnosis between NET and NEC. The combination of morphological features and grading improves the ability in this distinction, which has important clinical implications. NENs are graded between G1 and G3 on the basis of the mitotic count and Ki67 index. NECs are the most aggressive form of NENs, and they are always high-grade (defined as G3) neoplasms with an elevated proliferation rate. Morphologically, NECs show abundant necrosis, grow in sheets and present poor nested architecture. NETs can be divided into G1, G2 and G3 form. G1 and G2 are rather slow growth tumors. The morphology of NETs shows organoids structures and nested architectural pattern with minimal necrosis (3-7). The majority of these tumors occur in the gastrointestinal system and lung. However, as they can derive from any cell of the endocrine system, these malignancies can also originate in other sites such as thyroid, thymus, adrenal medulla, genito-urinary tract, etc. (8-11).

1.1 Lung Neuroendocrine Tumors

Lung NENs represent around 25% of all NENs and about 1-2% of all primary lung cancers. According to several parameters, such as the mitotic count per 2 mm^2, the extension of necrosis along with histopathological features and the expression of different biomarkers, these malignancies are classified into four subtypes: small cell lung carcinomas (SCLCs), large cell neuroendocrine carcinomas (LCNECs), typical carcinoids (TC) and atypical carcinoids (AC) (12). These tumors represent, considering all NENs, about 20%, 3%, 2%, and 0.2%, respectively (13).

LCNEC and SCLC are poorly-differentiated high-grade tumors, hence referred as NECs, which present a mitotic count >10 per 2 mm^2 (even more than 50 for SCLC) and extensive necrosis. LCNECs have large tumor cells with prominent nuclei and coarser chromatin, organoid nesting, and trabecular growth. On the other hand, SCLCs display small cells with dispersed chromatin and a high nuclear/cytoplasmic ratio. Moreover, NECs express several neuroendocrine biomarkers, such as synaptophysin (14, 15). Finally, both cancers display frequent aneuploidy and chromosomal alterations. The loss of both TP53 and RB1 appear to be crucial for the tumorigenesis, especially for SCLCs, but many other mutations are involved (16).

TC and AC, that belong to well-differentiated lung NENs (low/intermediate grade, respectively), are rather indolent tumors, and they can be referred as lung neuroendocrine tumors (LNETs). TC do not present any necrosis and their mitotic count is less than 2 mitoses per 2 mm^2, whereas AC show a more intermediate grade. In AC mitotic count is between 2-10 mitoses per 2 mm^2 and they can present foci of necrosis. TC show an organoid growth patterns and lack of a high amount of cytoplasm with inconspicuous nucleoli; while AC have more nuclear polymorphisms and irregularities on nucleoli and nuclear membrane. Notably, LNETs have a highly vascularized stroma (15, 17). In comparison with NEC, LNETs are characterized by a low mutational burden. The most common mutation (11-22% of LNETs) is an alteration of the MEN1 gene, which encodes for a scaffold protein involved in histone modification (18).

1.2 Medullary Thyroid Carcinoma

Several tumors occur in the thyroid gland (19). Among these, medullary thyroid carcinoma (MTC) represents about 5% of all thyroid malignancies and originates from the calcitonin-secreting parafollicular C cells. Although most of the cases (around 75%) occurs sporadically, the remaining exists in a hereditary form. In familial forms, over 95% of patients carry a “gain of function” germline mutation of the Rearranged during Transfection (RET) proto-oncogene. These mutations cause multiple endocrine neoplasia (MEN) type 2 syndromes (MEN2A and MEN2B) and isolated familial MTC (20-22). The RET gene encodes tyrosine kinase receptor involved in cell proliferation, survival, migration, and differentiation pathways and its constitutive activation causes MEN2 syndromes (23). MTCs have solid nests and sheets of round to polygonal and elongated cells with poorly defined cell borders. The stroma can be fibrotic and highly vascularized (24). Most MTCs, particularly sporadic forms, are well-differentiated tumors with a low growth rate and are able to produce calcitonin. Although, it is difficult to predict the clinical behaviour of MTC, a recent study validated a new grading system for MTC, that account for Ki67 index, mitotic count, and necrosis. This classification was able to predict overall survival in patients with MTC, showing a low-grade tumor in 75% of cases (25).

1.3 Current Therapeutic Strategies in LNET and MTC

In patients with LNET or MTC, surgery is currently the best therapeutic option. Although NETs are, by definition, low grade and indolent tumors, the occurrence of distant metastases is not a rare event at the time of diagnosis. Indeed, TC and AC develop distant metastases in approximately 10% and 20% of cases, respectively. Also, in MTC distant metastasis occur in 15–20% of patients at the diagnosis (26, 27). For these cases surgery is not curative and a medical management becomes fundamental (28). Although we still lack a standard procedure for NET medical treatment, several approaches are currently used. It has been demonstrated that somatostatin receptors have a role in the control of hormone secretion and cell proliferation in NENs (29). As a matter of fact, recent studies have been focused on the use of somatostatin analogs (SSAs) and peptide receptor radionuclide therapy (PRRT) against somatostatin receptors. Lanreotide and octreotide are the most commonly used somatostatin analogs (SSAs). Their effects on LNETs are still unclear, although two retrospective studies stated a potential positive impact of SSAs (30, 31). In MTC, SSAs have shown effectiveness in controlling MTC-related symptoms (32-35). In a phase II study on 19 patients, pasireotide showed a median progression free survival of 36 months and antiproliferative effects in postoperative MTC, without exerting severe side-effects (hyperglycaemia was the most common). The combination of this SSA with everolimus (an mTOR inhibitor) showed efficacy also in progressive MTC, with more intense adverse events, but still acceptable (36). The aim of PRRT is to selectively supply radiation to the tumor through a radionuclide linked to a chelating molecule and a peptide receptor ligand that bind somatostatin receptors. For NETs, ^{177}Lu-DOTATATE, which has been already approved in Europe and U.S., and ^{177}Lu-DOTA-EB-TATE, which is under studying in China, have shown interesting effects. However, although well-tolerated, these molecules have dose limitations, mainly due to toxicity on the bone marrow and related side-effects (37, 38). A retrospective study in patients with LNETs, presenting a sufficient level of somatostatin receptor expression, showed encouraging results for ^{177}Lu-DOTATATE treatment for these tumors, with a disease control rate of 88%, a median progression free survival of 23 months and an overall survival of 59 months (39). Few data exist on ^{90}Y-DOTATOC in LNETs. It was reported a 100% of disease control rate and an objective response rate between 0% and 50% following its use. Moreover, the most frequently adverse event observed was nephrotoxicity (40). In MTC, Satapath group observed a disease control rate of 86% for ^{177}Lu-DOTATATE in combination with capecitabine, a compound that induces DNA-damage

and synergizes with ^{177}Lu-DOTATATE. Maghsoomi et al. stated that PRRT (in particular they tested ^{90}Y-DOTATOC, ^{177}Lu-DOTA-TATE, and ^{111}-Indium-based agent) could stabilize the disease for few months. Therefore, the potential role of PRRT in the therapy of advanced MTC disease is still unclear, as authors suggested additional and larger randomized trials to further study the utility of this therapy (41, 42). The mTOR inhibitor everolimus showed a clinically significant improvement in patients with advanced, progressive, well-differentiated, non-functional LNETs (43). In a phase II trial on locally advanced MTC and patients with metastatic anaplastic thyroid cancer, everolimus alone showed a limited effect, although it was well tolerated (44). The authors hypothesized that this poor effect might be due to the activation of alternative survival pathways that bypass everolimus impact, suggesting a potential combination of this drugs with other molecules to enhance its effect. This assumption had been partially confirmed in other studies, where everolimus combined with other molecules (5-aza-20-deoxycytidine and pasireotide) showed promising results both in LNET and MTC, although further studies are required (36, 45, 46). Chemotherapy and external radiotherapy are other potential therapeutic options in advanced NETs. Unfortunately, both LNET and MTC are quite unresponsive to both treatments (47, 48).

An interesting class of drugs, recently used in the therapy of cancer, are the TKIs, a family of small molecules or peptides with the ability to inhibit either cytosolic or receptor tyrosine kinases with a relevant role in cancer cell proliferation, progression and tumor-induced angiogenesis. The utility of treatment with TKIs in LNET is still unclear. A recent study reported the first case of a patient affected by AC that harboured a RET fusion mutation. In this patient selpercatinib, a RET-specific TKI, exerted a relevant response with a 36% reduction in sum of target lesions (49). Another patient, suffering from an AC harbouring an epidermal growth factor receptor (EGFR) L858R mutation, achieved a partial response after treatment with a combination of icotinib (an EGFR TKI) and irinotecan plus cisplatin chemotherapy (50). A 49-years-old white female was diagnosed with an adenocarcinoma in the upper right lobe and a TC in the left lower lobe. After treatment with cisplatin and gemcitabine followed by radiotherapy, this patient showed a partial response of the adenocarcinoma and the TC remained unchanged. Notably, when the therapy changed to erlotinib (an EGFR TKI), the TC showed a complete response (51).

Interestingly, TKIs targeting RET represent a valid therapy in advanced MTC. Four TKIs have been approved for patients with advanced MTC: vandetanib, which targets RET, vascular endothelial growth factor receptor (VEGFR)-2/3 and EGFR (52, 53); cabozantinib,

a potent inhibitor of RET, VEGFR-2 and c-Met (54, 55); and recently selpercatinib and pralsetinib, two RET-specific inhibitors (56, 57). These molecules showed significant improvement in progression-free survival, however not all patients positively respond to these therapies. Some patients even displayed a progression of the disease after an initial response, due to the activation of alternative survival pathways (45, 58). Moreover, several side effects of the drugs limit their long-term use (59, 60).

Therefore, despite the development of novel drugs in cancer research over the last decade, there are no curative therapies for advanced NETs and novel treatment strategies seem mandatory.

1.4 Angiogenesis in NETs

Angiogenesis is an important step for tumor progression, as it provides oxygen supply and nutrients for cancer growth in response to hypoxia. Hypoxia leads the tumor cells to secrete angiogenic factors, including vascular endothelial growth factor (VEGF), basic fibroblast growth factor, plated-delivered endothelial growth factor and many others, which trigger vascular growth into the tumor microenvironment. Nonetheless, it is important not only that pro-angiogenic factors are overexpressed, but also that anti-angiogenic molecules, such as angiostatin and endostatin, are inhibited (Fig. 1) (61).

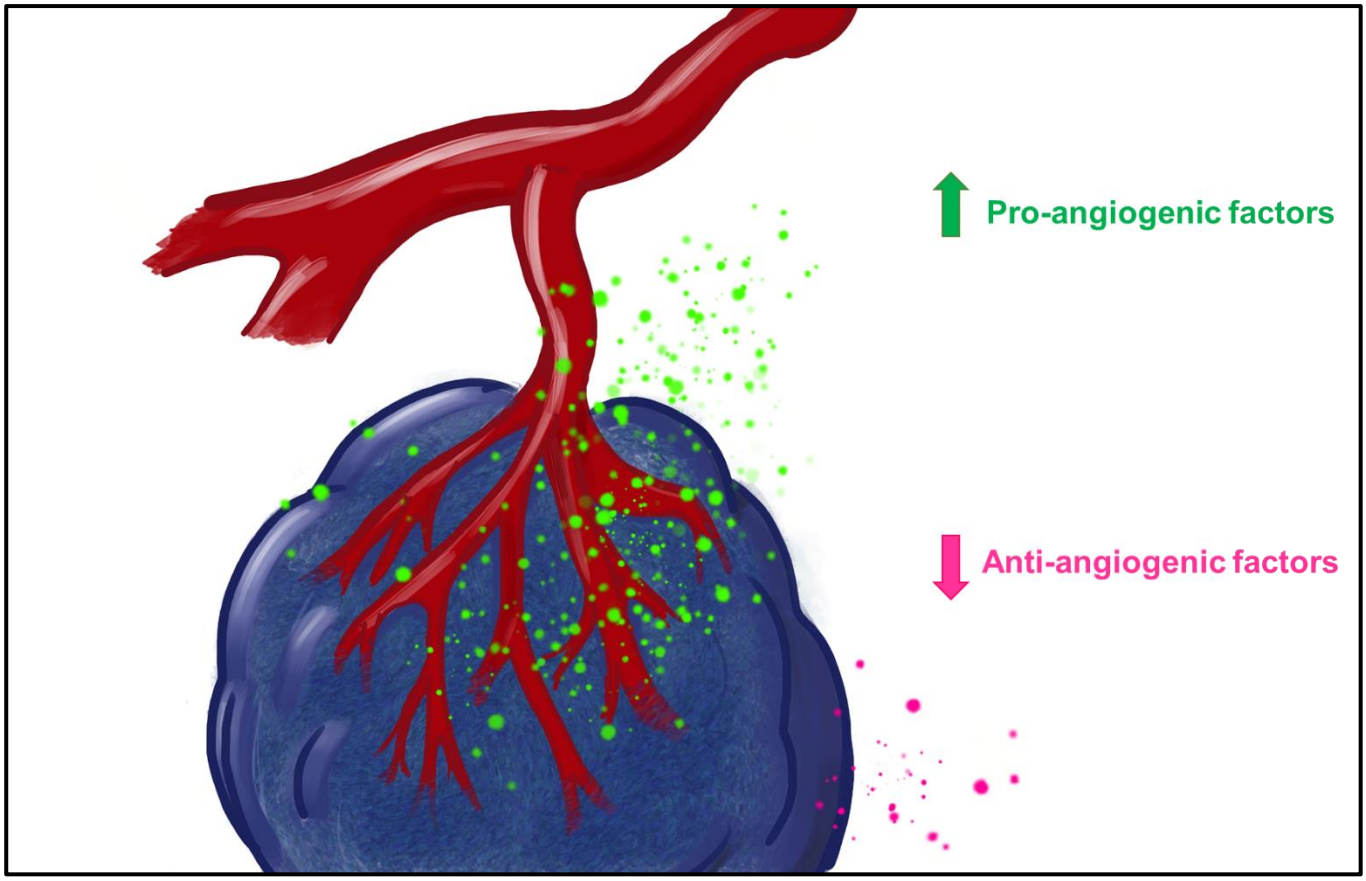

Fig. 1. Schematic representation of the dysregulation between pro- and anti-angiogenic factors caused by the tumor, which triggers novel angiogenesis toward the tumor itself.

In addition, the architectural structure of these novel vessels is abnormal as the constant secretion of pro-angiogenic factors from tumor cells does not allow a proper formation of tight junctions and basement membrane between endothelial cells. This situation leads to hyperpermeability of the tumor-induced vascular network and high heterogeneity in vessel caliber size, causing irregularities in the blood flow, with persisting hypoxia and poor perfusion that interfere with medical therapy. Finally, in normal angiogenesis, novel vessels are surrounded by pericytes, which stabilize vascular structure; while, during tumor-induced angiogenesis, pericytes are absent or poorly represented, facilitating the spread of tumor cells (62, 63).

In oncology the presence of high microvascular density in malignant tumors is often associated with poor prognosis. This association appears to be inverse in NENs, where low grade, well-differentiated NETs (such as LNET and MTC) are characterized by high vascularization and it appears to be a favourable prognostic feature. While a low vascular density has been commonly detected in NEC with an unfavourable prognosis (64). This characteristic, denominated as “neuroendocrine paradox”, may be due to the capacity of differentiated NET cells to promote a dense vascular network, like their normal tissue counterpart. In fact, endocrine glands are highly vascularized (65, 66).

In light of these insights, anti-angiogenic treatment may represent an interesting therapeutic strategy in low-grade NETs (67). An example came from studies in patients with pancreatic NETs. Sunitinib is a multi-receptor inhibitor targeting VEGFR1-3 and PDGFR-α and β, currently used in the therapy of metastatic, well-differentiated pancreatic NETs. A recent study assessed the clinical benefit of sunitinib in pancreatic NET patients by combining the data from a phase III trial (68) and an open-label phase IV trial (69). The objective response rate was considered as primary endpoint in this study. The combined analysis of the two trials revealed an objective response rate of 16.7% (and a progression free survival of 12.9 months) and confirmed the benefits for the patients treated with sunitinib (70). As we mentioned before, for MTC clinical therapy there are two multi-target TKIs (cabozantinib and vandetanib), that can potentially target tumor angiogenesis and RET (52-55). Their anti-angiogenic potentials were recently compared by Carra et al. 2021 (71), where cabozantinib showed a more relevant effect on tumor-induced angiogenesis *in vivo* in comparison with vandetanib, although their antiproliferative efficacy *in vitro* was similar. Furthermore, also LNET could benefit from a therapy that targets the angiogenesis, by inhibiting the PI3K/Akt/mTOR pathway, which is involved in several tumorigenic mechanisms, including

angiogenesis, through the combined use of the bioactive agent sulforaphane with acetazolamide. Moreover, acetazolamide interferes with carbonic anhydrase-dependent hypoxia mediated pathways, which promotes tumor-induced angiogenesis in hypoxic conditions, resulting in a potential inhibition of tumor vascularization (72). In 2014, Motylewska et al. tested the influence of angiomodulators (VEGF, endostatin, interferon-α, rapamycin, JV-36 and semaxinib) on TT and H727 cells, respectively an MTC and a LNET cell line. The study reported an antiproliferative effect for some of these compounds (interferon-α, rapamycin and semaxinib) in both tumor cell line.

1.5 Zebrafish Model

Zebrafish (*Danio rerio*) is a freshwater fish (Fig. 2) native to South Asia, belonging to the Cyprinidae family of the order Cypriniformes. In the last decades it has gained attention as a robust animal for studying development and disease. As a matter of fact, zebrafish offers several advantages over other animal models such as ease of maintenance, high fecundity, fast external development, optical clearance of embryos, small size, and low cost (73, 74).

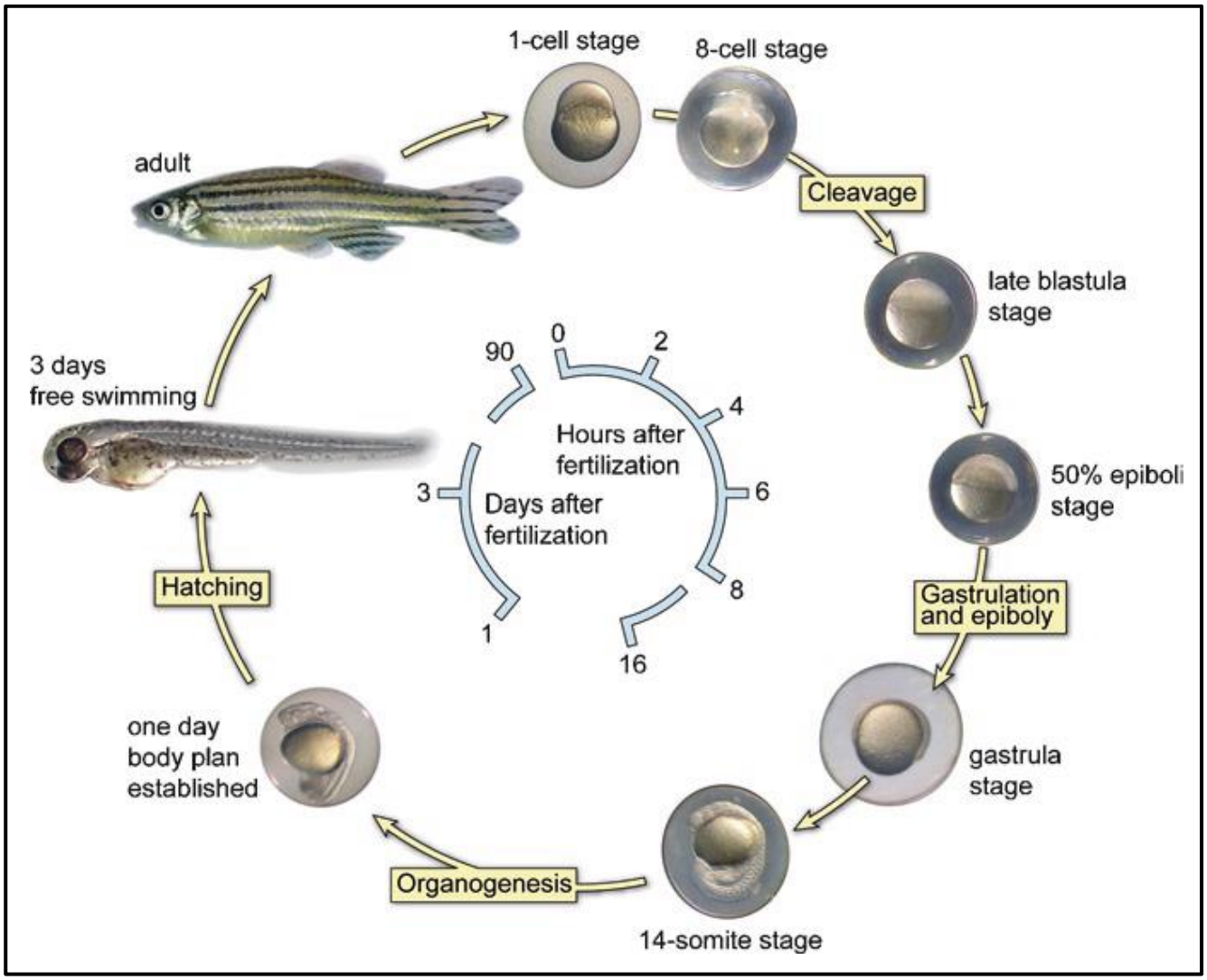

Fig. 2. A schematic representation of the embryonic developmental stages of zebrafish. Modified from: Willemsen R., Padje S., van Swieten J.C., Oostra B.A. (2011) Zebrafish (Danio rerio) as a Model Organism for Dementia. In: De Deyn P., Van Dam D. (eds) Animal Models of Dementia. Neuromethods, vol 48. Humana Press. https://doi.org/10.1007/978-1-60761-898-0_14 (75)

More recently, zebrafish emerged as a promising organism to model cancer *in vivo* due to the extensive evolutionary conservation of human cancer-associated genes, telomere biology and the relative ease of genetic manipulation of embryos by microinjection (76). Furthermore, thanks to the transparency of zebrafish embryos and larvae it is possible to follow tumor cell growth and dynamics at early stages of cancer development. In addition, zebrafish transgenic lines with fluorescently labelled tissues are available to track cancer cell growth, dissemination, and tumor microenvironment in real-time (77).

Interestingly, zebrafish has grown in popularity in the last decade as xenograft model, most often used to test drugs for their cytotoxic, anti-metastatic, or anti-angiogenic properties (78). Thus, zebrafish has rapidly become a new model for xenograft assays, as the adaptive immune system is not fully developed until the seventh day post fertilization. Therefore, within this period transplanted cancer cells will not be rejected by embryos. Most of the recent transplantation studies in zebrafish are in agreement to use embryonal stages of 48 hours post fertilization (hpf) as the stage for the implant. In fact, at this stage developmental migration is finished, so the injected cancer cells are likely to migrate, excluding the likelihood of passive transport during gastrulation (79). The literature identified variable site of transplantation for zebrafish xenograft, such as the yolk sac, cardinal vein, Duct of Cuvier, or the hindbrain. Depending on the site of transplantation and thanks to the transparency of the embryos, different phenotypes of tumorigenesis could be observed: tumor-induced angiogenesis, cancer cell invasion, extravasation, and formation of metastasis (73).

Zebrafish is also emerging as an optimal experimental model for the study of NETs as most of the features of the endocrine system are highly conserved between human and zebrafish. Moreover, there are several mutant and transgenic zebrafish lines that resemble different human endocrine diseases (80).

In 2017, our laboratory developed a zebrafish model to investigate tumor-induced angiogenesis in NETs, established by injecting human NET cells near to the developing subintestinal vein (SIV) plexus and common cardinal vein (CCV) in transgenic *Tg(fli1a:EGFP)*^{y1} zebrafish embryos. This transgenic zebrafish line expresses enhanced green fluorescent protein (EGFP) under the control of the fli1a promoter, thereby labelling all blood vessels and providing a live visual marker for vascular development. Moreover, zebrafish embryos require a low number of cells to properly create a tumor implant, making the model suitable for engraftment of primary cell cultures, using tumor samples from patients, often limited in number and size (81). The versatility of this model to study well-

differentiated NETs has been already assessed (71, 82, 83). The injection of human NET cells in 48 hours post-fertilization zebrafish embryos stimulates the migration and growth of sprouting vessels toward the implant within 2-3 days. At this stage, zebrafish embryos do not have a fully developed immune system and no graft rejection occurs. The use of fluorescently labelled tumor cells provides to investigate their metastatic behaviour into zebrafish in real-time.

Last but not least, zebrafish embryos are readily permeable to small molecules dissolved in their culture media. This provides to test molecules with antitumor activity. The rapidity of this procedure (within 5 days) makes this tool very useful to perform preclinical drug screening with small molecules, such as TKIs. This is of high importance in the emerging field of patient-derived xenograft (PDX), for a fast development of personalized therapy (84).

2. Aim of the thesis

The aims of this PhD project were to evaluate the antitumor activity of several novel TKIs in well-differentiated NET cell lines, with a focus on LNETs (NCI-H727, UMC-11 and NCI-H835) and MTC (TT and MZ-CRC-1). Tests were conducted through different approaches, both *in vitro (*proliferation assay, flow cytometry evaluation of cell cycle and apoptosis, cell migration examination) and *in vivo*, where we took advantage of an innovative zebrafish model.

Despite the development of novel drugs for cancer research, there are no curative therapies in patients with metastatic LNETs. Therefore, we investigated the antitumor activity of three TKIs, recently adopted in other NENs, with different targets: cabozantinib (targeting VEGFR2, c-Met, Kit, Axl and Flt3), axitinib (targeting VEGFR1, 2, 3 and PDGFRβ) and sulfatinib (targeting VEGFR 1, 2, and 3, and FGFR1).

In MTC there are already different drugs approved for medical treatment. However, the occurrence of several side effects and the onset of drug-resistance, limit their long-term use. In this respect, we tested three new molecules: sulfatinib, SPP86 (a RET-specific inhibitor) and SU5402 (a selective inhibitor of FGFR1, VEGFR-2 and PDGFRβ).

3. Materials and Methods

3.1 Reagents and Cell Culture

Sulfatinib (a multi-target TKI with affinity for VEGFR-1, -2 and 3 and FGFR-1), axitinib (an inhibitor of VEGFR-1, -2 and 3 and PDGFR-β), and SPP86 (a RET-specific inhibitor) were supplied by MedChemExpress (Monmouth Junction, NJ, USA). Cabozantinib (a multi-target inhibitor that blocks VEGFR2, c-Met, Kit, Axl and Flt3) was provided by Cayman Chemicals (Ann Arbor, MI, USA). SU5402 (an inhibitor of the FGF signaling pathway by targeting FGFR1 with affinity also for VEGFR2 and PDGFRβ) was supplied by Sigma-Aldrich (St. Louis, MI, USA). All drugs were dissolved in dimethyl sulfoxide solution (DMSO) at 10 mM. Culture media containing equivalent concentrations of only vehicle were used as controls in all experiments. All compounds were stored at −20°C and diluted with culture media before use.

Three human LNET cell lines NCI-H727, UMC-11 and NCI-H835, were obtained from American Type Culture Collection (ATCC, Manassas, VA, USA), whereas two human MTC cell lines TT and MZ-CRC-1, were kindly provided by Prof. Lips (Utrecht, the Netherland). Cells were maintained at 37°C in 5% CO_2 and cultured in T75 flasks filled with 10 mL of RPMI 1640 (EuroClone™, Milan, Italy) for LNETs and F-12K Kaighn's modification medium (Gibco™ Life technology) for MTC. Medium was supplemented with 10% heat-activated fetal bovine serum (FBS) (Invitrogen™) and 1% penicillin/streptomycin (EuroClone™, Milan, Italy), RMPI was also supplemented with 2mM of L-Glutammine (EuroClone™, Milan, Italy). Cells were harvested by trypsinization, resuspended in complete medium and then counted through optical microscope using a standard haemocytometer before plating. Cells used in all experiments were below 5 passages.

3.2 Proliferation assay

LNET and MTC cell lines were seeded in 96 well plates at their optimal culture concentration (NCI-H727: $3.5x10^3$ cell/well; UMC-11: $3.5x10^3$ cell/well; NCI-H835: $5x10^4$ cell/well; TT: $3x10^4$ cells/well; MZ-CRC-1: $3x10^4$ cells/well) in order to perform drug treatments on exponentially growing cells.

The following day, NCI-H727 and UMC-11 cell culture medium was replaced with medium containing sulfatinib, axitinib or cabozantinib and MTC cell culture media with medium containing sulfatinib, SPP86 of SU5402 for 3 days at different concentrations (from 0.05 to 50 µM for LNET, from 0.05 to 30µM for MTC). This medium was in turn replaced with fresh medium containing the compounds at the same concentrations and incubation was continued for a further 3 days. Cells cultured in medium with only vehicle was used as control.

After 6 days, MTT assay (3-(4,5-dimethylthiazol-2-yl)-2,5-diphenyltetrazolium bromide) was performed, as previously described (82). Briefly, after incubation at 37°C, each well was treated with MTT (0.5 mg/ml) and incubated at 37°C for 4 h. Cell proliferation was analysed by a colorimetric assay that consisted in a cellular reduction of MTT that lead to the final production of crystalline formazan. This product was dissolved in 100ml EtOH:DMSO (1:1) and read at 540 nm in a microplate reader.

For NCI-H835, as they are partially floating, medium containing sulfatinib, axitinib or cabozantinib was added to each well for 3 days at different concentrations (from 0.01 to 50µM), without replacing the medium in the well. After 3 days, the operation was repeated. At the end of incubation period, cells were analyzed by a cell viability assay, the CellTiter 96® AQueous One Solution Cell Proliferation Assay (MTS, Promega, cat. G3580), according to the manufacturer's instructions. Plates were then read at 490 nm in a microplate reader.

All the experiments were conducted in quadruplicates. Data are represented as the mean of all results obtained for each primary endometrial stromal culture as independent experiments.

3.3 Cell cycle evaluation

Cell lines were seeded in 6-well plates in duplicate at their optimal culture concentration, as described in the proliferation assay section.

The day after, the medium was replaced with fresh medium, either without (control) or with sulfatinib, axitinib or cabozantinib (LNET cell lines) or with sulfatinib, SPP86 or SU5402 (MTC cell lines) at their half maximal effective concentration (EC_{50}) for 3 days. Then, the medium was replaced with new one containing drugs at same different concentrations for

further 3 days, at the end of which cells were harvested by gentle trypsinization, washed with PBS and collected after centrifugation.

Propidium iodide (PI) (Sigma-Aldrich, USA) staining solution (50 µg/ml PI, 0.05% Triton X-100 and 0.6 µg/ml RNase A in 0.1% sodium citrate) was added to the pellets at 4°C for 30 minutes and cells were analyzed by flow cytometry, as previously reported (82).

Data were indicated as percentage of cells in G_0/G_1, S and G_2/M phases. All experiments were independently performed in triplicate for each sample.

3.4 Apoptosis assay

LNET and MTC cell lines were grown in six-well plates in duplicate and incubated with sulfatinib, axitinib or cabozantinib (LNET cell lines) or with sulfatinib, SPP86 of SU5402 (MTC cell lines), following the same protocol as for cell cycle analysis.

At 6 days of treatment cells were harvested by trypsinization, washed with PBS and centrifuged. 100 µl of 1 x binding buffer (BB: 1.4 M NaCl, 0.1 M HEPES/NaOH, pH 7.4, 25 mM CaCl2) was used to resuspend each cell sample. Then, 5 µl of Annexin V-FITC (BD Pharmingen, San Diego, CA, USA) and 10 µl PI (50 µg/ml in PBS) were added for 15 min at room temperature in dark for each sample. After a final addition of 400 µl of 1 x BB, stained cells were mesuared by FACScalibur flow cytometer (BD Biosciences, San Jose, CA, USA) on 10,000 events as previously described (82).

Three types of cell populations were identified by Cell-Quest Pro Software: Annexin-/PI- (live cells), Annexin+/PI- (early apoptotic cells) and Annexin+/PI+ (late apoptotic and necrotic cells), and the data were expressed as percentage of each population.

3.5 Wound-healing assay

All cell lines were plated in 6-well plates in duplicate (10^6 cells/well) and cultured to reach monolayer. Growth media was renewed as needed until 100% confluence was reached. At that time, cells were scratched rationally/orthogonally from the bottom of each well using a 10 µl sterile micropipette tip.

Cells were washed with PBS in order to remove cell debris then supplemented with growth medium without (control condition) or with sulfatinib, axitinib or cabozantinib (LNET cell lines) or with sulfatinib, SPP86 of SU5402 (MTC cell lines) at their EC_{50} concentration. We took pictures of the scratches at T0 and LNET cell lines were incubated with a TKI for 48h before taking novel pictures, while MTC cells were incubated for 72h. This discrepancy was due to the different metabolisms between pulmonary and medullary cells. However, before performing these experiments, we tested the effect of the EC_{50} concentration on cell viability after 3 days of incubation with the drugs. At this time, TKIs did not show any significant effect on cell survival. Images of defined wounds were acquired through Leica DM IRE 2 (Inverted Fluorescence Motorized Phase Contrast Microscope) using a 10x objective at different time point: right after the scratch (T0) and after 2 or 3 days according to the cell type (T_F).

The wound-healing area was measured with ImageJ software (National Institutes of Health, Bethesda, MD, USA). Results were reported as wound healing percentage using the equation:

$$\% \text{ wound-healing} = 100 \times [1 - (\text{wound area at } T_F / \text{wound area at T0})]$$

For each plate, at least 3 randomly selected images were acquired. All experiments were independently carried out in triplicate.

3.6 *In vivo* zebrafish assay for tumor-induced angiogenesis and migration

Embryo and adult zebrafish (*Danio rerio*) were raised and maintained according to Italian (D.Lgs 26/2014) and European laws (2010/63/EU and 86/609/EEC). All experiments were performed on *Tg(fli1a:EGFP)^{y1}* transgenic embryos, expressing EGFP (Enhanced Green Fluorescent Protein) under the control of the endothelial-specific gene promoter fli1a, allowing *in vivo* visualization of the entire vascular tree (85). At forty-eight hours post-fertilization embryos were anesthetized with 0.016% tricaine (Ethyl 3-aminobenzoate methanesulfonate salt, Sigma-Aldrich) and implanted with LNETs or TT cells, as previously described (80, 86). In brief, cells were labelled with a red fluorescent viable dye (CellTrackerTM CM-DiI, Invitrogen), resuspended with PBS (final concentration of 250.000 cells/µl), and grafted into the subperidermal space of *Tg(fli1a:EGFP)^{y1}* embryos, close to the

sub-intestinal vessel plexus by using a microinjector (100-1000 cells in each embryo). As a control for the implantation, embryos were injected with only PBS.

After tumor implantation, zebrafish embryos were treated for 24 hours with different doses of the specific inhibitor directly dissolved in embryo medium. These concentrations (0.25μM and 2.5μM) were identified on the basis of preliminary pharmacological experiments on *Tg(fli1a:EGFP)*^{y1} embryos without tumor xenograft, aimed to detect the toxicity range for each compound, limiting the presence of morphological abnormalities.

Assays were performed 3 times, with about 20 embryos in each experimental group.

As an arbitrary unit (A.U.) of tumor-induced angiogenesis, we calculated the total cumulative length of vessels sprouting from the sub-intestinal vein plexus and the common cardinal vein in each embryo by Fiji software. All images were taken at 24 hours post injection (hpi) with Leica M205 FA stereomicroscope equipped with a Leica DFC 450 C digital camera using the LAS software (Leica).

The presence of tumor cell clusters far from the injection site was detected by fluorescence microscopy and quantified by the “Analyze Particle” tool of Fiji software. In particular fluorescent cells along the tail were quantified at different time points: 0 (immediately after the injection) and 48 hours post injection.

The study was approved by the Institutional Ethics Committee and the Animal Welfare Body OPBA (University of Milan, approval number 16/18).

3.7 Statistical Analysis

Experiments were performed at least three times. Relative EC_{50} values and maximal inhibitory effect were calculated using nonlinear regression curve-fitting program. Statistical differences among groups were first evaluated by t-test or ANOVA test together with the followed post hoc test (Newman–Keuls). A p value <0.05 was considered significant. The values reported in the figures represent the mean ± standard error of the mean (SEM). For statistical analysis, GraphPad Prism 5.0 (GraphPad Software, San Diego, CA) was used.

4. Results

4.1 Effects of TKIs on cell viability

After 6 days of incubation, all TKIs significantly inhibited the viability of NET cells in a dose-dependent manner (Fig. 3, 4).

In NCI-H727 and NCI-H835 cell lines (Fig.3a and 3c) the growth inhibitory effect of sulfatinib was significantly more potent than that of axitinib and cabozantinib, as shown by the higher maximal inhibition ($p < 0.001$, fig.3, table 1). In UMC-11, both sulfatinib and cabozantinib exerted a maximal antiproliferative inhibition significantly higher than axitinib ($p < 0.05$) (fig.3, table 1).

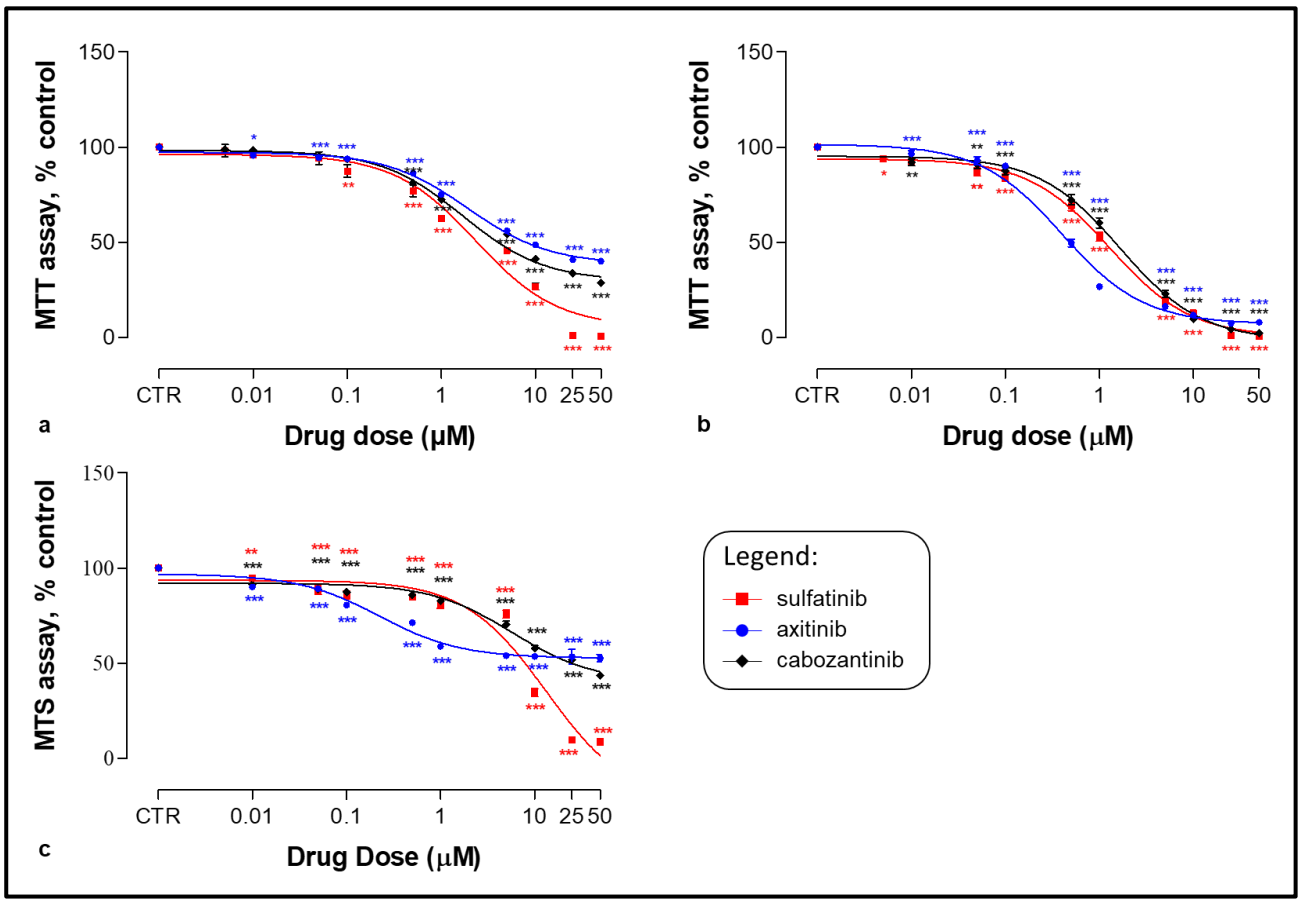

Fig. 3. Effect of sulfatinib (red), axitinib (blue) and cabozantinib (black) on cell proliferation in NCI-H727 (**a**), UMC-11 (**b**) and NCI-H835 (**c**) cell lines, as measured by MTT or MTS assays. Cells were incubated for 6 days with or without each drug at different concentrations, as described in Material and Methods section. Dose-response curves were expressed as nonlinear regression (curve fit) of log (concentration drug) versus the percentage of control (untreated cells). Values represent the

mean ± SEM of at least 3 independent experiments in 6 replicates. CTR values have been set to 100%. * $p < 0.05$; ** $p < 0.01$; *** $p < 0.001$. SEM, standard error of the mean; CTR, control; MTT, 3-(4,5-dymethylthiazol-2-yl)-2,5-diphenyltetrazolium bromide; MTS, 3-(4,5-dimethylthiazol-2-yl)-5-(3-carboxymethoxyphenyl)-2-(4-sulfophenyl)-2H-tetrazolium.

No significant difference has been observed between maximal inhibition of the three TKIs in TT cell lines (Fig.4a and table 1). However, the EC_{50} concentration of SPP86 was significantly lower than the EC_{50} of SU5402 ($p < 0.001$). In MZ-CRC-1 (Fig.4b and table 1) sulfatinib showed a higher maximal inhibition compared with SPP86 ($p < 0.05$) and SU5402 ($p < 0.01$). No difference between maximal inhibition of SSP86 and SU5402 was found; however, the EC_{50} concentration of SPP86 was significantly lower than SU5402 ($p < 0.001$). From these assays, we calculated the EC_{50} concentration for all the drugs that we used for the following experiments. In the Table.1, we resumed the EC_{50} concentration for each drug and their maximal inhibitory effect.

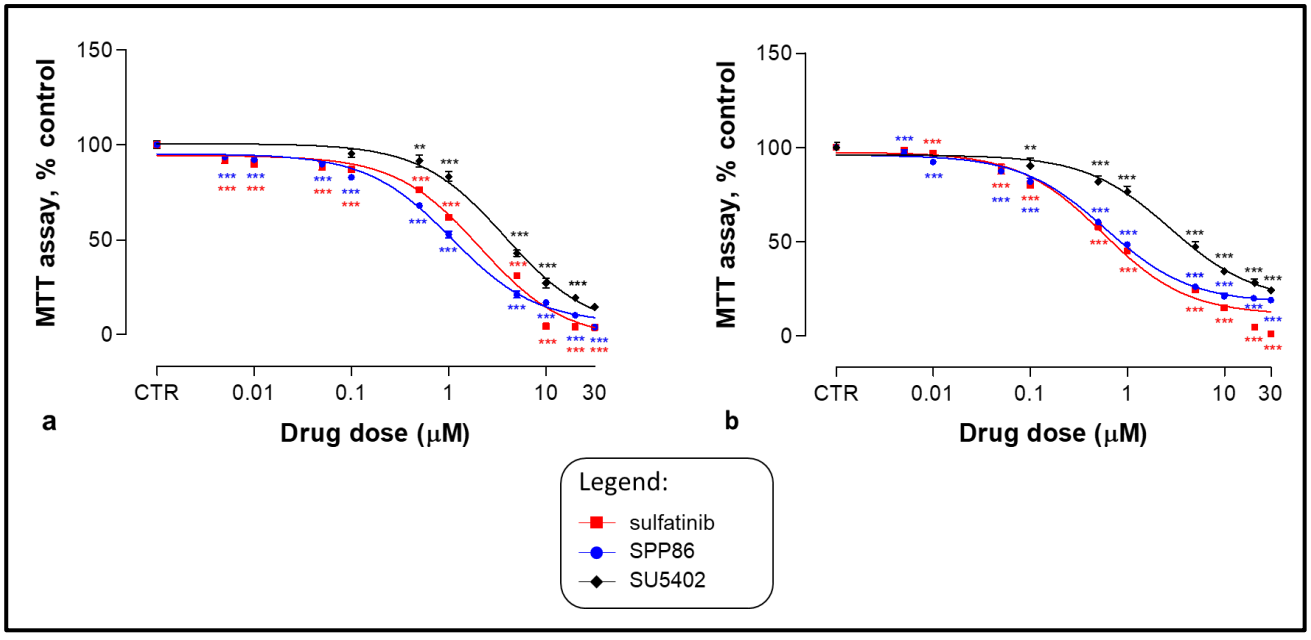

Fig. 4. Effect of sulfatinib (red), SPP86 (blue) and SU5402 (black) on cell proliferation in TT (**a**) and MZ-CRC-1 (**b**) cell lines, as measured by MTT assay. Cells were incubated for 6 days with or without each drug at different concentrations, as described in Material and Methods section. Dose-response curves were expressed as nonlinear regression (curve fit) of log (concentration drug) versus the percentage of control (untreated cells). Values represent the mean ± SEM of at least 3 independent experiments in 6 replicates. CTR values have been set to 100%. * $p < 0.05$; ** $p < 0.01$; *** $p < 0.001$. SEM, standard error of the mean; CTR, control; MTT, 3-(4,5-dymethylthiazol-2-yl)-2,5-diphenyltetrazolium bromide.

Table 1. Growth inhibition of LNET and MTC cell lines after 6 days of incubation with TKIs.

		EC_{50}	Maximal Inhibition
NCI-H727	Sulfatinib	2.3 µM	94.5%
	cabozantinib	1.7 µM	70.3%
	Axitinib	2 µM	61.4%
UMC-11	Sulfatinib	1.3 µM	100%
	cabozantinib	1.6 µM	100%
	Axitinib	0.4 µM	92.9%
NCI-H835	Sulfatinib	5.6µM	100%
	cabozantinib	0.007 µM	51%
	Axitinib	0.2 µM	47.3%
TT	Sulfatinib	2 µM	100%
	SPP86	1.3 µM	100%
	SU5402	3.6 µM	96.5%
MZ-CRC-1	Sulfatinib	0.5 µM	89.5%
	SPP86	0.7 µM	83.6%
	SU5402	2.6 µM	80.6%

4.2 Effects of TKIs on Cell Cycle

After 6 days of incubation, we analyzed the effects of these molecules on the cell cycle by flow cytometric analysis with PI-stained LNET and MTC cells (Fig. 5-6).

In NCI-H727 (Fig. 5a), while sulfatinib and cabozantinib had no relevant effect, axitinib reduced the number of cells in G_0/G_1 and S phases (-86.11%, $p < 0.001$ for G_0/G_1; -69.25%, $p < 0.05$ for S phase), while it increased the G_2/M phase (+93.42%, $p < 0.001$) in comparison with untreated control cells. In UMC-11 (Fig. 5b), sulfatinib and cabozantinib were able to significantly reduce cell percentage in S phase (-24.5%, $p < 0.01$ and -25.3%, $p < 0.001$, respectively). Axitinib perturbed all the cell cycle phases, reducing both G_0/G1 (-21.88%, $p < 0.01$) and S phases (-45.14%, $p < 0.001$), and increasing the fraction of cells in G_2/M phase (+58.53%, $p < 0.001$) compared with the control. All TKIs showed a limited effect on cell cycle phases in NCI-H835 cells. They moderately reduced cells in S phase (sulfatinib -25.41%, axitinib -22.59%, both $p < 0.05$; cabozantinib -29.27%, $p < 0.01$) and cabozantinib lightly increased cells in G_2/M phase (+14.91%, $p < 0.05$).

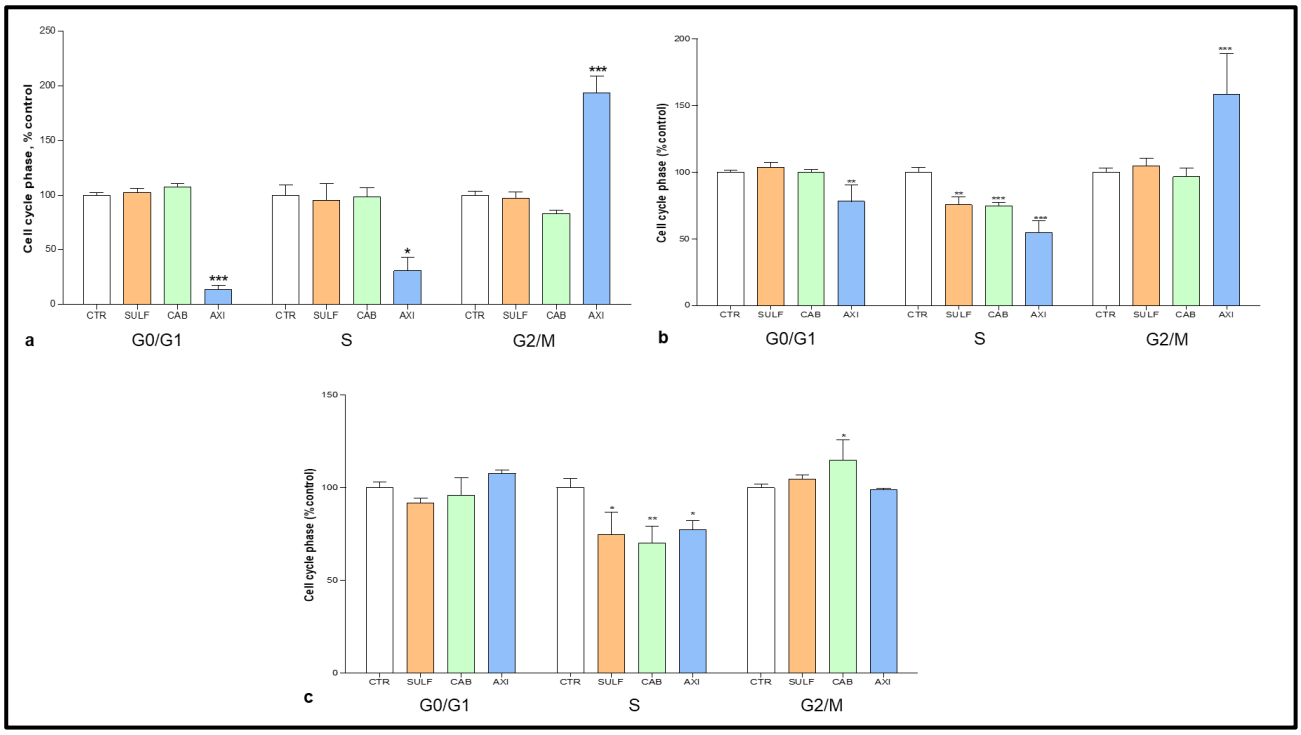

Fig. 5. Cell cycle analysis after 6 days of incubation with SULF, CAB and AXI in NCI-H727 (**a**), UMC-11 (**b**) and NCI-H835 (**c**) cell lines. Cells were detected by FACS analysis after staining with propidium iodide. CTR values have been set to 100%. Values represent the mean ± SEM of at least 3 independent experiments. * p < 0.05; ** p < 0.01; *** p < 0.001. SEM, standard error of the mean; CTR, control; SULF, sulfatinib; CAB, cabozantinib; AXI, axitinib.

In MTC cells (Fig. 6), the S phase was the most vulnerable. In TT cells, all compounds significantly decreased the number of cells in S phase, with sulfatinib and SPP86 having a slightly higher effect compared to SU5402 (-63.67%, -59.22% and -39.36%, respectively, $p < 0.001$ for all TKIs vs control). Sulfatinib and SPP86 also reduced the fraction of cells in G_2/M phase (-28.65%, $p < 0.01$; -18.9%, $p < 0.05$, respectively) in comparison with control. In MZ-CRC-1 cells the S phase was significantly impaired after SU5402 and SPP86 (-56.28% and -57.20%, respectively, both $p < 0.001$) with the latter having a relevant effect also in the G_2/M phase (-38.04%, $p < 0.001$).

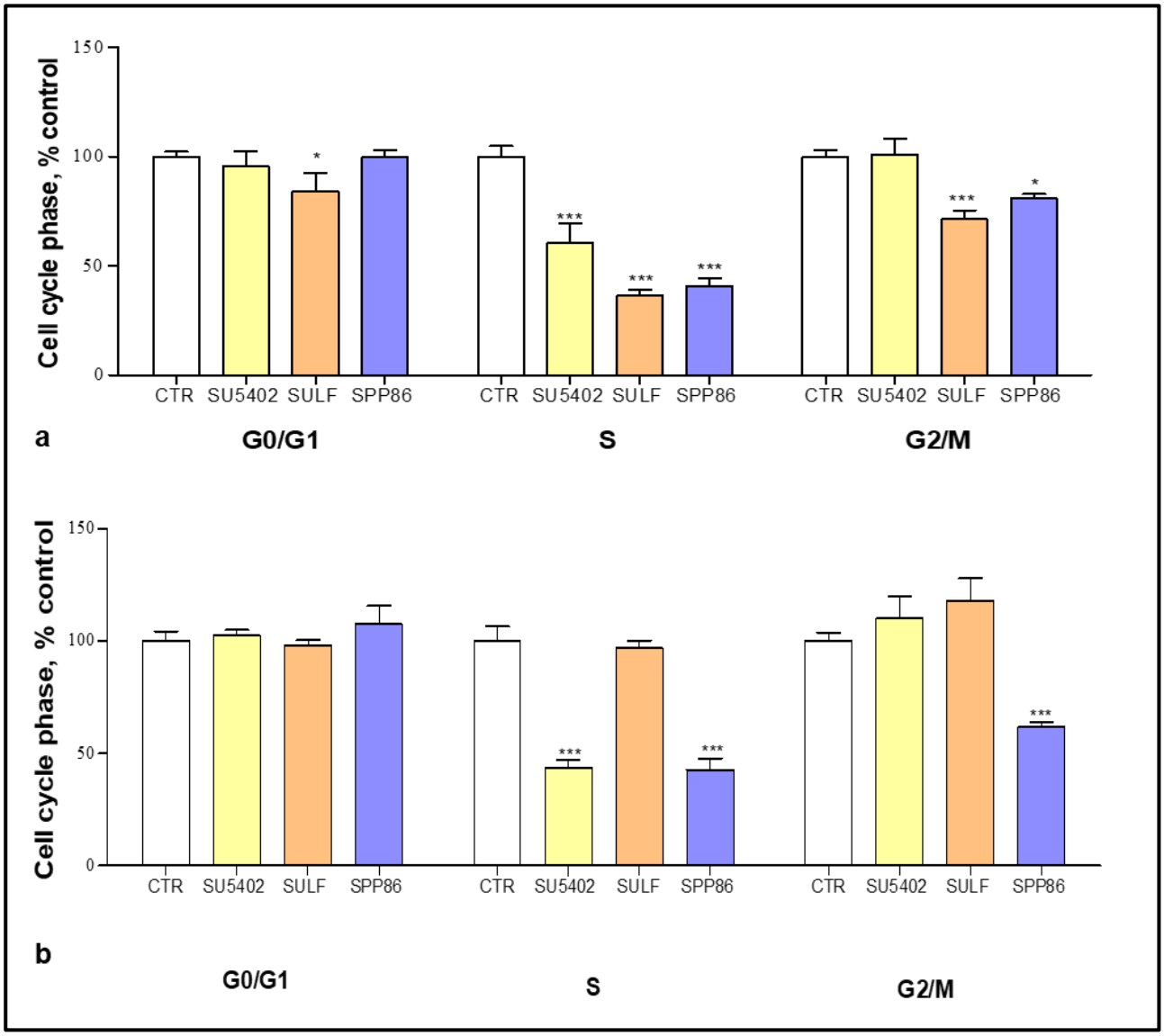

Fig. 6. Cell cycle analysis after 6 days of incubation with SU5402, SULF and SPP86 in TT (**a**) and MZ-CRC-1 (**b**) cell lines. Cells were detected by FACS analysis after staining with propidium iodide. CTR values have been set to 100%. Values represent the mean ± SEM of at least 3 independent experiments. * p < 0.05; *** p < 0.001. SEM, standard error of the mean; CTR, control; SULF, sulfatinib.

4.3 Effects of TKIs on Apoptosis/Necrosis

We studied the effects of TKIs on apoptosis through flow cytometry with Annexin V and PI staining.

In NCI-H727 (Fig. 7a), sulfatinib induced a relevant increase in the number of cells in late apoptosis (+161.2% vs. control, $p < 0.05$) and necrosis (+58.09% vs. control, $p < 0.05$). No statistically significant effect on apoptosis/necrosis was observed after incubation with cabozantinib and axitinib. In UMC-11 (Fig.7b) sulfatinib was able to induce a strong increase in the fraction of cells in early apoptosis (+159.5% vs. control, $p < 0.01$), while cabozantinib had no relevant effect. Axitinib exerted a significant increase in early (+74.83% vs. control, $p < 0.05$) and late apoptosis (+169.1% vs. control, $p < 0.01$). Finally, in NCI-H835 (Fig.5c), sulfatinib strongly increased the fractions of cells in late apoptosis (+158.5% vs. control, $p < 0.05$) and necrosis (+126.9% vs. control, $p < 0.001$). Similarly, cabozantinib slightly modified the fraction of cells in these phases (+67.42% vs. control, $p < 0.05$ for late apoptosis; +17.88% vs. control, $p < 0.05$ for necrosis), while after axitinib no relevant modification in any phase has been observed.

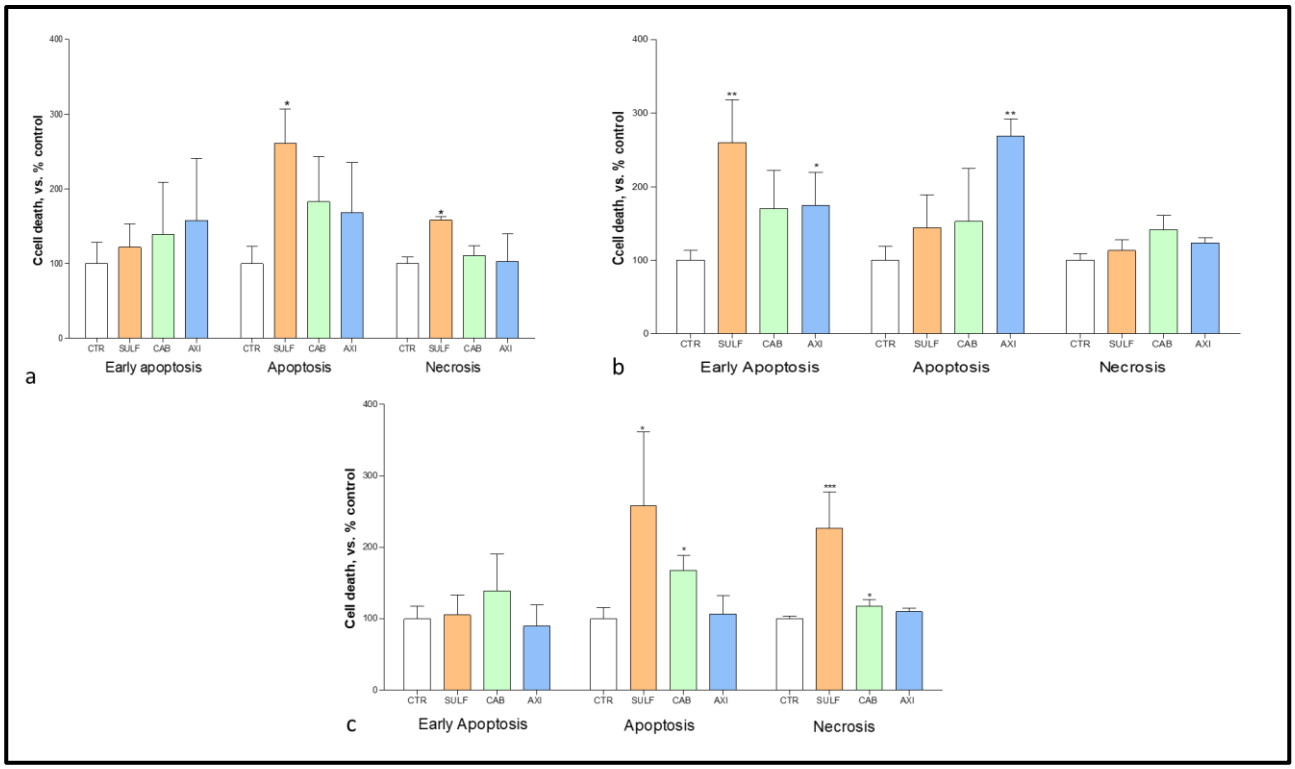

Fig. 7. Modulation of cell death analysis after 6 days of incubation with SULF, CAB and AXI in NCI-H727 (**a**), UMC-11 (**b**), and NCI-H835 (**c**) cell lines through flow cytometry with Annexin V and propidium iodide. The proportions of cells in early apoptosis, late apoptosis and necrosis are expressed as percentage compared with untreated CTR and represent the mean ± SEM of at least 3 independent experiments. * $p < 0.05$; ** $p < 0.01$. SEM, standard error of the mean; CTR, control; SULF, sulfatinib; CAB, cabozantinib; AXI, axitinib.

In MTC cells, the effects on apoptosis were similar for both cell lines. SU5402 did not show any relevant effect on cell death. On the other hand, both sulfatinib and SPP86 stimulated apoptosis. In TT cells (Fig. 8a) both drugs significantly increased the fractions of cells in early and late apoptosis and necrosis (sulfatinib vs control: +388 %, $p < 0.05$; +212.2%, $p < 0.001$; +32.05%, $p < 0.05$, respectively; SPP86 vs control: +440.2; +370.8% and +170%, all with $p < 0.001$, respectively). In MZ-CRC-1 cells (Fig. 8b), sulfatinib increased all fractions of cells compared to control (early apoptosis +141.1%, $p < 0.05$; late apoptosis +208.3%, $p < 0.001$, necrosis +95.19%, $p < 0.05$), while SPP86 had a relevant impact on late apoptosis (+207.4%, $p < 0.001$) and necrosis (+85.89%, $p < 0.05$).

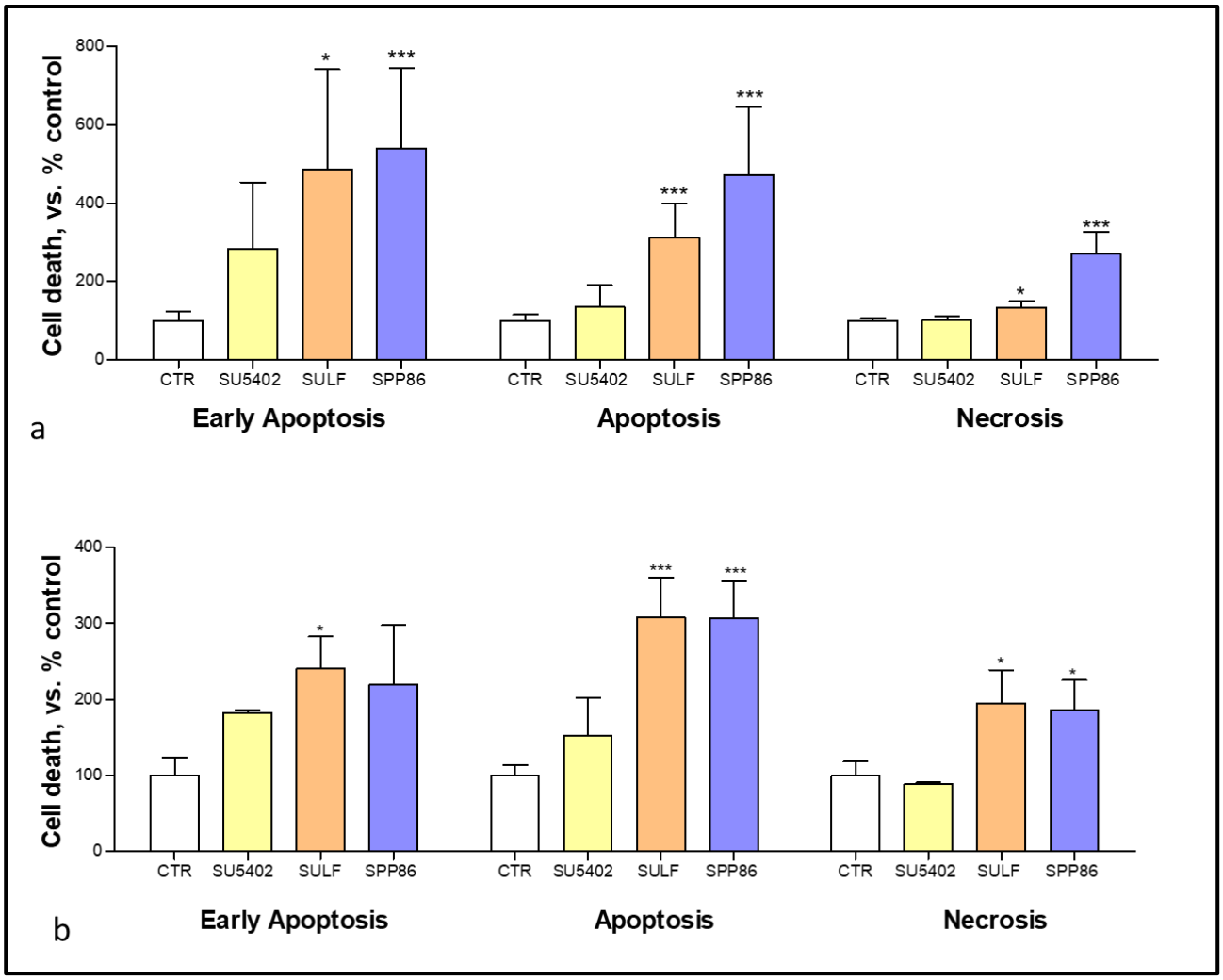

Fig. 8. Modulation of cell death analysis after 6 days of incubation with SU5402, SULF and SPP86 in TT (**a**) and MZ-CRC-1 (**b**) cell lines through flow cytometry with Annexin V and propidium iodide. The proportions of cells in early apoptosis, late apoptosis and necrosis are expressed as percentage compared with untreated CTR and represent the mean ± SEM of at least 3 independent experiments. * $p < 0.05$; *** $p < 0.001$. SEM, standard error of the mean; CTR, control; SULF, sulfatinib.

4.4 Effects of TKIs on Cell Migration

We investigated *in vitro* the impact of TKIs on cell migration through a wound-healing assay (Fig. 9-12).

In LNET cell lines (Fig. 9, 10), we performed this experiment only in NCI-H727 and UMC-11 since NCI-H835 cells lack substrate adherence and grow in suspension. In NCI-H727 only cabozantinib (Fig. 9) was able to significantly inhibit the migration process (-36.6% vs. control, $p < 0.001$). While in UMC-11 no relevant effect was observed for any TKI (Fig. 10).

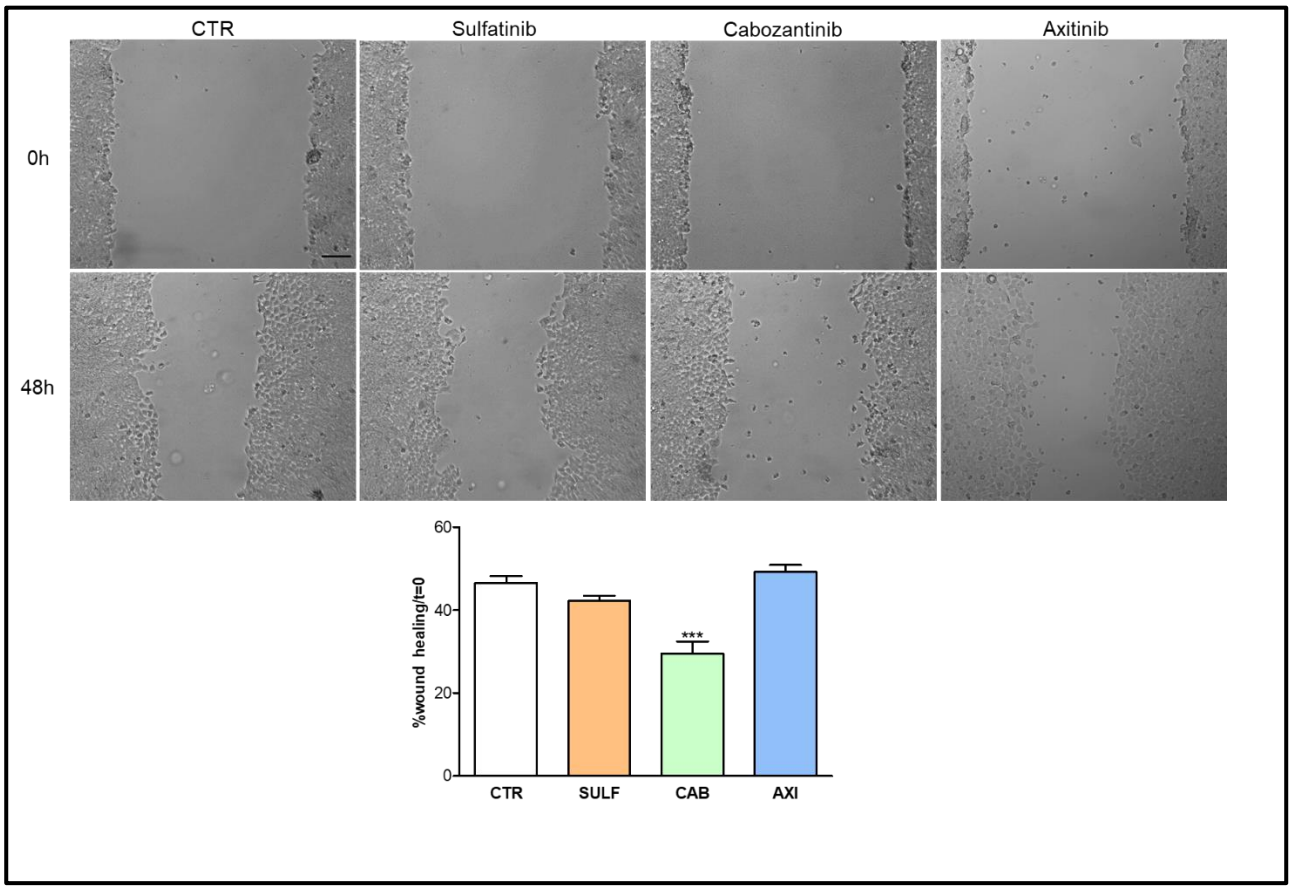

Fig. 9. Effect of SULF, CAB and AXI on NCI-H727 cell migration compared to untreated CTR. The area of wound was recorded at 0 and 2 days, and the percentage of wound healing with respect to T0 was calculated using the equation reported in Material and Methods section. Data were reported as mean ± SEM of at least 3 independent experiments. Scale bar 200 µm. *** $p < 0.001$. SEM, standard error of the mean; CTR, control; SULF, sulfatinib; CAB, cabozantinib; AXI, axitinib.

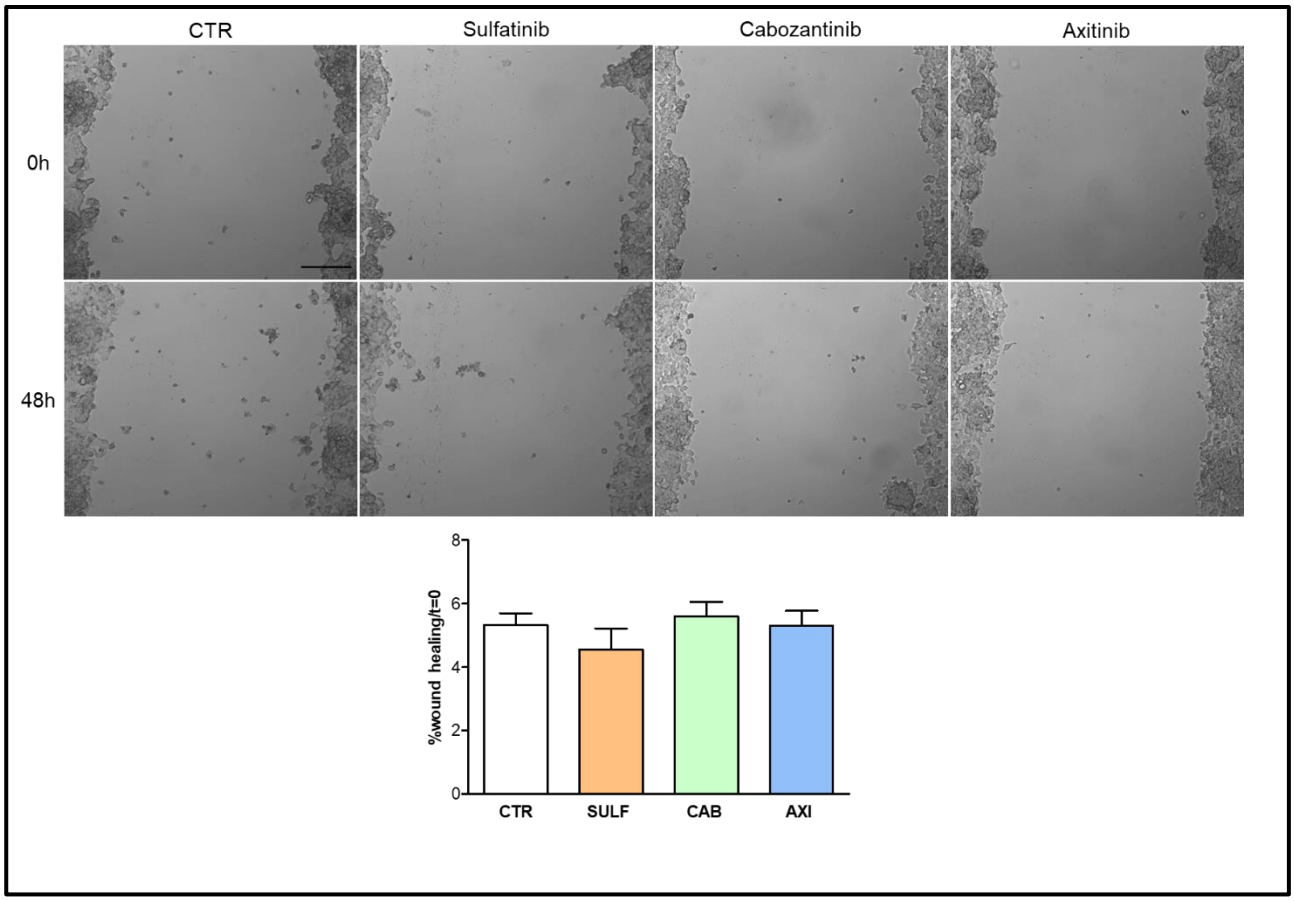

Fig. 10. Effect of SULF, CAB and AXI on UMC-11 cell migration compared to untreated CTR. The area of wound was recorded at 0 and 2 days, and the percentage of wound healing with respect to T0 was calculated using the equation reported in Material and Methods section. Data were reported as mean ± SEM of at least 3 independent experiments. Scale bar 200 μm. SEM, standard error of the mean; CTR, control; SULF, sulfatinib; CAB, cabozantinib; AXI, axitinib.

In TT cells (Fig. 11) SPP86 had the most relevant inhibitory effect on cell migration (-41.6% vs. control, $p < 0.001$), followed by sulfatinib (-38.5% vs. control, $p < 0.001$) and SU5402 (-30.3% vs control, $p < 0.001$). In MZ-CRC-1 cells (Fig. 12) both sulfatinib and SPP86 inhibited cell migration compared to untreated control (-36.1%, $p < 0.01$ and -38.6%, $p < 0.01$, respectively). While SU5402 was not able to significantly affect the wound-healing process.

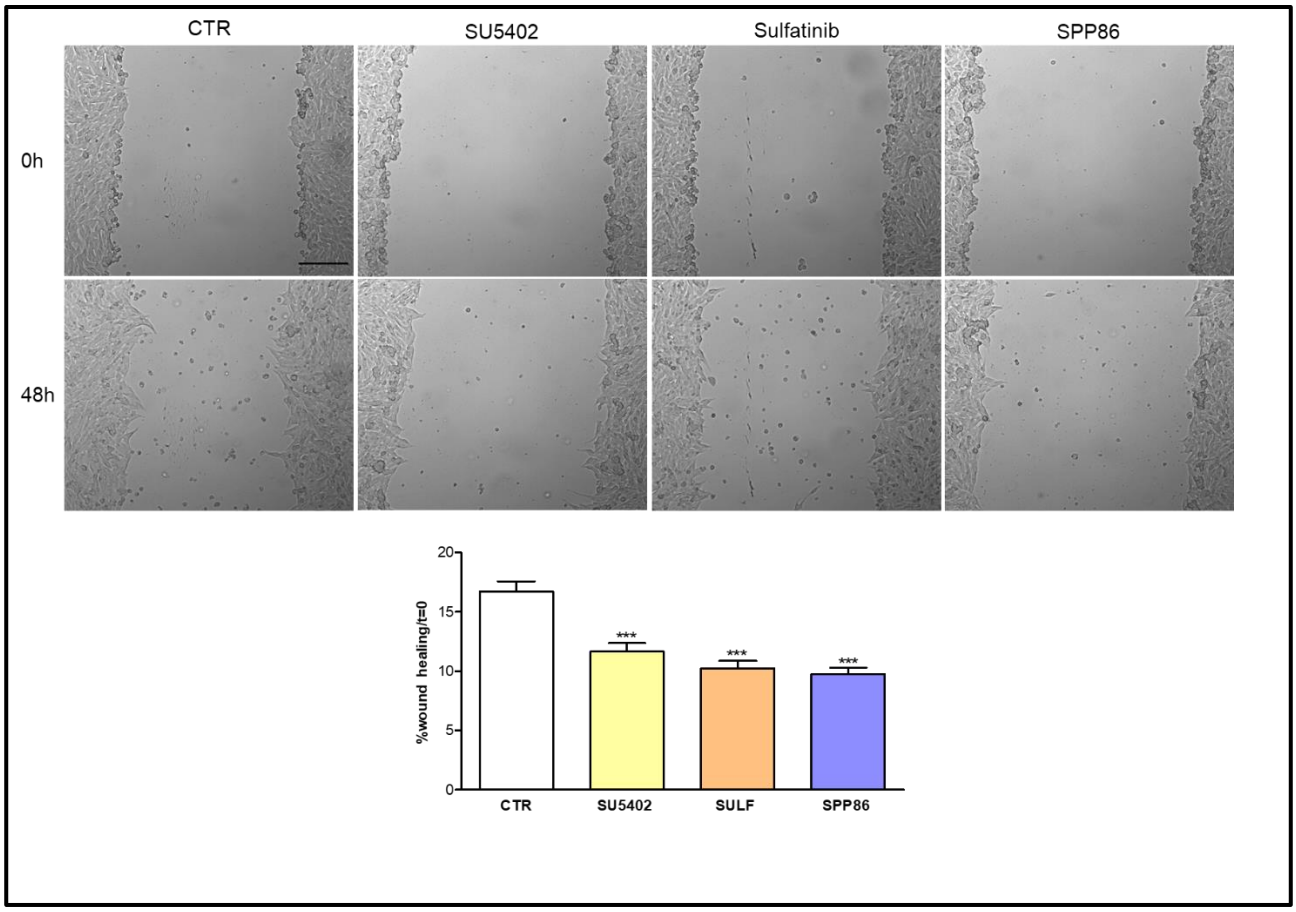

Fig. 11. Effect of SU5402, SULF and SPP86 on TT cell migration compared to untreated CTR. The area of wound was recorded at 0 and 3 days, and the percentage of wound healing with respect to T0 was calculated using the equation reported in Material and Methods section. Data were reported as mean ± SEM of at least 3 independent experiments. Scale bar 200 μm. *** $p < 0.001$. SEM, standard error of the mean; CTR, control; SULF, sulfatinib.

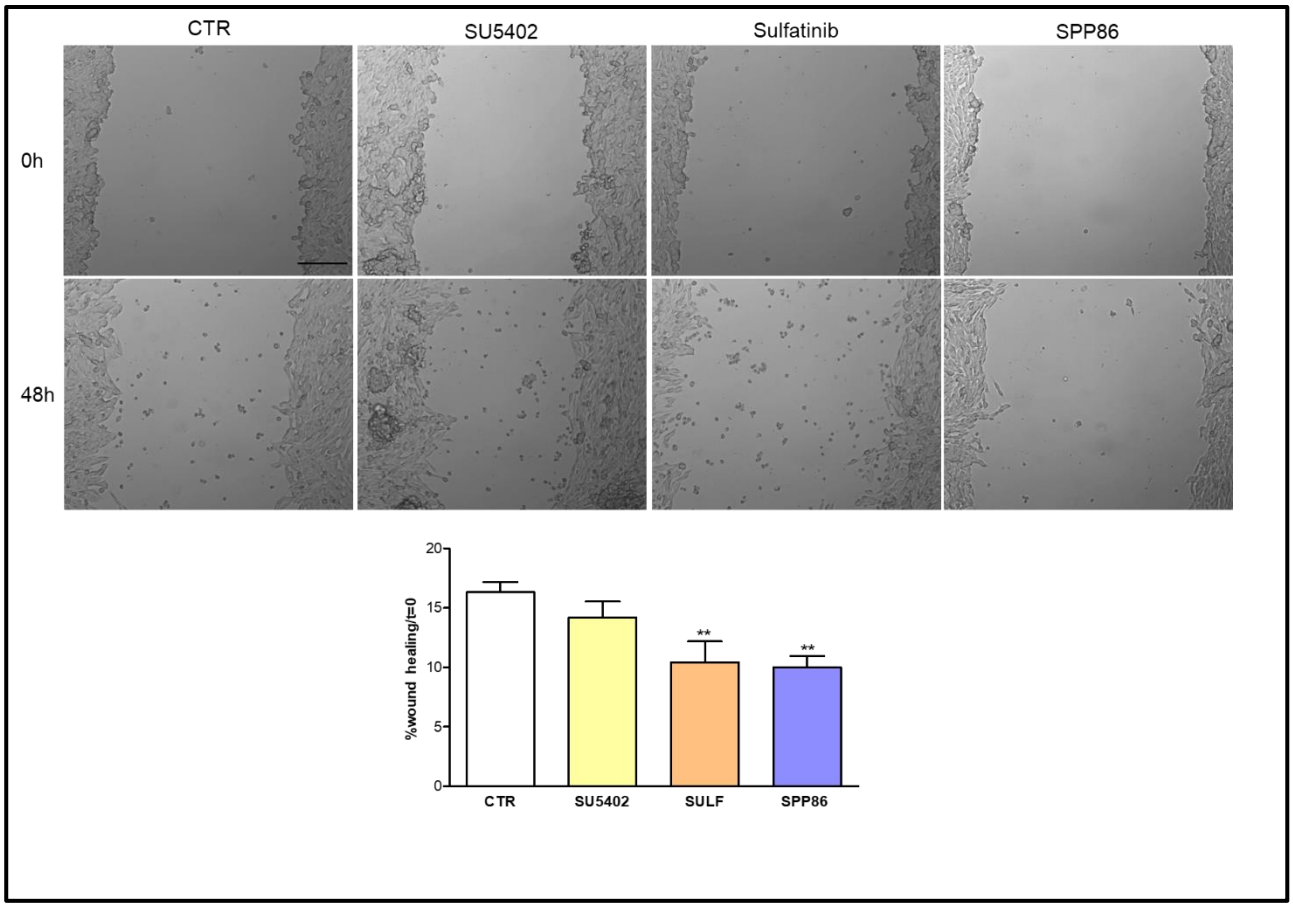

Fig. 12. Effect of SU5402, SULF and SPP86 on MZ-CRC-1 cell migration compared to untreated CTR. The area of wound was recorded at 0 and 3 days, and the percentage of wound healing with respect to T0 was calculated using the equation reported in Material and Methods section. Data were reported as mean ± SEM of at least 3 independent experiments. Scale bar 200 μm. ** $p < 0.01$. SEM, standard error of the mean; CTR, control; SULF, sulfatinib.

4.5 Effects of TKIs on *in vivo* Tumor-Induced Angiogenesis

We analyzed the effects of TKIs on tumor-induced angiogenesis through an innovative zebrafish platform.

All LNET cell lines (NCI-H727, UMC-11 and NCI-H835) strongly stimulated angiogenesis, leading to the formation of new endothelial structures, which sprouted from the SIV plexus and CCV toward the tumor as early as 24 hpi. In grafted *Tg(fli1a:EGFP)^{y1}* embryos (Fig. 13-15), cabozantinib and axitinib drastically affected the vascular network induced by the tumor cell injection, in a dose-dependent manner, highlighting a strong reduction of peritumoral endothelial structures as early as 24 hpi. This effect was less evident after incubation with sulfatinib.

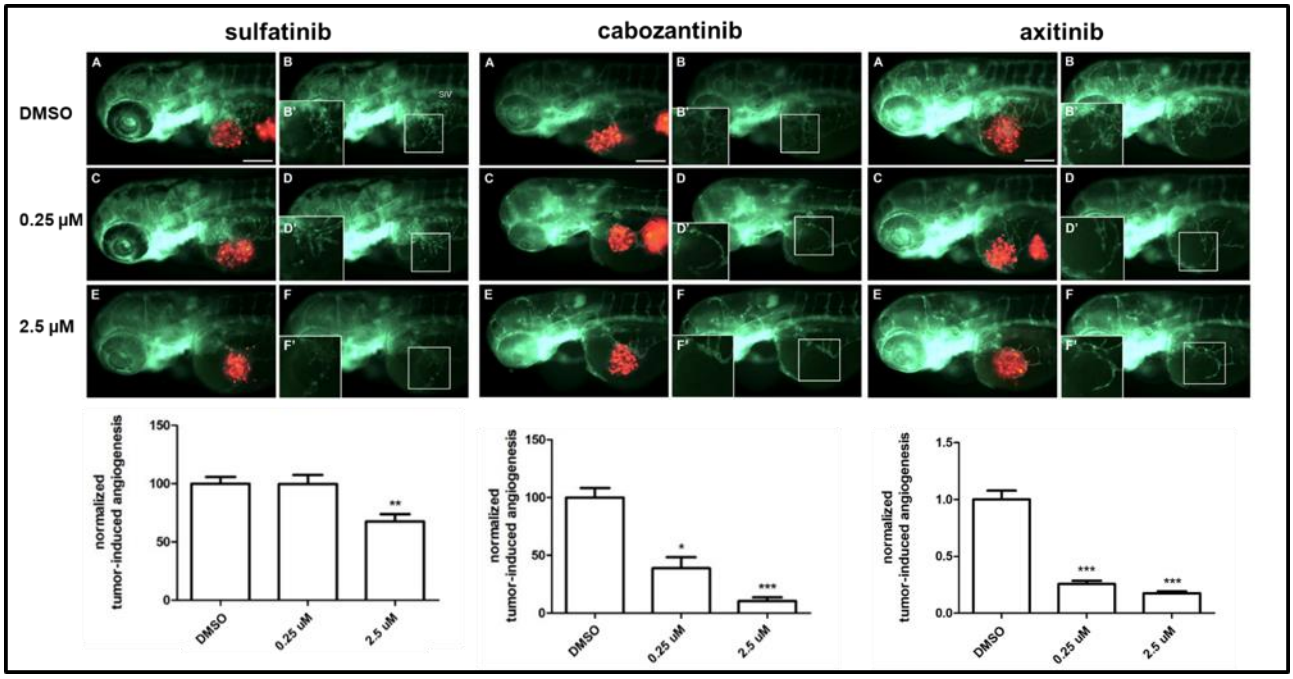

Fig. 13. Effect of treatment with sulfatinib, cabozantinib and axitinib on NCI-H727 cell-induced angiogenesis. For each inhibitor there is a representative image of an injected and treated embryo (with drug-vehicle or specific concentration). The red channel, corresponding of NCI-H727 cells, was omitted in panel **B**, **D** and **F** of each drug to highlight the tumor-induced microvascular network sprouting from the SIV. Digital magnifications of the graft region are shown in white-boxed regions **B'**, **D'** and **F'**. Graphs below report the results of tumor-induced angiogenesis quantification at 24h post-injection. All images are oriented so that rostral is to the left and dorsal is at the top. Scale bar in **A**, 100µm. SIV, subintestinal vein.

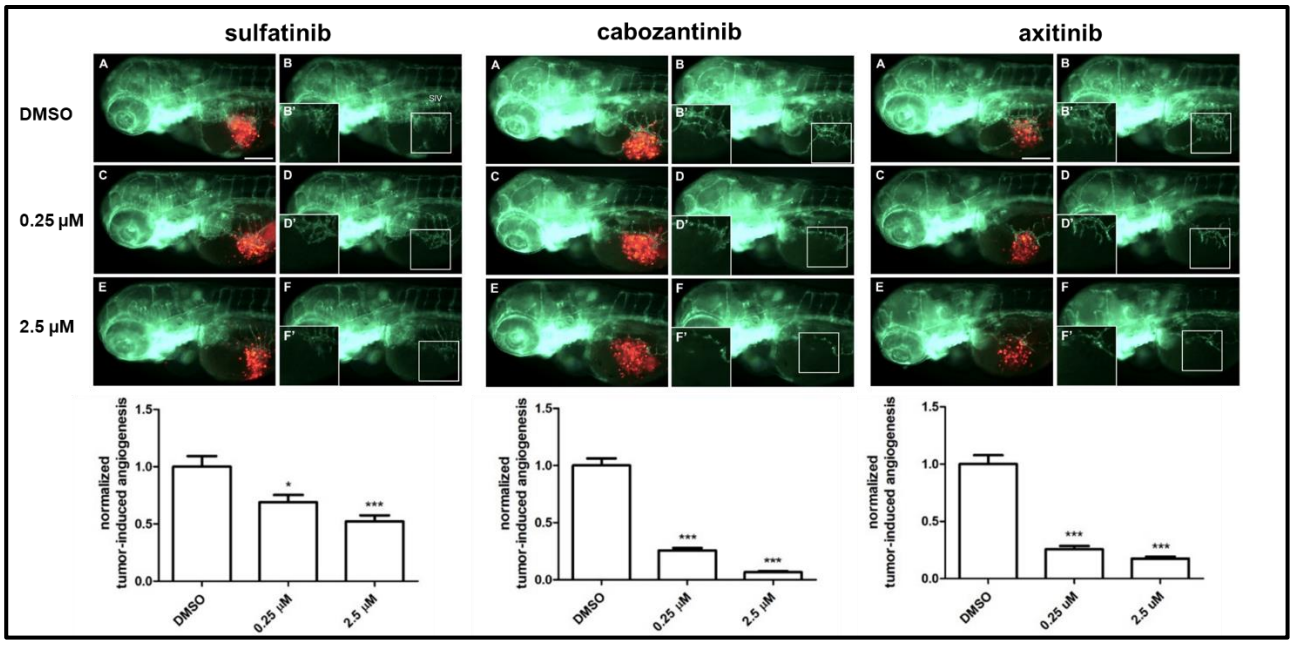

Fig. 14. Effect of treatment with sulfatinib, cabozantinib and axitinib on UMC-11 cell-induced angiogenesis. For each inhibitor there is a representative image of an injected and treated embryo (with drug-vehicle or specific concentration). The red channel, corresponding of UMC-11 cells, was omitted in panel **B**, **D** and **F** of each drug to highlight the tumor-induced microvascular network sprouting from the SIV. Digital magnifications of the graft region are shown in white-boxed regions **B'**, **D'** and **F'**. Graphs below report the results of tumor-induced angiogenesis quantification at 24h post-injection. All images are oriented so that rostral is to the left and dorsal is at the top. Scale bar in **A**, 100µm. SIV, subintestinal vein.

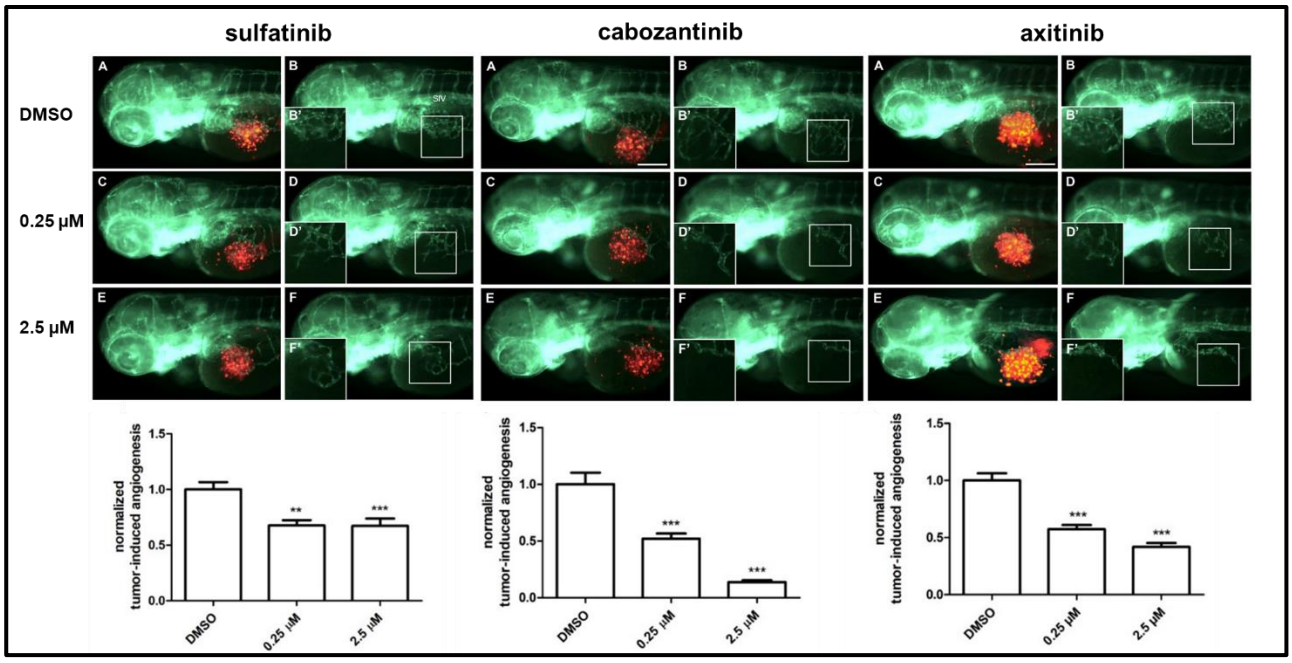

Fig. 15. Effect of treatment with sulfatinib, cabozantinib and axitinib on NCI-H835 cell-induced angiogenesis. For each inhibitor there is a representative image of an injected and treated embryo (with drug-vehicle or specific concentration). The red channel, corresponding of NCI-H835 cells, was omitted in panel **B**, **D** and **F** of each drug to highlight the tumor-induced microvascular network sprouting from the SIV. Digital magnifications of the graft region are shown in white-boxed regions **B'**, **D'** and **F'**. Graphs below report the results of tumor-induced angiogenesis quantification at 24h post-injection. All images are oriented so that rostral is to the left and dorsal is at the top. Scale bar in **A**, 100µm. SIV, subintestinal vein.

For MTC, these experiments were conducted only in TT cells (Fig. 16), since MZ-CRC-1 induced only a moderate induction of angiogenesis in zebrafish embryos. SU5402 lightly reduced the formation of novel vessel at high concentration (2.5µM), although this effect was not statistically significant. On the other hand, sulfatinib and SPP86 displayed a significant and similar inhibition of TT-induced angiogenesis compared to controls.

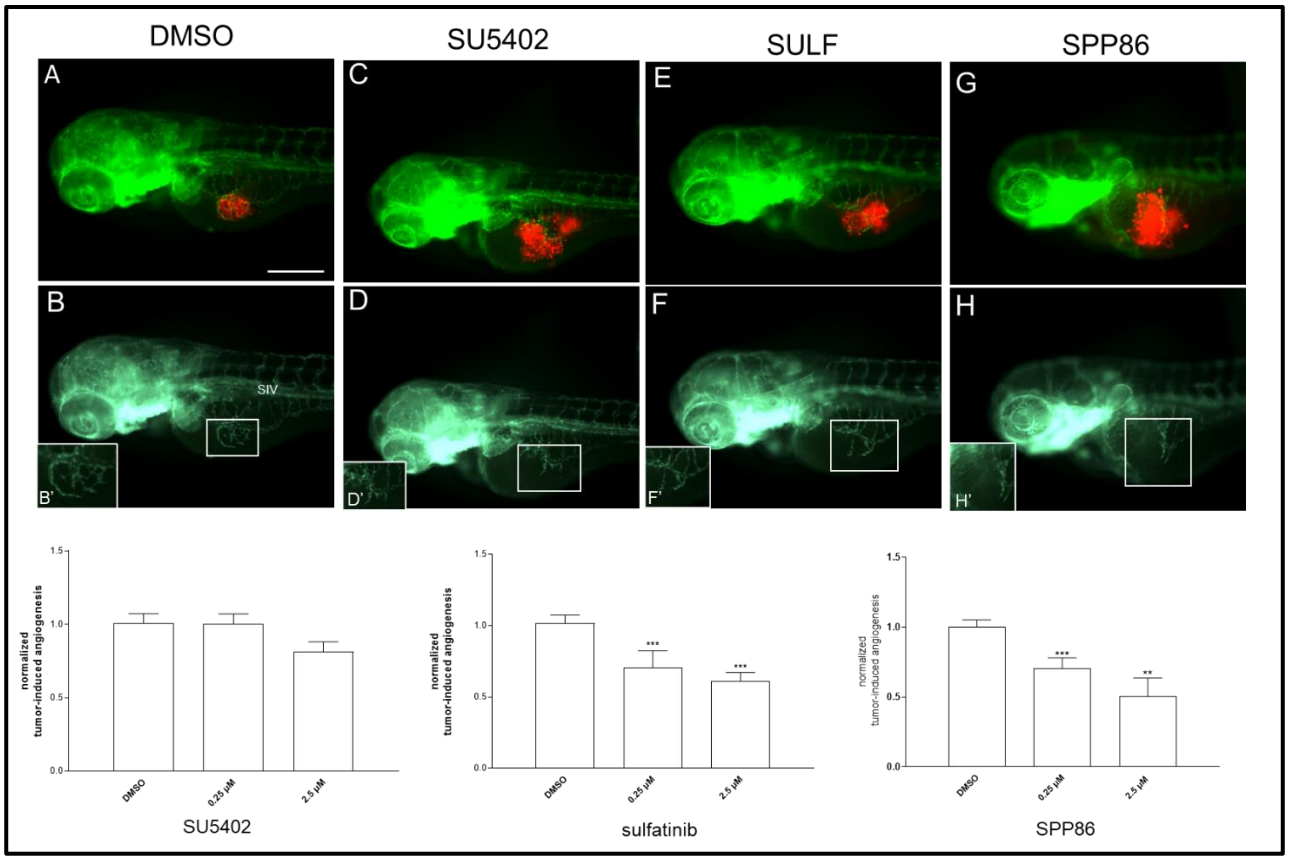

Fig. 16. Effect of treatment with SU5402, sulfatinib and SPP86 on TT cell-induced angiogenesis. For each inhibitor there is a representative image of an injected and treated embryo (with drug-vehicle or specific concentration). The red channel, corresponding of TT cells, was omitted in panel **B**, **D, F and H** of each drug to highlight the tumor-induced microvascular network sprouting from the SIV. Digital magnifications of the graft region are shown in white-boxed regions **B'**, **D', F'** and **H'**. Graphs below report the results of tumor-induced angiogenesis quantification at 24h post-injection. All images are oriented so that rostral is to the left and dorsal is at the top. Scale bar in **A**, 100µm. SIV, subintestinal vein.

4.6 Effects of TKIs on *in vivo* Migration

Finally, we tested the potential anti-metastatic effect of these drugs. At 48 hpi we counted the number of fluorescent spots containing a variable number of cells, located away from the site of inoculation, particularly in the tail.

A possible technical drawback with tumor xenograft in zebrafish embryos is represented by the possibility that tumor cells could be accidentally and directly introduced into the blood vessels during the injection process. To prevent this possibility, embryos have been observed within 1 hour after the implant and those showing cells into the yolk sac or in the circulatory system were excluded from further analysis.

In embryos correctly engrafted with LNET cells (Fig. 17), the presence of circulating fluorescent spots progressively increased, especially in the tail, within 48 hpi for all cell lines. Cabozantinib was the only TKI able to significantly inhibit cell migration *in vivo*. Although the number of the spots identified in the tail was low, sulfatinib and axitinib appeared to have no effect on this metastatic process.

In both TT and MZ-CRC-1 cells the number of fluorescent spots located in the tail was extremely low for a proper analysis.

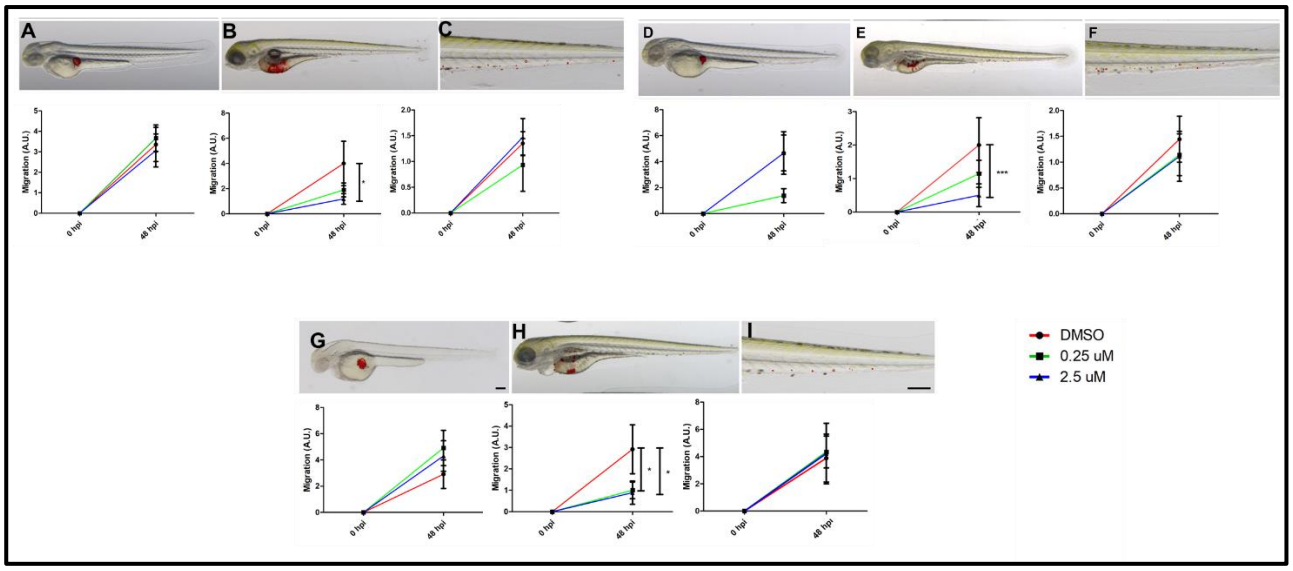

Fig. 17. Effect of SULF (**A**, **D** and **G**), CAB (**B**, **E** and **H**) and AXI (**C**, **F** and **I**) on invasiveness of NCI-H727 (**A**-**C**), UMC-11 (**D**-**F**) and NCI-H835 (**G**-**I**) cells in grafted embryos. Quantification of cells spreading in the tail of embryos injected with NCI-H835, UMC-11, NCI-H727 and NCI-H720 cells at 0 and 48 hpi after 0.25 and 2.5 μM of axitinib. As arbitrary unit (A.U) of migration we considered the number of fluorescent particles in the tail. Scale bar in **I**, 100μm. Graphed values represent the mean ± S.E.M. ***p<0.001 vs DMSO.

5. Discussion

The only curative solution for the treatment of NENs is represented by surgical resection. However, in some cases these malignancies are locally unresectable or in advanced stage with distant metastasis. Several studies evaluated the antitumor activity of medical strategies in advanced NENs (87). Despite some of these therapies showed promising results and are currently approved and adopted in the clinic, the high heterogeneity of these neoplasms together with the onset of drug-resistance and the occurrence of side-effects limited the use of most of these compounds (88).

In the present work, we studied the effects of TKIs on two different types of low-grade, well-differentiated NETs: LNETs and MTC. We selected few TKIs recently developed and adopted in other NENs. Cabozantinib is already approved for MTC treatment, therefore we tested its efficacy in LNETs, along with sulfatinib and axitinib, two novel multi-target TKIs that mainly address VEGFRs. The reason is to exploit the high vascularization of these tumors and their high expression of VEGFRs (89, 90). Similarly, sulfatinib has been tested in MTC cells, due to the high expression of VEGFR also in this tumor (91). In addition, we selected SPP86, a RET-specific inhibitor that was not studied so far, and SU5402, an inhibitor of the FGFR1, a survival pathway activated in most NENs.

5.1 Lung Neuroendocrine tumors

In LNET cell lines, all TKIs displayed a significant inhibition of cell viability. Overall, sulfatinib had the major impact compared to cabozantinib and axitinib, particularly in NCI-H727 and NCI-H835 cells. This effect was confirmed by the study of apoptosis through the flow cytometry with Annexin V and PI staining. In this assay, we observed a more potent pro-apoptotic activity after sulfatinib compared to the other two drugs. The cell cycle analysis showed that axitinib was the only TKI to significantly affect the cell cycle distribution of NCI-H727 cells. It strongly reduced percentage of cells in G_0/G_1 and S phases, while it increased cell percentage in G_2/M phase. In UMC-11, axitinib showed a similar but milder effect compared to NCI-H727. Moreover, also sulfatinib and cabozantinib significantly reduced cell percentage of cells in S phase. Finally, in NCI-H835 the most affected phase was the S phase, reduced by all three TKIs. In addition, cabozantinib was also able to slightly increase cells in G_2/M phase.

The wound healing assay showed a significant inhibition of cell migration only after incubation with cabozantinib in NCI-H727 cells, whereas in UMC-11 no relevant effect was observed after treatment with sulfatinib, cabozantinib and axitinib.

Interestingly, cabozantinib inhibited the tumor-induced angiogenesis in the zebrafish model more efficiently than the other drugs in all three LNET cell lines. Axitinib resulted to be a potent antiangiogenic compound, although slightly milder than cabozantinib, while sulfatinib was the less potent compound. Cabozantinib confirmed its higher efficacy also to impair the metastatic potential of LNET cells. This TKI was the only one to arrest cell migration, evaluated through a wound-healing assay, and to inhibit the formation of micrometastasis in zebrafish embryos.

It is known that LNETs are characterized by a highly vascularized network and a low proliferation rate (92). Anti-angiogenic therapy might be an interesting strategy in LNETs and few preliminary studies have recently suggested its efficacy. Sunitinib is a TKI acting on VEGFR-1-3 and PDGFR-α, -β. In 2008, a two-cohort, phase II study evaluated the efficacy of this TKI in patients with pancreatic NETs and advanced carcinoids (also including lung carcinoids, about 36% of the patients). This study reported an overall objective response rate for sunitinib higher in pancreatic tumors (16.7%) than in carcinoid tumors (2.4%). Despite its higher effects in pancreatic tumors, in both populations sunitinib was associated with a preserved quality of life. Although they could not unravel the mechanism by which this drug impacted on tumor growth, the authors hypothesized that targeting angiogenic factors could have contributed to the anti-tumor activity observed in this study (93). In a phase II study, that included 44 patients with metastatic carcinoids (4 of which with LNET as primary tumor), was observed the effect of bevacizumab, a monoclonal antibody that selectively target VEGF, and pegylated interferon-a-2b. All patients were on a stable dose of octreotide. The study was divided into 2 stages. In the first stage, patients were split into 2 groups (22 patients per group): one group received bevacizumab, the other received pegylated interferon. In the second stage, patients received both agents. Bevacizumab alone showed the most encouraging effects, as 21 of the 22 patients achieved a partial response or stable disease, while only 16 out of 22 for the other drug. Moreover, bevacizumab led to a reduction in tumor blood flow (94).

Although the impact of an angiogenesis-targeted therapy is still under investigation in LNET, the results obtained in this PhD project suggest cabozantinib as a potential candidate in the therapy of patients with highly vascularized LNET. Indeed, its fascinating outcome in

inhibiting tumor-induced angiogenesis in our zebrafish model could fit with the high vascularization of this neoplasm. Moreover, the relevant effects of cabozantinib in inhibiting tumor dissemination in our *in vivo* model could represent an enthralling strategy to prevent development of metastasis.

A potential future prospect would be to evaluate the effect of cabozantinib in reducing tumor-induced vessel disorganization. As tumor vessel are “leaky”, drug deliverance is often impaired. Some studies have recently focused on stabilizing newly formed blood vessels in order to fix this situation and improving medical therapy. Anisimov et al. designed a chimeric molecule targeting both VEGF and angiopoietin-1. This compound was able to inhibit tumor-induced angiogenesis and to promote the formation of stable vessels (95). Moreover, vascular stabilization has also been reported to improve immune state of tumor microenvironment. Normalization of blood vessels reduces the gather of immunosuppressive cells, restores proper functions of connective tissue and stimulates maturation of dendritic cells (96). For these reasons, it could be fascinating to explore these mechanisms also in LNETs, due to their high vascularization.

5.2 Medullary Thyroid Carcinoma

In MTC, sulfatinib, SPP86 and SU5402 inhibited cell viability of both TT and MZ-CRC-1 cell lines in a dose-dependent manner. While SU5402 was the drug with the milder effect in both cell lines, both SPP86 and sulfatinib showed a relevant inhibition of cell viability. Consistently, these two molecules shared a similar effect in the analysis of cell death, as both of them were able to increase the fractions of cells in early and late apoptosis and necrosis. SPP86 appeared to be the most effective compound in affecting the cell cycle. It was able to decrease the percentage of cells in S phase and in G_2/M phase for both TT and MZ-CRC-1 cell lines. *In vivo*, both sulfatinib and SPP86 were able to significantly decrease tumor-induced angiogenesis of implanted TT cells. Therefore, both sulfatinib and SPP86 potentially represent interesting compounds suitable for novel therapies in patients with MTC. SPP86 is a RET-specific inhibitor (97). Almost all patients affected by MTC are characterized by a mutation of the proto-oncogene RET (60, 98), which makes this receptor a suitable target for MTC therapy (99). Currently, cabozantinib and vandetanib are considered the first-line therapy in patients with advanced MTC (100). However, the long-term use of these two inhibitors has strong limitations mainly due to their multi-target profile, which leads to several side effects (59, 101-104). Studying molecules that specifically

address RET receptor could be of high importance to limit the onset of adverse effects. As our work showed a comparable effect between SPP86, a RET-specific inhibitor, and sulfatinib, a multi-target VEGFR and FGFR inhibitor, SPP86 is expected to have a relevant clinical role in the therapy of this tumor. In fact, targeting only RET, that is specifically mutated in MTC, could potentially prevent several side-effects limiting the long-term use of the multi-target TKIs currently approved for MTC treatment (cabozantinib and vandetanib). This year, two RET-specific molecules have been approved by the FDA for the therapy of RET-altered MTC: selpercatinib and pralsetinib (105-108). However, some cases of acquired resistance to these inhibitors have been already reported. They showed vulnerability to non-gatekeepers mutations of RET, thus conferring resistance to those tumors harbouring these mutations, such as RET G810 and L730 mutations (109, 110). In the literature there are no data about the efficacy of SPP86 in patients with advanced MTC and no specificity or resistance to particular RET mutations has been reported so far. There are only few *in vitro* studies on this compound showing a high selectivity for RET (IC_{50} of 8nM) and capacity to inhibit RET signalling in cancer cell lines at low concentrations (111, 112). For these reasons, it is not currently possible to determine whether SPP86 is more potent than selpercatinib and pralsetinib. Our study revealed promising effects on cell proliferation, cell cycle and apoptosis and cell migration *in vitro*, and a significant impact on tumor-induced angiogenesis in our *in vivo* model. Therefore, it may be interesting to compare in future the antitumor activity of SPP86 with selpercatinib and pralsetinib, including a detailed analysis on specific RET-mutations addressed by SPP86, to understand whether it could be a feasible alternative for a RET-specific therapy.

6. Conclusions

The present PhD project revealed a significant reduction of cell viability for all the TKIs tested both in LNET and MTC cell lines. This effect appeared to be mainly mediated by cell cycle modulation and induction of apoptosis. Despite sulfatinib resulted the most potent compound in terms of inhibition of LNET cell proliferation, cabozantinib showed *in vivo* the most effective impact in reducing tumor-induced angiogenesis. Consistently, cabozantinib was the only TKI able to inhibit *in vivo* the dissemination of implanted LNET cells. According to these data, cabozantinib could represent a potential candidate in the therapy of patients with highly vascularized LNET.

In MTC cell lines, SPP86 and sulfatinib displayed a similar antitumor activity both *in vitro* and *in vivo*, suggesting a good efficacy of specific RET inhibitors (SPP86) with potentially less adverse effects than multitarget TKIs.

In addition, this study showed that the zebrafish model for NETs represents an innovative tool for drug screening with several advantages compared with rodent models: rapidity of procedure, animal immune suppression is not required, lower number of tumor cells for implant and the optical transparency provides a real-time monitoring of cell-stromal interactions and cancer progression in living animals. The possibility to implant PDXs opens a promising scenario for the identification of personalized therapies in patients with advanced LNETs and MTC.

Acknowledgments

I would like to thank my tutor Prof. Giovanni Vitale for the opportunity to conduct my PhD thesis in his group. Here, I met amazing people and colleagues from whom I learned a lot and who helped me to improve as a person and a scientist.

Therefore, I am profoundly grateful to my friends and colleagues Alessandra, Germano, Silvia, and Celeste for teaching me, helping me, and supporting me.

I wish to thank all the colleagues from Istituto Auxologico Italiano and Università degli Studi di Milano.

I would like to thank Università degli Studi di Milano for the fellowship provided during my PhD project.

I would also like to thank Istituto Auxologico Italiano for the chance to work in its facilities.

My sincere thanks to my family, my parents and my brother, for the support throughout all these years.

Last but not least, I am profoundly grateful to Laura, for supporting me and putting up with me, especially for the last months of my PhD.

Thank you all.

References

1. Oronsky B, Ma PC, Morgensztern D, Carter CA. Nothing But NET: A Review of Neuroendocrine Tumors and Carcinomas. Neoplasia. 2017 Dec;19(12):991-1002. doi: 10.1016/j.neo.2017.09.002. Epub 2017 Nov 5. PMID: 29091800; PMCID: PMC5678742.
2. Dasari A, Shen C, Halperin D, Zhao B, Zhou S, Xu Y, Shih T, Yao JC. Trends in the Incidence, Prevalence, and Survival Outcomes in Patients With Neuroendocrine Tumors in the United States. JAMA Oncol. 2017 Oct 1;3(10):1335-1342. doi: 10.1001/jamaoncol.2017.0589. PMID: 28448665; PMCID: PMC5824320.
3. Kim JY, Hong SM, Ro JY. Recent updates on grading and classification of neuroendocrine tumors. Ann Diagn Pathol. 2017 Aug;29:11-16. doi: 10.1016/j.anndiagpath.2017.04.005. Epub 2017 Apr 13. PMID: 28807335.
4. Klöppel G. Neuroendocrine Neoplasms: Dichotomy, Origin and Classifications. Visc Med. 2017 Oct;33(5):324-330. doi: 10.1159/000481390. Epub 2017 Oct 16. PMID: 29177160; PMCID: PMC5697503.
5. Apostolidis L, Dal Buono A, Merola E, Jann H, Jäger D, Wiedenmann B, Winkler EC, Pavel M. Multicenter Analysis of Treatment Outcomes for Systemic Therapy in Well Differentiated Grade 3 Neuroendocrine Tumors (NET G3). Cancers (Basel). 2021 Apr 16;13(8):1936. doi: 10.3390/cancers13081936. PMID: 33923759; PMCID: PMC8073753.
6. Assarzadegan N, Montgomery E. What is New in the 2019 World Health Organization (WHO) Classification of Tumors of the Digestive System: Review of Selected Updates on Neuroendocrine Neoplasms, Appendiceal Tumors, and Molecular Testing. Arch Pathol Lab Med. 2021 Jun 1;145(6):664-677. doi: 10.5858/arpa.2019-0665-RA. PMID: 32233993.
7. Vesterinen T, Säilä J, Blom S, Pennanen M, Leijon H, Arola J. Automated assessment of Ki-67 proliferation index in neuroendocrine tumors by deep learning. APMIS. 2022 Jan;130(1):11-20. doi: 10.1111/apm.13190. Epub 2021 Nov 22. PMID: 34741788.
8. Chen H, Sippel RS, O'Dorisio MS, Vinik AI, Lloyd RV, Pacak K; North American Neuroendocrine Tumor Society (NANETS). The North American Neuroendocrine Tumor Society consensus guideline for the diagnosis and management of neuroendocrine tumors: pheochromocytoma, paraganglioma, and medullary thyroid

cancer. Pancreas. 2010 Aug;39(6):775-83. doi: 10.1097/MPA.0b013e3181ebb4f0. PMID: 20664475; PMCID: PMC3419007.

9. Bohnenberger H, Dinter H, König A, Ströbel P. Neuroendocrine tumors of the thymus and mediastinum. J Thorac Dis. 2017 Nov;9(Suppl 15):S1448-S1457. doi: 10.21037/jtd.2017.02.02. PMID: 29201448; PMCID: PMC5690954.
10. Fine SW. Neuroendocrine tumors of the prostate. Mod Pathol. 2018 Jan;31(S1):S122-132. doi: 10.1038/modpathol.2017.164. PMID: 29297494.
11. Kefeli M, Usubütün A. An Update of Neuroendocrine Tumors of the Female Reproductive System. Turk Patoloji Derg. 2015;31 Suppl 1:128-44. doi: 10.5146/tjpath.2015.01320. PMID: 26177323.
12. Filosso P.L., Fontana E.C., Roffinella M. (2021) Primary Neuroendocrine Tumors of the Lung. In: Cloyd J.M., Pawlik T.M. (eds) Neuroendocrine Tumors. Springer, Cham. https://doi.org/10.1007/978-3-030-62241-1_13
13. Rekhtman N. Neuroendocrine tumors of the lung: an update. Arch Pathol Lab Med. 2010 Nov;134(11):1628-38. doi: 10.5858/2009-0583-RAR.1. PMID: 21043816.
14. Metovic J, Barella M, Bianchi F, Hofman P, Hofman V, Remmelink M, Kern I, Carvalho L, Pattini L, Sonzogni A, Veronesi G, Harari S, Forest F, Papotti M, Pelosi G. Morphologic and molecular classification of lung neuroendocrine neoplasms. Virchows Arch. 2021 Jan;478(1):5-19. doi: 10.1007/s00428-020-03015-z. Epub 2021 Jan 21. PMID: 33474631; PMCID: PMC7966641.
15. Fisseler-Eckhoff A, Demes M. Neuroendocrine tumors of the lung. Cancers (Basel). 2012 Jul 31;4(3):777-98. doi: 10.3390/cancers4030777. PMID: 24213466; PMCID: PMC3712715.
16. Uccella S, La Rosa S, Metovic J, Marchiori D, Scoazec JY, Volante M, Mete O, Papotti M. Genomics of High-Grade Neuroendocrine Neoplasms: Well-Differentiated Neuroendocrine Tumor with High-Grade Features (G3 NET) and Neuroendocrine Carcinomas (NEC) of Various Anatomic Sites. Endocr Pathol. 2021 Mar;32(1):192-210. doi: 10.1007/s12022-020-09660-z. Epub 2021 Jan 12. PMID: 33433884.
17. Borczuk AC. Pulmonary Neuroendocrine Tumors. Surg Pathol Clin. 2020 Mar;13(1):35-55. doi: 10.1016/j.path.2019.10.002. Epub 2019 Nov 29. PMID: 32005434.
18. Volante M, Mete O, Pelosi G, Roden AC, Speel EJM, Uccella S. Molecular Pathology of Well-Differentiated Pulmonary and Thymic Neuroendocrine Tumors: What Do Pathologists Need to Know? Endocr Pathol. 2021 Mar;32(1):154-168. doi:

10.1007/s12022-021-09668-z. Epub 2021 Feb 27. PMID: 33641055; PMCID: PMC7960615.

19. Baloch ZW, LiVolsi VA. Neuroendocrine tumors of the thyroid gland. Am J Clin Pathol. 2001 Jun;115 Suppl: S56-67. doi: 10.1309/7NK9-VUAL-9WU2-KJ19. PMID: 11993691.
20. Thomas CM, Asa SL, Ezzat S, Sawka AM, Goldstein D. Diagnosis and pathologic characteristics of medullary thyroid carcinoma-review of current guidelines. Curr Oncol. 2019 Oct;26(5):338-344. doi: 10.3747/co.26.5539. Epub 2019 Oct 1. PMID: 31708652; PMCID: PMC6821118.
21. Araque KA, Gubbi S, Klubo-Gwiezdzinska J. Updates on the Management of Thyroid Cancer. Horm Metab Res. 2020 Aug;52(8):562-577. doi: 10.1055/a-1089-7870. Epub 2020 Feb 10. PMID: 32040962; PMCID: PMC7415555.
22. Larouche V, Akirov A, Thomas CM, Krzyzanowska MK, Ezzat S. A primer on the genetics of medullary thyroid cancer. Curr Oncol. 2019 Dec;26(6):389-394. doi: 10.3747/co.26.5553. Epub 2019 Dec 1. PMID: 31896937; PMCID: PMC6927790.
23. Murakumo Y, Jijiwa M, Asai N, Ichihara M, Takahashi M. RET and neuroendocrine tumors. Pituitary. 2006;9(3):179-92. doi: 10.1007/s11102-006-0263-4. PMID: 17036197.
24. Asa SL, Mete O (2016) Cytology and Pathology: Pitfalls and Challenges. In: Wang TS, Evans DB (eds) Medullary Thyroid Cancer. Chapter 4. Springer International Publishing Switzerland, pp 33–45.
25. Xu B, Fuchs TL, Ahmadi S, Alghamdi M, Alzumaili B, Bani MA, Baudin E, Chou A, De Leo A, Fagin JA, Ganly I, Glover A, Hartl D, Kanaan C, Khneisser P, Najdawi F, Nigam A, Papachristos A, Repaci A, Spanheimer PM, Solaroli E, Untch BR, Barletta JA, Tallini G, Al Ghuzlan A, Gill AJ, Ghossein RA. International Medullary Thyroid Carcinoma Grading System: A Validated Grading System for Medullary Thyroid Carcinoma. J Clin Oncol. 2021 Nov 3: JCO2101329. doi: 10.1200/JCO.21.01329. Epub ahead of print. PMID: 34731032. Gustafsson BI, Kidd M, Modlin IM. Neuroendocrine tumors of the diffuse neuroendocrine system. Curr Opin Oncol. 2008 Jan;20(1):1-12. doi: 10.1097/CCO.0b013e3282f1c595. PMID: 18043250.
26. Melosky B. Advanced typical and atypical carcinoid tumours of the lung: management recommendations. Curr Oncol. 2018 Jun;25(Suppl 1):S86-S93. doi: 10.3747/co.25.3808. Epub 2018 Jun 13. PMID: 29910651; PMCID: PMC6001761.

27. Barletta JA, Nosé V, Sadow PM. Genomics and Epigenomics of Medullary Thyroid Carcinoma: From Sporadic Disease to Familial Manifestations. Endocr Pathol. 2021 Mar;32(1):35-43. doi: 10.1007/s12022-021-09664-3. Epub 2021 Jan 25. PMID: 33492588.
28. Gustafsson BI, Kidd M, Modlin IM. Neuroendocrine tumors of the diffuse neuroendocrine system. Curr Opin Oncol. 2008 Jan;20(1):1-12. doi: 10.1097/CCO.0b013e3282f1c595. PMID: 18043250.
29. Gatto F, Hofland LJ. The role of somatostatin and dopamine D2 receptors in endocrine tumors. Endocr Relat Cancer. 2011 Dec 1;18(6):R233-51. doi: 10.1530/ERC-10-0334. PMID: 22135243.
30. Sullivan I, Le Teuff G, Guigay J, Caramella C, Berdelou A, Leboulleux S, Déandréis D, Hadoux J, Ducreux M, Duvillard P, Adam J, Scoazec JY, Baudin E, Planchard D. Antitumour activity of somatostatin analogues in sporadic, progressive, metastatic pulmonary carcinoids. Eur J Cancer. 2017 Apr; 75:259-267. doi: 10.1016/j.ejca.2016.11.034. Epub 2017 Feb 27. PMID: 28242503.
31. Bongiovanni A, Recine F, Riva N, Foca F, Liverani C, Mercatali L, Nicolini S, Pieri F, Amadori D, Ibrahim T. Outcome Analysis of First-line Somatostatin Analog Treatment in Metastatic Pulmonary Neuroendocrine Tumors and Prognostic Significance of 18FDG-PET/CT. Clin Lung Cancer. 2017 Jul;18(4):415-420. doi: 10.1016/j.cllc.2016.11.004. Epub 2016 Nov 21. PMID: 27956089.
32. Smid WM, Dullaart RP. Octreotide for medullary thyroid carcinoma associated diarrhoea. Neth J Med. 1992 Jun;40(5-6):240-3. PMID: 1436261.
33. Vitale G, Tagliaferri P, Caraglia M, Rampone E, Ciccarelli A, Bianco AR, Abbruzzese A, Lupoli G. Slow release lanreotide in combination with interferon-alpha2b in the treatment of symptomatic advanced medullary thyroid carcinoma. J Clin Endocrinol Metab. 2000 Mar;85(3):983-8. doi: 10.1210/jcem.85.3.6435. PMID: 10720027.
34. Díez JJ, Iglesias P. Somatostatin analogs in the treatment of medullary thyroid carcinoma. J Endocrinol Invest. 2002 Oct;25(9):773-8. doi: 10.1007/BF03345511. PMID: 12398235.
35. Vitale G, Lupoli G, Guarrasi R, Colao A, Dicitore A, Gaudenzi G, Misso G, Castellano M, Addeo R, Facchini G, Del Prete S, Caraglia M. Interleukin-2 and lanreotide in the treatment of medullary thyroid cancer: in vitro and in vivo studies. J Clin Endocrinol Metab. 2013 Oct;98(10): E1567-74. doi: 10.1210/jc.2013-1443. Epub 2013 Jul 24. PMID: 23884781.

36. Faggiano A, Modica R, Severino R, Camera L, Fonti R, Del Prete M, Chiofalo MG, Aria M, Ferolla P, Vitale G, Pezzullo L, Colao A. The antiproliferative effect of pasireotide LAR alone and in combination with everolimus in patients with medullary thyroid cancer: a single-center, open-label, phase II, proof-of-concept study. Endocrine. 2018 Oct;62(1):46-56. doi: 10.1007/s12020-018-1583-7. Epub 2018 Mar 23. PMID: 29572709.
37. Liu Q, Zang J, Sui H, Ren J, Guo H, Wang H, Wang R, Jacobson O, Zhang J, Cheng Y, Zhu Z, Chen X. Peptide Receptor Radionuclide Therapy of Late-Stage Neuroendocrine Tumor Patients with Multiple Cycles of 177Lu-DOTA-EB-TATE. J Nucl Med. 2021 Mar;62(3):386-392. doi: 10.2967/jnumed.120.248658. Epub 2020 Aug 21. Erratum in: J Nucl Med. 2021 Jul 1;62(7):1015. PMID: 32826319; PMCID: PMC8049339.
38. Mittra ES. Neuroendocrine Tumor Therapy: 177Lu-DOTATATE. AJR Am J Roentgenol. 2018 Aug;211(2):278-285. doi: 10.2214/AJR.18.19953. Epub 2018 Jun 27. PMID: 29949416.
39. Zidan L, Iravani A, Oleinikov K, Ben-Haim S, Gross DJ, Meirovitz A, Maimon O, Akhurst T, Michael M, Hicks RJ, Grozinsky-Glasberg S, Kong G. Efficacy and safety of 177Lu-DOTATATE in lung neuroendocrine tumors: a bi-center study. J Nucl Med. 2021 May 28: jnumed.120.260760. doi: 10.2967/jnumed.120.260760. Epub ahead of print. PMID: 34049983.
40. Camus B, Cottereau AS, Palmieri LJ, Dermine S, Tenenbaum F, Brezault C, Coriat R. Indications of Peptide Receptor Radionuclide Therapy (PRRT) in Gastroenteropancreatic and Pulmonary Neuroendocrine Tumors: An Updated Review. J Clin Med. 2021 Mar 18;10(6):1267. doi: 10.3390/jcm10061267. PMID: 33803817; PMCID: PMC8003169.
41. Satapathy S, Mittal BR, Sood A, Verma R, Panda N. Efficacy and safety of concomitant 177Lu-DOTATATE and low-dose capecitabine in advanced medullary thyroid carcinoma: a single-centre experience. Nucl Med Commun. 2020 Jul;41(7):629-635. doi: 10.1097/MNM.0000000000001205. PMID: 32371670.
42. Maghsoomi Z, Emami Z, Malboosbaf R, Malek M, Khamseh ME. Efficacy and safety of peptide receptor radionuclide therapy in advanced radioiodine-refractory differentiated thyroid cancer and metastatic medullary thyroid cancer: a systematic review. BMC Cancer. 2021 May 20;21(1):579. doi: 10.1186/s12885-021-08257-x. PMID: 34016077; PMCID: PMC8139052.

43. Fazio N, Buzzoni R, Delle Fave G, Tesselaar ME, Wolin E, Van Cutsem E, Tomassetti P, Strosberg J, Voi M, Bubuteishvili-Pacaud L, Ridolfi A, Herbst F, Tomasek J, Singh S, Pavel M, Kulke MH, Valle JW, Yao JC. Everolimus in advanced, progressive, well-differentiated, non-functional neuroendocrine tumors: RADIANT-4 lung subgroup analysis. Cancer Sci. 2018 Jan;109(1):174-181. doi: 10.1111/cas.13427. Epub 2017 Nov 9. PMID: 29055056; PMCID: PMC5765303.
44. Lim SM, Chang H, Yoon MJ, Hong YK, Kim H, Chung WY, Park CS, Nam KH, Kang SW, Kim MK, Kim SB, Lee SH, Kim HG, Na II, Kim YS, Choi MY, Kim JG, Park KU, Yun HJ, Kim JH, Cho BC. A multicenter, phase II trial of everolimus in locally advanced or metastatic thyroid cancer of all histologic subtypes. Ann Oncol. 2013 Dec;24(12):3089-94. doi: 10.1093/annonc/mdt379. Epub 2013 Sep 19. PMID: 24050953.
45. Vitale G, Dicitore A, Pepe D, Gentilini D, Grassi ES, Borghi MO, Gelmini G, Cantone MC, Gaudenzi G, Misso G, Di Blasio AM, Hofland LJ, Caraglia M, Persani L. Synergistic activity of everolimus and 5-aza-2'-deoxycytidine in medullary thyroid carcinoma cell lines. Mol Oncol. 2017 Aug;11(8):1007-1022. doi: 10.1002/1878-0261.12070. Epub 2017 Jun 21. PMID: 28453190; PMCID: PMC5537710.
46. Baudin, Berruti, A., Giuliano, M., Mansoor, W., Bobirca, C., Houtsma, E., Fagan, N., Oberg, K. E., & Ferolla, P. (2021). First long-term results on efficacy and safety of long-acting pasireotide in combination with everolimus in patients with advanced carcinoids (NET) of the lung/thymus: Phase II LUNA trial. Journal of Clinical Oncology, 39(15_suppl), 8574–8574. https://doi.org/10.1200/JCO.2021.39.15_suppl.8574
47. Links TP, Verbeek HH, Hofstra RM, Plukker JT. Endocrine tumours: progressive metastatic medullary thyroid carcinoma: first- and second-line strategies. Eur J Endocrinol. 2015 Jun;172(6): R241-51. doi: 10.1530/EJE-14-0726. Epub 2015 Jan 27. PMID: 25627652.
48. Baudin E, Caplin M, Garcia-Carbonero R, Fazio N, Ferolla P, Filosso PL, Frilling A, de Herder WW, Hörsch D, Knigge U, Korse CM, Lim E, Lombard-Bohas C, Pavel M, Scoazec JY, Sundin A, Berruti A; ESMO Guidelines Committee. Electronic address: clinicalguidelines@esmo.org. Lung and thymic carcinoids: ESMO Clinical Practice Guidelines for diagnosis, treatment and follow-up☆. Ann Oncol. 2021 Apr;32(4):439-451. doi: 10.1016/j.annonc.2021.01.003. Epub 2021 Jan 19. Erratum in: Ann Oncol. 2021 Nov;32(11):1453-1455. PMID: 33482246.

49. Kander EM, Shah MH, Zhou Y, Goyal A, Palmer JD, Owen DH, Shilo K, Patel G, Raval RR, Gonzalez J, Nguyen M, Olek E, Kherani J, Rothenberg SM, Konda B. Response to the Selective RET Inhibitor Selpercatinib (LOXO-292) in a Patient With RET Fusion-positive Atypical Lung Carcinoid. Clin Lung Cancer. 2021 May;22(3): e442-e445. doi: 10.1016/j.cllc.2020.06.011. Epub 2020 Jun 18. PMID: 32660930.
50. Chen YQ, Li YF, Zhang CY, Zhang SL, Lv ZY, Dong S, Chen HJ, Zhang XC, Wu YL, Yang JJ. Response to Icotinib Plus Chemotherapy in Pulmonary Atypical Carcinoid Harboring the EGFR L858R Mutation: A Brief Report. JTO Clin Res Rep. 2021 Nov 19;2(12):100258. doi: 10.1016/j.jtocrr.2021.100258. PMID: 34917992; PMCID: PMC8668983.
51. Drpa G, Sreter KB, Manojlovic S, Kukulj S. Erlotinib for coexisting typical bronchial carcinoid and advanced lung adenocarcinoma: does the epidermal growth factor receptor mutation status matter? Anticancer Drugs. 2018 Mar;29(3):281-285. doi: 10.1097/CAD.0000000000000587. PMID: 29280916.
52. Wells SA Jr, Robinson BG, Gagel RF, Dralle H, Fagin JA, Santoro M, Baudin E, Elisei R, Jarzab B, Vasselli JR, Read J, Langmuir P, Ryan AJ, Schlumberger MJ. Vandetanib in patients with locally advanced or metastatic medullary thyroid cancer: a randomized, double-blind phase III trial. J Clin Oncol. 2012 Jan 10;30(2):134-41. doi: 10.1200/JCO.2011.35.5040. Epub 2011 Oct 24. Erratum in: J Clin Oncol. 2013 Aug 20;31(24):3049. PMID: 22025146; PMCID: PMC3675689.
53. Ton GN, Banaszynski ME, Kolesar JM. Vandetanib: a novel targeted therapy for the treatment of metastatic or locally advanced medullary thyroid cancer. Am J Health Syst Pharm. 2013 May 15;70(10):849-55. doi: 10.2146/ajhp120253. PMID: 23640345.
54. Yakes FM, Chen J, Tan J, Yamaguchi K, Shi Y, Yu P, Qian F, Chu F, Bentzien F, Cancilla B, Orf J, You A, Laird AD, Engst S, Lee L, Lesch J, Chou YC, Joly AH. Cabozantinib (XL184), a novel MET and VEGFR2 inhibitor, simultaneously suppresses metastasis, angiogenesis, and tumor growth. Mol Cancer Ther. 2011 Dec;10(12):2298-308. doi: 10.1158/1535-7163.MCT-11-0264. Epub 2011 Sep 16. PMID: 21926191.
55. Bentzien F, Zuzow M, Heald N, Gibson A, Shi Y, Goon L, Yu P, Engst S, Zhang W, Huang D, Zhao L, Vysotskaia V, Chu F, Bautista R, Cancilla B, Lamb P, Joly AH, Yakes FM. In vitro and in vivo activity of cabozantinib (XL184), an inhibitor of RET, MET, and VEGFR2, in a model of medullary thyroid cancer. Thyroid. 2013

Dec;23(12):1569-77. doi: 10.1089/thy.2013.0137. Epub 2013 Sep 17. PMID: 23705946; PMCID: PMC3868259.

56. Sherman EJ, Wirth LJ, Shah MH, Cabanillas ME, Robinson B, Laskin JJ, Kroiss M, Subbiah V, Drilon AE, Wright J, Soldatenkova V, French PP, Italiano, A, Weiler D. Selpercatinib efficacy and safety in patients with RET-altered thyroid cancer: A clinical trial update. Journal of clinical oncology, 2021-05-20, Vol.39 (15_suppl), p.6073-6073
57. U.S. Food & Drug Administration. FDA approves selpercatinib for lung and thyroid cancers with RET gene mutations or fusions. Available at: https://www.fda.gov/drugs/resources-information-approved-drugs/fda-approves-selpercatinib-lung-and-thyroid-cancers-ret-gene-mutations-or-fusions
58. Cabanillas ME, Habra MA. Lenvatinib: Role in thyroid cancer and other solid tumors. Cancer Treat Rev. 2016 Jan;42:47-55. doi: 10.1016/j.ctrv.2015.11.003. Epub 2015 Dec 2. PMID: 26678514.
59. Holden SN, Eckhardt SG, Basser R, de Boer R, Rischin D, Green M, Rosenthal MA, Wheeler C, Barge A, Hurwitz HI. Clinical evaluation of ZD6474, an orally active inhibitor of VEGF and EGF receptor signaling, in patients with solid, malignant tumors. Ann Oncol. 2005 Aug;16(8):1391-7. doi: 10.1093/annonc/mdi247. Epub 2005 May 19. PMID: 15905307.
60. Pacini F, Elisei R, Romei C, Pinchera A. RET proto-oncogene mutations in thyroid carcinomas: clinical relevance. J Endocrinol Invest. 2000 May;23(5):328-38. doi: 10.1007/BF03343732. PMID: 10882153.
61. Nishida N, Yano H, Nishida T, Kamura T, Kojiro M. Angiogenesis in cancer. Vasc Health Risk Manag. 2006;2(3):213-9. doi: 10.2147/vhrm.2006.2.3.213. PMID: 17326328; PMCID: PMC1993983.
62. Lugano R, Ramachandran M, Dimberg A. Tumor angiogenesis: causes, consequences, challenges and opportunities. Cell Mol Life Sci. 2020 May;77(9):1745-1770. doi: 10.1007/s00018-019-03351-7. Epub 2019 Nov 6. PMID: 31690961; PMCID: PMC7190605.
63. Majidpoor J, Mortezaee K. Angiogenesis as a hallmark of solid tumors - clinical perspectives. Cell Oncol (Dordr). 2021 Aug;44(4):715-737. doi: 10.1007/s13402-021-00602-3. Epub 2021 Apr 9. PMID: 33835425.
64. Marion-Audibert AM, Vullierme MP, Ronot M, Mabrut JY, Sauvanet A, Zins M, Cuilleron M, Sa-Cunha A, Lévy P, Rode A. Routine MRI With DWI Sequences to

Detect Liver Metastases in Patients With Potentially Resectable Pancreatic Ductal Carcinoma and Normal Liver CT: A Prospective Multicenter Study. AJR Am J Roentgenol. 2018 Nov;211(5):W217-W225. doi: 10.2214/AJR.18.19640. Epub 2018 Sep 21. PMID: 30240298.

65. Teulé A, Casanovas O. Relevance of angiogenesis in neuroendocrine tumors. Target Oncol. 2012 Jun;7(2):93-8. doi: 10.1007/s11523-012-0217-x. Epub 2012 May 17. PMID: 22592949.
66. Scoazec JY. Angiogenesis in neuroendocrine tumors: therapeutic applications. Neuroendocrinology. 2013;97(1):45-56. doi: 10.1159/000338371. Epub 2012 Jun 7. PMID: 22538258.
67. Lopes-Coelho F, Martins F, Pereira SA, Serpa J. Anti-Angiogenic Therapy: Current Challenges and Future Perspectives. Int J Mol Sci. 2021 Apr 5;22(7):3765. doi: 10.3390/ijms22073765. PMID: 33916438; PMCID: PMC8038573.
68. Raymond E, Dahan L, Raoul JL, Bang YJ, Borbath I, Lombard-Bohas C, Valle J, Metrakos P, Smith D, Vinik A, Chen JS, Hörsch D, Hammel P, Wiedenmann B, Van Cutsem E, Patyna S, Lu DR, Blanckmeister C, Chao R, Ruszniewski P. Sunitinib malate for the treatment of pancreatic neuroendocrine tumors. N Engl J Med. 2011 Feb 10;364(6):501-13. doi: 10.1056/NEJMoa1003825. Erratum in: N Engl J Med. 2011 Mar 17;364(11):1082. PMID: 21306237.
69. Raymond E, Kulke MH, Qin S, Yu X, Schenker M, Cubillo A, Lou W, Tomasek J, Thiis-Evensen E, Xu JM, Croitoru AE, Khasraw M, Sedlackova E, Borbath I, Ruff P, Oberstein PE, Ito T, Jia L, Hammel P, Shen L, Shrikhande SV, Shen Y, Sufliarsky J, Khan GN, Morizane C, Galdy S, Khosravan R, Fernandez KC, Rosbrook B, Fazio N. Efficacy and Safety of Sunitinib in Patients with Well-Differentiated Pancreatic Neuroendocrine Tumours. Neuroendocrinology. 2018;107(3):237-245. doi: 10.1159/000491999. Epub 2018 Jul 10. PMID: 29991024.
70. Fazio N, Kulke M, Rosbrook B, Fernandez K, Raymond E. Updated Efficacy and Safety Outcomes for Patients with Well-Differentiated Pancreatic Neuroendocrine Tumors Treated with Sunitinib. Target Oncol. 2021 Jan;16(1):27-35. doi: 10.1007/s11523-020-00784-0. Epub 2021 Jan 7. PMID: 33411058; PMCID: PMC7810649.
71. Carra S, Gaudenzi G, Dicitore A, Saronni D, Cantone MC, Plebani A, Ghilardi A, Borghi MO, Hofland LJ, Persani L, Vitale G. Vandetanib versus Cabozantinib in Medullary Thyroid Carcinoma: A Focus on Anti-Angiogenic Effects in Zebrafish

Model. Int J Mol Sci. 2021 Mar 16;22(6):3031. doi: 10.3390/ijms22063031. PMID: 33809722; PMCID: PMC8002338.

72. Mokhtari RB, Qorri B, Baluch N, Sparaneo A, Fabrizio FP, Muscarella LA, Tyker A, Kumar S, Cheng HM, Szewczuk MR, Das B, Yeger H. Next-generation multimodality of nutrigenomic cancer therapy: sulforaphane in combination with acetazolamide actively target bronchial carcinoid cancer in disabling the PI3K/Akt/mTOR survival pathway and inducing apoptosis. Oncotarget. 2021 Jul 20;12(15):1470-1489. doi: 10.18632/oncotarget.28011. PMID: 34316328; PMCID: PMC8310668.
73. Hason M, Bartůněk P. Zebrafish Models of Cancer-New Insights on Modeling Human Cancer in a Non-Mammalian Vertebrate. Genes (Basel). 2019 Nov 15;10(11):935. doi: 10.3390/genes10110935. PMID: 31731811; PMCID: PMC6896156.
74. Avdesh A, Chen M, Martin-Iverson MT, Mondal A, Ong D, Rainey-Smith S, Taddei K, Lardelli M, Groth DM, Verdile G, Martins RN. Regular care and maintenance of a zebrafish (Danio rerio) laboratory: an introduction. J Vis Exp. 2012 Nov 18;(69): e4196. doi: 10.3791/4196. PMID: 23183629; PMCID: PMC3916945.
75. Willemsen R, Padje S, van Swieten JC, Oostra BA (2011) Zebrafish (Danio rerio) as a Model Organism for Dementia. In: De Deyn P., Van Dam D. (eds) Animal Models of Dementia. Neuromethods, vol 48. Humana Press. https://doi.org/10.1007/978-1-60761-898-0_14
76. Fazio M, Ablain J, Chuan Y, Langenau DM, Zon LI. Zebrafish patient avatars in cancer biology and precision cancer therapy. Nat Rev Cancer. 2020 May;20(5):263-273. doi: 10.1038/s41568-020-0252-3. Epub 2020 Apr 6. PMID: 32251397; PMCID: PMC8011456.
77. White R, Rose K, Zon L. Zebrafish cancer: the state of the art and the path forward. Nat Rev Cancer. 2013 Sep;13(9):624-36. doi: 10.1038/nrc3589. PMID: 23969693; PMCID: PMC6040891.
78. Wyatt RA, Trieu NPV, Crawford BD. Zebrafish Xenograft: An Evolutionary Experiment in Tumour Biology. Genes (Basel). 2017 Sep 5;8(9):220. doi: 10.3390/genes8090220. PMID: 28872594; PMCID: PMC5615353.
79. Haldi M, Ton C, Seng WL, McGrath P. Human melanoma cells transplanted into zebrafish proliferate, migrate, produce melanin, form masses and stimulate angiogenesis in zebrafish. Angiogenesis. 2006;9(3):139-51. doi: 10.1007/s10456-006-9040-2. Epub 2006 Oct 19. PMID: 17051341.

80. Vitale G, Gaudenzi G, Dicitore A, Cotelli F, Ferone D, Persani L. Zebrafish as an innovative model for neuroendocrine tumors. Endocr Relat Cancer. 2014 Jan 21;21(1):R67-83. doi: 10.1530/ERC-13-0388. PMID: 24292602.
81. Gaudenzi G, Albertelli M, Dicitore A, Würth R, Gatto F, Barbieri F, Cotelli F, Florio T, Ferone D, Persani L, Vitale G. Patient-derived xenograft in zebrafish embryos: a new platform for translational research in neuroendocrine tumors. Endocrine. 2017 Aug;57(2):214-219. doi: 10.1007/s12020-016-1048-9. Epub 2016 Aug 2. PMID: 27481363.
82. Dicitore A, Cantone MC, Gaudenzi G, Saronni D, Carra S, Borghi MO, Albertelli M, Ferone D, Hofland LJ, Persani L, Vitale G. Efficacy of a Novel Second-Generation Somatostatin-Dopamine Chimera (TBR-065) in Human Medullary Thyroid Cancer: A Preclinical Study. Neuroendocrinology. 2021;111(10):937-950. doi: 10.1159/000512366. Epub 2020 Oct 19. PMID: 33075795.
83. Dicitore A, Saronni D, Gaudenzi G, Carra S, Cantone MC, Borghi MO, Persani L, Vitale G. Long-term effects of somatostatin analogues in rat GH-secreting pituitary tumor cell lines. J Endocrinol Invest. 2021 Jun 14. doi: 10.1007/s40618-021-01609-1. Epub ahead of print. PMID: 34128215.
84. Li XY, Huang LT, Wu JQ, He MF, Zhu SH, Zhan P, Lv TF, Song Y. Zebrafish Xenograft Model of Human Lung Cancer for Evaluating Osimertinib Resistance. Biomed Res Int. 2019 Jun 27; 2019:3129748. doi: 10.1155/2019/3129748. PMID: 31346515; PMCID: PMC6620834.
85. Lawson ND, Weinstein BM. In vivo imaging of embryonic vascular development using transgenic zebrafish. Dev Biol. 2002 Aug 15;248(2):307-18. doi: 10.1006/dbio.2002.0711. PMID: 12167406.
86. Cirello V, Gaudenzi G, Grassi ES, Colombo C, Vicentini L, Ferrero S, Persani L, Vitale G, Fugazzola L. Tumor and normal thyroid spheroids: from tissues to zebrafish. Minerva Endocrinol. 2018 Mar;43(1):1-10. doi: 10.23736/S0391-1977.17.02610-4. Epub 2017 Jan 31. PMID: 28146140.
87. Dong M, Phan AT, Yao JC. New strategies for advanced neuroendocrine tumors in the era of targeted therapy. Clin Cancer Res. 2012 Apr 1;18(7):1830-6. doi: 10.1158/1078-0432.CCR-11-2105. Epub 2012 Feb 15. PMID: 22338018.
88. Mansoori B, Mohammadi A, Davudian S, Shirjang S, Baradaran B. The Different Mechanisms of Cancer Drug Resistance: A Brief Review. Adv Pharm Bull. 2017

Sep;7(3):339-348. doi: 10.15171/apb.2017.041. Epub 2017 Sep 25. PMID: 29071215; PMCID: PMC5651054.

89. Sartelet H, Decaussin M, Devouassoux G, Nawrocki-Raby B, Brichon PY, Brambilla C, Brambilla E. Expression of vascular endothelial growth factor (VEGF) and its receptors (VEGF-R1 [Flt-1] and VEGF-R2 [KDR/Flk-1]) in tumorlets and in neuroendocrine cell hyperplasia of the lung. Hum Pathol. 2004 Oct;35(10):1210-7. doi: 10.1016/j.humpath.2004.07.009. PMID: 15492987.
90. Yao JC. Neuroendocrine tumors. Molecular targeted therapy for carcinoid and islet-cell carcinoma. Best Pract Res Clin Endocrinol Metab. 2007 Mar;21(1):163-72. doi: 10.1016/j.beem.2007.01.006. PMID: 17382271.
91. Capp C, Wajner SM, Siqueira DR, Brasil BA, Meurer L, Maia AL. Increased expression of vascular endothelial growth factor and its receptors, VEGFR-1 and VEGFR-2, in medullary thyroid carcinoma. Thyroid. 2010 Aug;20(8):863-71. doi: 10.1089/thy.2009.0417. PMID: 20615131.
92. Piro R, Tonelli R, Taddei S, Marchioni A, Musci G, Clini E, Facciolongo N. Atypical diagnosis for typical lung carcinoid. BMC Pulm Med. 2019 Sep 2;19(1):168. doi: 10.1186/s12890-019-0929-0. PMID: 31477066; PMCID: PMC6719370.
93. Kulke MH, Lenz HJ, Meropol NJ, Posey J, Ryan DP, Picus J, Bergsland E, Stuart K, Tye L, Huang X, Li JZ, Baum CM, Fuchs CS. Activity of sunitinib in patients with advanced neuroendocrine tumors. J Clin Oncol. 2008 Jul 10;26(20):3403-10. doi: 10.1200/JCO.2007.15.9020. PMID: 18612155.
94. Yao JC, Phan A, Hoff PM, Chen HX, Charnsangavej C, Yeung SC, Hess K, Ng C, Abbruzzese JL, Ajani JA. Targeting vascular endothelial growth factor in advanced carcinoid tumor: a random assignment phase II study of depot octreotide with bevacizumab and pegylated interferon alpha-2b. J Clin Oncol. 2008 Mar 10;26(8):1316-23. doi: 10.1200/JCO.2007.13.6374. PMID: 18323556.
95. Anisimov A, Tvorogov D, Alitalo A, Leppänen VM, An Y, Han EC, Orsenigo F, Gaál EI, Holopainen T, Koh YJ, Tammela T, Korpisalo P, Keskitalo S, Jeltsch M, Ylä-Herttuala S, Dejana E, Koh GY, Choi C, Saharinen P, Alitalo K. Vascular endothelial growth factor-angiopoietin chimera with improved properties for therapeutic angiogenesis. Circulation. 2013 Jan 29;127(4):424-34. doi: 10.1161/CIRCULATIONAHA.112.127472. PMID: 23357661.

96. Zheng R, Li F, Li F, Gong A. Targeting tumor vascularization: promising strategies for vascular normalization. J Cancer Res Clin Oncol. 2021 Sep;147(9):2489-2505. doi: 10.1007/s00432-021-03701-8. Epub 2021 Jun 19. PMID: 34148156.
97. Alao JP, Michlikova S, Dinér P, Grøtli M, Sunnerhagen P. Selective inhibition of RET mediated cell proliferation *in vitro* by the kinase inhibitor SPP86. BMC Cancer. 2014 Nov 20;14:853. doi: 10.1186/1471-2407-14-853. PMID: 25409876; PMCID: PMC4252022.
98. Wohllk N, Cote GJ, Bugalho MM, Ordonez N, Evans DB, Goepfert H, Khorana S, Schultz P, Richards CS, Gagel RF. Relevance of RET proto-oncogene mutations in sporadic medullary thyroid carcinoma. J Clin Endocrinol Metab. 1996 Oct;81(10):3740-5. doi: 10.1210/jcem.81.10.8855832. PMID: 8855832.
99. Thein KZ, Velcheti V, Mooers BHM, Wu J, Subbiah V. Precision therapy for RET-altered cancers with RET inhibitors. Trends Cancer. 2021 Dec;7(12):1074-1088. doi: 10.1016/j.trecan.2021.07.003. Epub 2021 Aug 12. PMID: 34391699; PMCID: PMC8599646.
100. Kim M, Kim BH. Current Guidelines for Management of Medullary Thyroid Carcinoma. Endocrinol Metab (Seoul). 2021 Jun;36(3):514-524. doi: 10.3803/EnM.2021.1082. Epub 2021 Jun 22. PMID: 34154310; PMCID: PMC8258323.
101. Thornton K, Kim G, Maher VE, Chattopadhyay S, Tang S, Moon YJ, Song P, Marathe A, Balakrishnan S, Zhu H, Garnett C, Liu Q, Booth B, Gehrke B, Dorsam R, Verbois L, Ghosh D, Wilson W, Duan J, Sarker H, Miksinski SP, Skarupa L, Ibrahim A, Justice R, Murgo A, Pazdur R. Vandetanib for the treatment of symptomatic or progressive medullary thyroid cancer in patients with unresectable locally advanced or metastatic disease: U.S. Food and Drug Administration drug approval summary. Clin Cancer Res. 2012 Jul 15;18(14):3722-30. doi: 10.1158/1078-0432.CCR-12-0411. Epub 2012 Jun 4. PMID: 22665903.
102. Elisei R, Schlumberger MJ, Müller SP, Schöffski P, Brose MS, Shah MH, Licitra L, Jarzab B, Medvedev V, Kreissl MC, Niederle B, Cohen EE, Wirth LJ, Ali H, Hessel C, Yaron Y, Ball D, Nelkin B, Sherman SI. Cabozantinib in progressive medullary thyroid cancer. J Clin Oncol. 2013 Oct 10;31(29):3639-46. doi: 10.1200/JCO.2012.48.4659. Epub 2013 Sep 3. Erratum in: J Clin Oncol. 2014 Jun 10;32(17):1864. PMID: 24002501; PMCID: PMC4164813.

103. Milling RV, Grimm D, Krüger M, Grosse J, Kopp S, Bauer J, Infanger M, Wehland M. Pazopanib, Cabozantinib, and Vandetanib in the Treatment of Progressive Medullary Thyroid Cancer with a Special Focus on the Adverse Effects on Hypertension. Int J Mol Sci. 2018 Oct 20;19(10):3258. doi: 10.3390/ijms19103258. PMID: 30347815; PMCID: PMC6214082.

104. Cappagli V, Moriconi D, Bonadio AG, Giannese D, La Manna G, Egidi MF, Comai G, Vischini G, Bottici V, Elisei R, Viola D. Proteinuria is a late-onset adverse event in patients treated with cabozantinib. J Endocrinol Invest. 2021 Jan;44(1):95-103. doi: 10.1007/s40618-020-01272-y. Epub 2020 May 3. PMID: 32363491.

105. Wirth LJ, Robinson B, Boni V, Tan DSW, McCoach C, Massarelli E, Hess LM, Jen MH, Kherani J, Olek E, Subbiah V. Patient-Reported Outcomes with Selpercatinib Treatment Among Patients with RET-Mutant Medullary Thyroid Cancer in the Phase I/II LIBRETTO-001 Trial. Oncologist. 2021 Sep 13. doi: 10.1002/onco.13977. Epub ahead of print. PMID: 34516023.

106. Jozaghi Y, Zafereo M, Williams MD, Gule-Monroe MK, Wang J, Grubbs EG, Vaporciyan A, Hu MI, Busaidy N, Dadu R, Waguespack SG, Subbiah V, Cabanillas M. Neoadjuvant selpercatinib for advanced medullary thyroid cancer. Head Neck. 2021 Jan;43(1):E7-E12. doi: 10.1002/hed.26527. Epub 2020 Nov 9. PMID: 33169506; PMCID: PMC7756223.

107. Locantore P, Novizio R, Corsello A, Paragliola RM, Pontecorvi A, Corsello SM. Discovery, preclinical development, and clinical application of pralsetinib in the treatment of thyroid cancer. Expert Opin Drug Discov. 2021 Oct 27:1-7. doi: 10.1080/17460441.2022.1995351. Epub ahead of print. PMID: 34702125.

108. Kim J, Bradford D, Larkins E, Pai-Scherf LH, Chatterjee S, Mishra-Kalyani PS, Wearne E, Helms WS, Ayyoub A, Bi Y, Sun J, Charlab R, Liu J, Zhao H, Liang D, Ghosh S, Philip R, Pazdur R, Theoret MR, Beaver JA, Singh H. FDA Approval Summary: Pralsetinib for the Treatment of Lung and Thyroid Cancers With RET Gene Mutations or Fusions. Clin Cancer Res. 2021 Oct 15;27(20):5452-5456. doi: 10.1158/1078-0432.CCR-21-0967. Epub 2021 May 27. PMID: 34045295.

109. Subbiah V, Shen T, Terzyan SS, Liu X, Hu X, Patel KP, Hu M, Cabanillas M, Behrang A, Meric-Bernstam F, Vo PTT, Mooers BHM, Wu J. Structural basis of acquired resistance to selpercatinib and pralsetinib mediated by non-gatekeeper RET mutations. Ann Oncol. 2021 Feb;32(2):261-268. doi: 10.1016/j.annonc.2020.10.599. Epub 2020 Nov 5. PMID: 33161056; PMCID: PMC7883646.

110. Lin JJ, Gainor JF. An early look at selective RET inhibitor resistance: new challenges and opportunities. Br J Cancer. 2021 May;124(11):1757-1758. doi: 10.1038/s41416-021-01344-7. Epub 2021 Mar 23. PMID: 33758332; PMCID: PMC8144197.

111. Dinér P, Alao JP, Söderlund J, Sunnerhagen P, Grøtli M. Preparation of 3-substituted-1-isopropyl-1H-pyrazolo[3,4-d]pyrimidin-4-amines as RET kinase inhibitors. J Med Chem. 2012 May 24;55(10):4872-6. doi: 10.1021/jm3003944. Epub 2012 May 16. PMID: 22559926.

112. Alao JP, Michlikova S, Dinér P, Grøtli M, Sunnerhagen P. Selective inhibition of RET mediated cell proliferation in vitro by the kinase inhibitor SPP86. BMC Cancer. 2014 Nov 20;14:853. doi: 10.1186/1471-2407-14-853. PMID: 25409876; PMCID: PMC4252022.

List of figures and tables

- **Fig. 1.** Schematic representation of tumor-induced angiogenesis……. Pag.14
- **Fig. 2.** Schematic representation of zebrafish developmental stages……... Pag. 17
- **Fig. 3.** Proliferation assay on LNET cell lines…… Pag. 26
- **Fig. 4.** Proliferation assay on MTC cell lines……. Pag. 27
- **Table 1.** EC_{50} and maximal inhibition of every drug for all cell lines……. Pag. 28
- **Fig. 5.** Cell cycle analysis on LNET cell lines…… Pag. 29
- **Fig. 6.** Cell cycle analysis on MTC cell lines……. Pag. 30
- **Fig. 7.** Apoptosis analysis on LNET cell lines……..…….. Pag. 32
- **Fig. 8.** Apoptosis analysis on MTC cell lines……. Pag. 33
- **Fig. 9.** Effect of TKIs on NCI-H727 migration…..…… Pag. 34
- **Fig. 10.** Effect of TKIs on UMC-11 migration…… Pag. 35
- **Fig. 11.** Effect of TKIs on TT migration……... Pag. 36
- **Fig. 12.** Effect of TKIs on MZ-CRC-1 migration……. Pag. 37
- **Fig. 13.** Effect of TKIs on NCI-H727-induced angiogenesis *in vivo*……... Pag. 38
- **Fig. 14.** Effect of TKIs on UMC-11-induced angiogenesis *in vivo*…….. Pag. 39
- **Fig. 15.** Effect of TKIs on NCI-H835-induced angiogenesis *in vivo*……... Pag. 40
- **Fig. 16.** Effect of TKIs on TT-induced angiogenesis *in vivo*……... Pag. 41
- **Fig. 17.** Effect of TKIs on cell migration *in vivo*……. Pag. 42

Dissemination of the results

The results sharing to the scientific community is one of the fundamental goals of any scientific research. For this reason, it is our intention to publish in international peer-reviewed journals the results achieved through this project, with a particular preference for Journals with open-access policies. The “non-expert” public will be reached by advertising our project in all available social and scientific events. Several outreach activities will be used, such as articles in non-specialised press, public talks, workshops for patients with NETs, etc. During my PhD program, some of these have been already published or presented at one congress.

Publications

- Gaudenzi G, Dicitore A, Carra S, **Saronni D**, Pozza C, Giannetta E, Persani L, Vitale G. MANAGEMENT OF ENDOCRINE DISEASE: Precision medicine in neuroendocrine neoplasms: an update on current management and future perspectives. Eur J Endocrinol. 2019 May 1. pii: EJE-19-0021.R1. doi: 10.1530/EJE-19-0021. [Epub ahead of print] Review. PMID: 31048562

- Carra S, Gaudenzi G, Dicitore A, **Saronni D**, Cantone MC, Plebani A, Ghilardi A, Borghi MO, Hofland LJ, Persani L, Vitale G. Vandetanib versus Cabozantinib in Medullary Thyroid Carcinoma: A Focus on Anti-Angiogenic Effects in Zebrafish Model. Int J Mol Sci. 2021 Mar 16;22(6):3031. doi: 10.3390/ijms22063031. PMID: 33809722; PMCID: PMC8002338.

- Vitale G, Cozzolino A, Malandrino P, Minotta R, Puliani G, **Saronni D**, Faggiano A, Colao A. Role of FGF System in Neuroendocrine Neoplasms: Potential Therapeutic Applications. Front Endocrinol (Lausanne). 2021 Apr 14;12:665631. doi: 10.3389/fendo.2021.665631. PMID: 33935975; PMCID: PMC8080021.

Oral communication

- Congresso SIE 2019 Roma, 30 Maggio - 1° giugno 2019. Comunicazione Orale: Targeting of fibroblast growth factor receptor pathway as a new anti-tumor strategy for medullary thyroid cancer. **Saronni D**, Dicitore A, Gaudenzi G, Carra S, Borghi MO, Persani L, Vitale G.

Summary of the project for the public

Il mio progetto di dottorato ha avuto come scopo quello di valutare l'attività antitumorale di nuovi inibitori delle tirosin-chinasi nei tumori neuroendocrini, nello specifico in linee cellulari di tumori neuroendocrini a lenta crescita e altamente vascolarizzati, quali tumori polmonari di basso grado ed il carcinoma midollare della tiroide. Tale valutazione è stata condotta attraverso esperimenti *in vitro* al fine di valutare gli effetti dei farmaci sulla vitalità e morte cellulare. Infine, abbiamo valutato *in vivo* l'efficacia dei farmaci sull'angiogenesi indotta dal tumore (formazione di nuovi vasi in grado di fornire ossigeno e sostanze nutritive essenziali alla crescita tumorale) e sul potenziale metastatico, utilizzando un innovativo modello animale con embrioni di zebrafish. Abbiamo osservato una riduzione della vitalità cellulare dose-dipendente, confermata da un aumento della morte cellulare, per tutti i farmaci usati. Nelle linee tumorali del polmone il cabozantinib ha mostrato la maggiore inibizione dell'angiogenesi, rendendolo così potenzialmente utile nella clinica per queste neoplasie. Nel carcinoma midollare della tiroide, il RET-inibitore SPP86 ha mostrato capacità antitumorali, sia *in vitro* che *in vivo*, simili al sulfatinib, rendendolo un potenziale farmaco da valutare in futuri trials clinici.

The goal of my PhD project was to evaluate the antitumor activity of novel TKIs on NETs, in particular on low-grade, highly vascularized NET cell lines, such as LNET and MTC. This evaluation was conducted *in vitro* with assays to analyse the effects on cell viability and cell death. *In vivo* we evaluated the efficacy of drugs on tumor-induced angiogenesis (formation of new blood vessels contributing to the dissemination of tumor cells and supplying nutrients and oxygen for cancer growing) and the development of metastasis, taking advantage of an innovative zebrafish model. We observed a dose-dependent reduction of cell viability, confirmed by an increase in cell death after treatment with all tested compounds. However, for LNET cells, cabozantinib showed the highest impact on *in vivo* angiogenesis, making it an interesting molecule for the clinical treatment of these tumors. In MTC, the RET-inhibitor SPP86 showed an anti-tumor activity, both *in vitro* and *in vivo*, comparable with sulfatinib, suggesting a potential use in future clinical trials.

Appendix

MANAGEMENT OF ENDOCRINE DISEASE

Precision medicine in neuroendocrine neoplasms: an update on current management and future perspectives

Germano Gaudenzi[1], Alessandra Dicitore[2], Silvia Carra[3], Davide Saronni[2], Carlotta Pozza[4], Elisa Giannetta[4], Luca Persani[2,3] and **Giovanni Vitale[1,2]**

[1]Istituto Auxologico Italiano, IRCCS, Laboratorio Sperimentale di Ricerche di Neuroendocrinologia Geriatrica ed Oncologica, Milan, Italy, [2]Department of Clinical Sciences and Community Health (DISCCO), University of Milan, Milan, Italy, [3]Laboratory of Endocrine and Metabolic Research, Istituto Auxologico Italiano IRCCS, Milan, Italy, and [4]Department of Experimental Medicine, Sapienza University of Rome, Rome, Italy

Correspondence should be addressed to G Vitale
Email
giovanni.vitale@unimi.it

Abstract

Neuroendocrine neoplasms (NENs) are traditionally considered as a single group of rare malignancies that originate from the highly spread neuroendocrine system. The clinical management is complex due to the high heterogeneity of these neoplasms in terms of clinical aggressiveness and response to the therapy. Indeed, a multidisciplinary approach is required to reach a personalization of the therapy, including cancer rehabilitation. In this review, we discuss the possibility to adopt a precision medicine (PM) approach in the management of NENs. To this purpose, we summarize current knowledge and future perspectives about biomarkers and preclinical *in vitro* and *in vivo* platforms, potentially useful to inform clinicians about the prognosis and for tailoring therapy in patients with NENs. This approach may represent a breakthrough in the therapy and tertiary prevention of these tumors.

European Journal of Endocrinology
(2019) **180**, R1–R10

European Journal of Endocrinology

Introduction

Neuroendocrine neoplasms (NENs) are a group of neoplasms derived from the neuroendocrine system, expressing markers of neuroendocrine differentiation, such as chromogranin A (CgA), synaptophysin and neuron-specific enolase (NSE), as well as several hormones (1). Although surgery remains the cornerstone of treatment for localized tumors, most patients with NENs are diagnosed once metastases have occurred. These patients require a chronic medical management defined through a multidisciplinary approach. The main factors

Invited Author's profile

Giovanni Vitale is an associate professor in endocrinology at the University of Milan – Italy – and director of the Laboratory of Geriatric and Oncologic Neuroendocrinology Research at Istituto Auxologico Italiano IRCCS. His research interests involve the development of new therapeutic strategies in the field of neuroendocrine tumors with a translational approach from bench to bedside. In recent years, he has developed an innovative preclinical model for neuroendocrine tumors based on xenograft in zebrafish embryos.

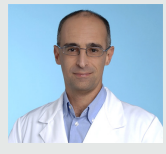

https://eje.bioscientifica.com
https://doi.org/10.1530/EJE-19-0021

Published by Bioscientifica Ltd.

that currently play an important role in establishing the treatment are substantially the grade and the stage of the tumor, the anatomic site of origin and the presence of a functioning syndrome. However, clinical efficacy of current treatment strategies is limited by the high biological heterogeneity of these neoplasms in the clinical aggressiveness and response to the therapy (2). In this context, a precision medicine (PM)-based strategy, through the biomarker-driven approach and preclinical models, could be helpful for the management of NENs (Fig. 1).

Biomarkers in PM for NENs

Tissue biomarkers, routinely used in the clinical practice, have a diagnostic role in verifying the neuroendocrine phenotype (CgA, synaptophysin and NSE), determining the grade (Ki-67 and mitotic count) and discriminating between functioning (secreting serotonin, insulin, gastrin, glucagon, VIP, somatostatin, catecholamines, PTHrp, ACTH, GH, ADH, calcitonin, GNRH, CRH, etc.) or non-functioning tumors (3). However, currently available neuroendocrine phenotype markers have some limitations in the diagnostic phase when dosed in the blood. Despite being long identified as the most relevant NEN-related serum marker, the utility of circulating CgA is limited for the diagnosis of NEN. CgA assays still lack standardization, thus limiting not only clinical management but also the comparison between different analyses. Moreover, the test specificity is hampered by non-oncological causes, such as benign diseases and iatrogenic conditions (proton pump inhibitors and histamine type-2 receptor antagonists), and by the fact that a variety of non-NEN malignancies are characterized by increased CgA levels (4, 5, 6). Another limitation of CgA assays is the sensitivity that ranges between 32 and 92% and is dependent on the type of NEN, the functional status and the size of the tumor (3). Circulating NSE is also not relevant for the diagnosis of NEN, being not actively secreted but released by tumor cells with an intense cytolysis in poorly differentiated NEN (4). Conversely, the 24 h urinary 5-hydroxyindoloacetic acid (5-HIAA) has a potential diagnostic utility as all markers of functioning endocrine syndromes. 5-HIAA is increased in typical carcinoid syndrome, and therefore, represents a crucial marker, particularly in ileal NENs associated with carcinoid syndrome where the sensitivity and specificity can reach 85 and 100%, respectively (4).

In addition to diagnostic biomarkers, another area of interest for NENs includes the research of biomarkers with a prognostic value. Ki-67 index and mitotic count are routinely used to determine the tumor grading and

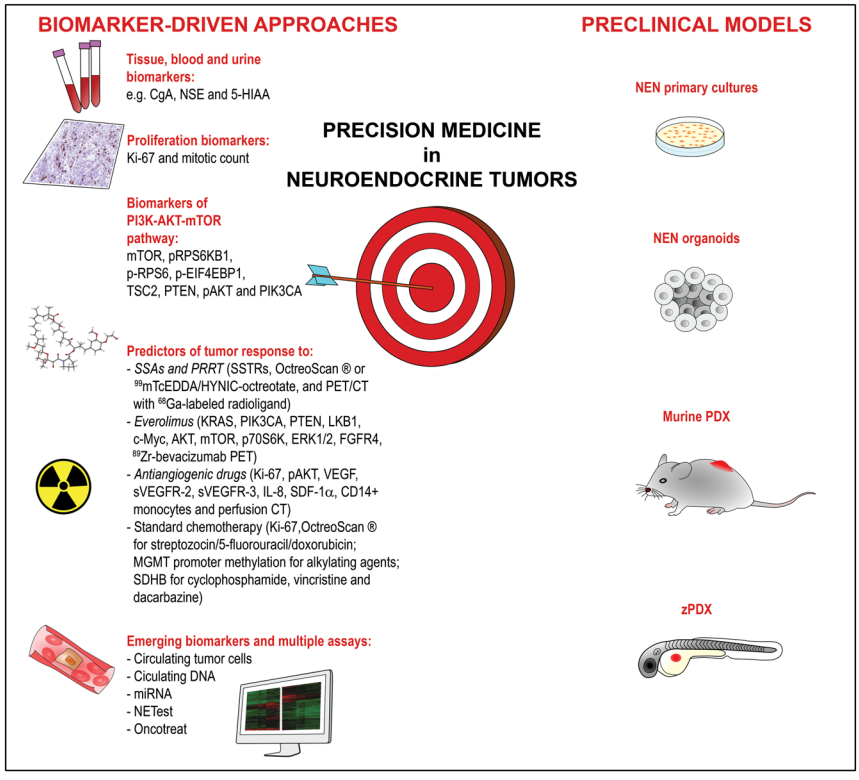

Figure 1
Overview of available biomarker-driven approaches and preclinical models for the development of PM in NENs. CgA, chromogranin A; NEN, neuroendocrine neoplasm; NSE, neuron-specific enolase; PDX, patient-derived xenograft; PET-CT, positron emission tomography/computed tomography; PRRT, peptide receptor radionuclide therapy; SSAs, somatostatin analogs; sVEGFR-2/3, soluble VEGF receptor-2/3; zPDX, zebrafish PDX.

cell proliferation rate. While Ki-67 index has a prognostic role in gastroenteropancreatic (GEP)-NENs, relatively less data support the same use for bronchial NENs (7, 8). The mitotic count has been shown to be prognostic in most of the NENs (9, 10). Elevated CgA and NSE levels are associated with poor progression-free survival (PFS) and overall survival (OS) in NENs. In addition, NSE expression is usually elevated in poorly differentiated NENs (11).

Other studies have been focused on the research of prognostic biomarkers between members of PI3K-AKT-mTOR pathway (12). In this context, the overexpression of mTOR protein has been suggested as a negative prognostic factor (13). In pancreatic NENs mutations in PI3K–AKT–mTOR pathway genes have been reported in 15% of patients. These genetic alterations seem to confer worse prognosis than other mutations linked to NENs (14). Genetic alterations of *TSC2* have been reported in 8% of pancreatic NENs and resulted to be associated with a reduced OS (15). On the other hand, although loss of 10q, the region containing *PTEN*, was present in about 30% of pancreatic NENs (16) and mutations in *PIK3CA*/*PTEN* have been found in 22% of poorly differentiated NENs, no prognostic value has been reported for these genetic modifications (17, 18). Indeed, given the complexity of this pathway, increased by the cross-talk with other molecular signaling, further studies are needed to get new insights into the prognostic role of its genetic and molecular alterations.

A great interest in the research of NEN biomarkers is represented by the identification of predictors of tumor response to the medical therapy. Although Ki-67 and mitotic count are currently used in the decision making of NENs treatment, technical issues about measurement of these parameters and tumor heterogeneity may weaken their predictive role (19). In addition, none of conventional circulating biomarkers have shown a high predictive accuracy (20). However, recent studies have investigated the potential predictive role of therapeutic response to current anti-cancer therapy for several biomarkers in NENs. These biomarkers are grouped on the basis of therapeutic interventions as follows:

- *Somatostatin analogs (SSAs) and peptide receptor radionuclide therapy (PRRT):* Although most clinicians agree that the presence of somatostatin receptors (SSTRs) should be verified before treatment with SSAs is initiated (21), only few studies showed that SSTR expression can predict the response to the therapy with SSAs in NENs (22, 23, 24). However, in CLARINET and PROMID trials, showing a significant delay in disease progression after treatment with SSA, SSTR scintigraphy was positive in 100 and 86% of enrolled patients, respectively (25, 26). One of the most clinically relevant therapeutic innovation in NEN has been the development of PRRT through the use of SSAs labeled with beta-emitting radionuclides, in patients with unresectable grade 1 or 2 NENs and high SSTR expression (27). In these cases, nuclear medicine imaging, such as scintigraphy with ^{111}Indium pentetreotide (OctreoScan®) or ^{99}mTcEDDA/HYNIC-octreotate and positron emission tomography (PET) with ^{68}Ga-labeled radioligands, has some predictive ability in determining the functional response.
- *mTOR inhibitors:* Although in several clinical studies, no valid biomarker has been identified so far to predict response to mTOR inhibitors, such as everolimus, few preclinical studies have recently explored mechanisms involved in the resistance to mTOR inhibitors. These data would be useful in future for the identification of predictive biomarkers. Besides KRAS and PIK3CA mutations, that conferred resistance to everolimus therapy (28), it has been showed that loss of PTEN and LKB1 with activation of c-Myc decreased sensitivity to treatment with mTOR inhibitors in pancreatic NEN cell lines (29). Evidence collected on human bronchial NEN primary cultures suggested that lower expression of mTOR, p70S6K, AKT and ERK1/2 could be predictive markers of resistance to mTOR inhibitors (30). Other genetic alterations correlated with resistance to everolimus therapy, such as the FGFR4-G388R single nucleotide polymorphism (31).

  Given that mTOR inhibition reduced VEGF-A secretion in three murine GEP-NEN cell lines (32), it has been proposed that levels of this cytokine could measure the response to everolimus (33). However, circulating VEGF-A in NEN patients treated with everolimus has not shown a clear predictive value yet. The tumor uptake of ^{89}Zr-bevacizumab, a radioactive-labeled VEGF-A antibody, diminished during everolimus treatment in patients with well-differentiated NENs. Therefore, serial ^{89}Zr-bevacizumab PET might be useful as an early predictive imaging-based biomarker for the treatment with everolimus or other drugs targeting VEGF system in NEN patients (33).
- *Antiangiogenic therapies:* Sunitinib is a multi-targeted tyrosine kinase inhibitor. Among tissue biomarkers, low Ki-67 and pAKT expression correlated with a better response to sunitinib in NENs (34). The predictive role of circulating levels of VEGF, soluble VEGF receptors (sVEGFR-2 and sVEGFR-3), IL-8 and stromal

cell-derived factor (SDF)-1α, have been analyzed in patients with pancreatic NEN and carcinoid tumors treated with sunitinib. Baseline level of sVEGFR-2 resulted more elevated in patients with pancreatic NEN and longer OS (35), as previously reported in NEN patients treated with pazopanib, another tyrosine kinase inhibitor (36). In carcinoid patients low pre-treatment IL-8 levels were associated with longer PFS and OS. In addition, low baseline concentrations of sVEGFR-3 and SDF-1α were associated with longer PFS and OS in both pancreatic NENs and carcinoid tumors patients (35). A significant increase from baseline of VEGF, IL-8 and SDF-1α, and a decrease in sVEGFR-2 and sVEGFR-3 were observed in patients with NENs at the end of the first cycle of treatment with sunitinib (35).

Bevacizumab, a VEGF monoclonal antibody, is another targeted therapy used in advanced NENs. In patients with metastatic or unresectable NEN, the decrease in blood flow and blood volume observed through perfusion CT during treatment with bevacizumab and everolimus correlated with RECIST response (37). However, larger prospective studies are needed for validation of these potential predictive biomarkers.

- *Standard chemotherapy:* Ki-67 has been proposed for selecting patients for chemotherapy in NENs due to the direct association between tumor grade and response (38). However, clinically useful threshold for Ki-67 has not well defined (38). Other predictive biomarkers have been currently identified for cytotoxic drugs. In pancreatic NENs, a positive OctreoScan® was predictive of an objective response to streptozocin/5-fluorouracil/doxorubicin (39). Moreover, it has been reported that MGMT promoter methylation status and protein deficiency were associated with a better response rate to alkylating agents (40, 41). In pheochromocytomas and paraganglioma patients with SDHB mutations showed a higher risk for developing metastatic disease, but they responded better than non-mutation carriers to the therapy with cyclophosphamide, vincristine and dacarbazine (42).

In the last years, due to a better understanding of molecular mechanisms involved in the development of NENs (43) and advances in the technologies, a new generation of biomarkers and multiple assays have been recently developed. Preliminary data are available in NENs:

- *Circulating tumor cells (CTCs)* could provide prognostic information in real time and in terms of tumor progression and OS in NENs (44, 45). Patients with a negative CTC count showed a better prognosis in terms of PFS and OS as compared to patients with ≥1 CTC. In addition, a >50% reduction of CTCs count after the treatment was associated with a better outcome (45). Therefore, CTC detection could be also an attractive method to monitor disease progression and response during the treatment. In addition, the molecular characterization of isolated CTCs might have clinical relevance for therapeutic decision making through the identification of specific molecular targets (45). SSTRs have been recently measured in CTCs isolated from patients with GEP-NENs (46). This could be useful in future for the selection of patients to treat with SSAs or PPRT. A recent study showed that CTC copy number alteration may represent a new predictor of response to chemotherapy in patients with small-cell lung cancer (47).
- *Circulating tumor DNA (ctDNA)* consists of short nuclear fragments (~166 bp) released in the blood from apoptotic or necrotic tumor cells. ctDNA analysis can be potentially useful for NEN management. It has been observed that the ctDNA levels rise during tumor progression, whereas decline after therapy. In this way, ctDNA levels surveillance could guide drug treatment and provide a more comprehensive representation of the mutational landscape of the NEN, as recently reported in few anecdotal reports (48, 49). In addition, changes in allele frequencies over time could reflect subclonal evolution, supplying the opportunity to adjust the therapy in order to overcome newly developing resistance. Finally, it has been noted an upward trend in ctDNA concentration earlier than current biomarkers, useful for an earlier prediction of disease recurrence (50).
- *miRNAs* are endogenous small non-coding RNAs that control post-transcriptional eukaryotic gene expression. Their tissue and blood levels have been associated to prognosis and prediction of therapeutic outcome in several cancers. As reported by Zatelli *et al.*, few evidences are currently available about the prognostic potential of miRNAs in NENs and they are limited to their tissue expression in lung NENs, pancreatic NENs, medullary thyroid cancer and pheochromocytoma (51).
- *NETest* is a multianalyte liquid biopsy procedure that measures the circulating expression level of 51 genes involved in cancerogenesis, cell proliferation, signaling, secretion and metastasis formation through a peripheral blood real-time polymerase chain reaction.

This procedure has been tested in GEP and pulmonary NENs. The NETest provides with high sensitivity (85–98%) and specificity (93–97%) information about the diagnosis, completeness of surgical resection and the presence of residual disease in patients with NENs. This test can also predict the therapeutic efficacy of SSAs and PRRT (52). Moreover, NETest is standardized, reproducible and is not influenced by age, gender, ethnicity, fasting or proton pump inhibitors (53).

- *OncoTreat* is an innovative platform based on the systematic prioritization of anti-cancer drugs. The rationale of OncoTreat starts from the ability of drugs to invert the expression profile of master regulator proteins, whose coordinated activity is necessary for the modulation of tumor check points (54). OncoTreat was set up in a cohort of 212 patients with GEP-NEN. In the first phase, a transcriptome analysis identified several master regulator proteins that include key regulators of neuroendocrine lineage progenitor state and immunoevasion. In the second phase, a prioritization of small molecules was performed by a transcriptome analysis aimed at identifying which molecules were able to invert the activity of GEP-NEN master regulator proteins in H-STS cells, a cell line derived from GEP-NEN patient (55). Interestingly, results of this study lead FDA to approve the Investigational New Drug Application for entinostat in GEP-NENs (54). Therefore, OncoTreat appears to be a promising strategy for the development of PM applications, ideally complemented by preclinical models to predict which drugs a patient will respond to.

The promising role of preclinical models in PM

Although the biomarker-driven approach is contributing to the evolution of tailored therapies for some tumors, the characterization of the genetic and molecular profiles of tumor cells does not often translate into a successful clinical outcome, due to the spatial and temporal heterogeneity of these cells (56). Several preclinical models have been indicated as promising platform for the development of PM applications, able to capture the heterogeneous nature of human cancers. For instance, short-term primary culture cells derived from solid tumors, also known as *ex vivo*, have gained significant importance in personalized cancer therapy (57). Recently, a human platform technology called CANscript™ has been developed to predict the response to anti-cancer drugs in patients with head and neck squamous cell carcinoma and colorectal cancer. Thin tumor sections were cultured *ex vivo*, on grade-matched tumor matrix support in a medium addicted with autologous patient serum and treated with selected drugs. Then, the clinical response was predicted from several parameters detected on *ex vivo* cultures, by a sophisticated machine-learning trained algorithm, showing a 100% sensitivity and 92% specificity (58).

Nowadays, patient-derived xenografts (PDXs) in mice represent the most robust and investigated experimental platform for the development of PM applications (59). To generate PDXs, solid tumors, collected after surgery or biopsy procedures, are inoculated as pieces or single-cell suspensions subcutaneously into the flank or in the same organ, as the original tumor of the animal. Several mouse strains, having different degrees of immunosuppression are currently available for these studies (60). Although an engraftment-associated selection has been reported, PDXs preserve the histological organization, the genetic and epigenetic mutational profile and the gene expression patterns, as in the patient counterpart. PDXs have showed also a high potential in predicting drug response to pharmacological treatments, as demonstrated in colorectal cancer (61). PDXs have been recently used to perform co-clinical studies, in which patient-derived tumor cells, isolated from a patient enrolled in a clinical trial, are implanted into immunocompromised mice that are subsequently treated with the same drugs of the patient to emulate clinical response (62). Compared to conventional phase I/II clinical trials, PDX-based co-clinical studies have the advantage of analyzing and integrating preclinical and clinical data in a real-time manner. This aspect is crucial to study mechanisms of drug resistance and to explore the therapies that can be administered to the patient (60).

Preclinical models for PM in NENs

Several preclinical models have been recently developed in NENs (Fig. 1) with relevant advantages and potential application in the clinical management of this tumor (Table 1).

In vitro models

Although human immortalized NEN cell lines have significantly contributed to the study of pathways involved in carcinogenesis and the screening of

Table 1 Advantages and limitations of NEN preclinical models.

	Advantages	Limitations
Immortalized cell lines	• Unlimited lifespan • Easy to handle and manipulate • Large number of cells • Study of pathways involved in carcinogenesis and preliminary drug screening	• Lack of cellular heterogeneity • Accumulation of genetic changes over time • Loss of well-differentiated neuroendocrine phenotype
Primary cultures (2D and 3D organoids)	• Fast procedure • Identification of novel molecular targets and drug screening	• Possible loss of tumor heterogeneity • Difficulties in the culture establishment due to the low proliferation rate of NENs
Murine patient-derived xenografts	• Realistic heterogeneity of tumor cells • Preservation of genetic and epigenetic characteristics of primary tumor • Preclinical drug screening and co-clinical trials • High prognostic and predictive potential	• Large number of tumor cells • Long time to establish • Immunosuppressed animals limit a realistic tumor microenvironment • Difficulties to generate mouse xenograft models able to metastasize • Possibility of engraftment-associated selection • Low engraftment rate for NENs
Zebrafish patient-derived xenografts	• Small number of tumor cells for the implant • Possibility to implant high number of embryos • Real-time visualization • Fast model for the analysis of tumor-induced angiogenesis and migration • Lack of an acquired immune system in embryos and larvae • High engraftment rate • Preclinical drug screening and co-clinical trials • High predictive potential	• Difficulties in orthotopic implantation • Difficulties in long-term analyses • Several organs or systems are still developing in embryos • Little knowledge about the maintenance of tumor microenvironment in zebrafish

compounds with antitumor activity and related drug resistance mechanisms (63), they have some limitations, such as the accumulation of genetic changes over time in culture and the lack of cellular heterogeneity. In addition, some NEN cell lines do not display well-differentiated neuroendocrine phenotype or have a very low expression of some key receptors for drug treatment (such as SSTRs). In this context, experimental data obtained from NEN cell lines should be carefully validated with primary cell cultures derived from NEN patients (64), even if establishment of these cells could be difficult, due to the low proliferation rate of NEN cells. In the context of PM, the main advantage of primary tumor cell culture is the possibility to evaluate the potential efficacy of several antitumor compounds in a short time, through a system where intratumor heterogeneity and the original genetic signature of the tumor are preserved (57). NEN primary cell cultures could also be used to perform preliminary preclinical studies for the identification of novel druggable molecular targets.

Powerful *in vitro* platforms, which can facilitate the development of PM strategies, have been recently set up using 3D patient-derived organoid cultures also in NENs (65). Organoids can be cultured from a small sample size, derived from needle biopsy and generated from different areas of the tumor in order to better mimic genetic and phenotypic heterogeneity of the tumor (66). These models could serve as a platform to combine high-throughput drug screening and genomic analysis on patient-derived tumor samples, thus offering a unique opportunity to stratify and identify efficacious therapies for individual patients.

In vivo models

NEN-PDX murine models of MTC (67) and high-grade pulmonary NENs (68) have been used in preclinical research to investigate the efficacy of experimental anti-cancer drugs. NEN-PDX murine models recapitulate some peculiarity of tumors in patients. For instance, the gastric neuroendocrine carcinoma PDX model GA0087 has showed a metastatic behavior supported by the high expression of VEGF-A as in patients with gastric NEC (69). A genomewide analysis on a PDX model of neuroendocrine prostate cancer in mice has showed that CBX2 and EZH2, members of the polycomb group family

of transcriptional repressors, are upregulated, as in patients with this disease (70). PDXs of pancreatic NEN can develop resistance to everolimus. In this study, the inhibitor of the mTOR pathway sapanisertib showed a potent antitumor effect also on everolimus-resistant PDXs, leading to the suggestion of a new alternative pharmacological strategy for everolimus-resistant NEN (71). However, the use of murine NEN-PDX models is very limited in the research of PM strategies probably due to the rarity of NENs, the limited size of post-surgical samples for most of these tumors and the low rate of successful tumor engraftment (72).

Recently, zebrafish PDX (zPDX) has been suggested as promising platform for the development of PM applications (73, 74). Fior and collaborators have demonstrated that zPDX has a strong predictive potential in patients with colorectal cancer treated with chemotherapy and biological therapy (74). In this respect, we have recently set up a NEN-zPDX platform, based on the injection of red fluorescent labeled NEN cells into the subperidermal cavity of *Tg(fli1a:EGFP)*^{y1} zebrafish embryos (73, 75). This transgenic line, expressing the enhanced green fluorescent protein (EGFP) in the endothelial cells of the entire vascular tree, offers the possibility to estimate the proangiogenic potential and the metastatic behavior of injected tumor cells derived from each patient tissue. In addition to the advantages due to the intrinsic features of the zebrafish model, as the high fecundity, the outer fertilization and the optical transparency, our PDX platform can overcome some general drawbacks of murine engraftment procedure. Although mouse is considered the gold standard for PDXs, several limitations have been reported, such as the large number of tumor cells to be implanted (about 1 million for each animal) and the long time required for the implantation (from several weeks to months), the need of immunosuppressed animals to avoid transplant rejection and the difficulties to generate mouse xenotransplant models able to metastasize (76). We have demonstrated that NEN PDXs can stimulate angiogenesis in zebrafish embryos within few days and without the need of immunosuppression, because the adaptive immune response is not completely developed during the early development of zebrafish (73). Compared to mouse tumor models, in which the spread of tumor cells cannot be analyzed in real time after the transplantation, the transparency of zebrafish embryos allows to follow in real time the invasive behavior of fluorescent-labeled tumor cells (73). Besides, in zebrafish model, the possibility to study the effects of small tumor implants (100 cells/embryo) resulted particularly suitable for NENs, where post-surgical availability of tumor cells is often limited. Interestingly, the success of NEN cells transplantation in zebrafish embryos resulted to be extraordinary higher compared than that reported for murine PDXs (72).

In the near future, additional studies will be fundamental to clarify if NEN zPDXs and NEN patients might have similar response to the available therapeutic options, as recently reported for colorectal cancer (74). These studies could be supported by the versatility of zebrafish embryos in drug screening. Indeed, because of the permeability of zebrafish embryos to small molecules, a number of compounds can be added directly to the embryo water, whereas larger or not water-soluble molecules need to be injected into the body of the embryo to ensure drug uptake. The effects of antitumor compounds on tumor-induced angiogenesis, invasiveness, metastatic dissemination and tumor cell proliferation can be easily evaluated by epifluorescence microscopy and confocal microscopy within 3 days after implantation.

Conclusions

Several biomarkers are routinely used for the classification of NENs and are currently relevant for the treatment selection. Although several prognostic and predictive biomarkers, which could support tailoring therapies have been recently identified (Fig. 1), most of them are far from being routinely adopted in clinical practice and further insights are needed.

Few available preclinical *in vitro* and *in vivo* models, derived from NEN patient cells, have provided first evidences of preserving molecular and behavioral features of the original NEN. The most promising preclinical platforms for PM in NENs are PDXs in mice and zebrafish embryos (Fig. 1). However, additional studies are needed to analyze the predictive potential of these innovative tools, as well as their translatability into the clinical practice, in order to improve the survival and quality of life in patients with advanced NENs.

Declaration of interest
The authors declare that there is no conflict of interest that could be perceived as prejudicing the impartiality of this review.

Funding
This work was supported by the ministerial research project: PRIN 2017Z3N3YC.

References

1 Rindi G & Wiedenmann B. Neuroendocrine neoplasms of the gut and pancreas: new insights. *Nature Reviews Endocrinology* 2012 **8** 54–64. (https://doi.org/10.1038/nrendo.2011.120)

2 Uri I & Grozinsky-Glasberg S. Current treatment strategies for patients with advanced gastroenteropancreatic neuroendocrine tumors (GEP-NETs). *Clinical Diabetes and Endocrinology* 2018 **4** 16. (https://doi.org/10.1186/s40842-018-0066-3)

3 Hofland J, Zandee WT & de Herder WW. Role of biomarker tests for diagnosis of neuroendocrine tumours. *Nature Reviews: Endocrinology* 2018 **14** 656–669. (https://doi.org/10.1038/s41574-018-0082-5)

4 Ferolla P, Faggiano A, Mansueto G, Avenia N, Cantelmi MG, Giovenali P, Del Basso De Caro ML, Milone F, Scarpelli G, Masone S *et al*. The biological characterization of neuroendocrine tumors: the role of neuroendocrine markers. *Journal of Endocrinological Investigation* 2008 **31** 277–286. (https://doi.org/10.1007/BF03345602)

5 Marotta V, Nuzzo V, Ferrara T, Zuccoli A, Masone M, Nocerino L, Del Prete M, Marciello F, Ramundo V, Lombardi G *et al*. Limitations of chromogranin A in clinical practice. *Biomarkers* 2012 **17** 186–191. (https://doi.org/10.3109/1354750X.2012.654511)

6 Marotta V, Zatelli MC, Sciammarella C, Ambrosio MR, Bondanelli M, Colao A & Faggiano A. Chromogranin A as circulating marker for diagnosis and management of neuroendocrine neoplasms: more flaws than fame. *Endocrine-Related Cancer* 2018 **25** R11–R29. (https://doi.org/10.1530/ERC-17-0269)

7 Strosberg J, Nasir A, Coppola D, Wick M & Kvols L. Correlation between grade and prognosis in metastatic gastroenteropancreatic neuroendocrine tumors. *Human Pathology* 2009 **40** 1262–1268. (https://doi.org/10.1016/j.humpath.2009.01.010)

8 Pelosi G, Rindi G, Travis WD & Papotti M. Ki-67 antigen in lung neuroendocrine tumors: unraveling a role in clinical practice. *Journal of Thoracic Oncology* 2014 **9** 273–284. (https://doi.org/10.1097/JTO.0000000000000092)

9 Pape UF, Berndt U, Muller-Nordhorn J, Bohmig M, Roll S, Koch M, Willich SN & Wiedenmann B. Prognostic factors of long-term outcome in gastroenteropancreatic neuroendocrine tumours. *Endocrine-Related Cancer* 2008 **15** 1083–1097. (https://doi.org/10.1677/ERC-08-0017)

10 Beasley MB, Thunnissen FB, Brambilla E, Hasleton P, Steele R, Hammar SP, Colby TV, Sheppard M, Shimosato Y, Koss MN *et al*. Pulmonary atypical carcinoid: predictors of survival in 106 cases. *Human Pathology* 2000 **31** 1255–1265. (https://doi.org/10.1053/hupa.2000.19294)

11 Lawrence B, Gustafsson BI, Kidd M, Pavel M, Svejda B & Modlin IM. The clinical relevance of chromogranin A as a biomarker for gastroenteropancreatic neuroendocrine tumors. *Endocrinology and Metabolism Clinics of North America* 2011 **40** 111–134, viii. (https://doi.org/10.1016/j.ecl.2010.12.001)

12 Zatelli MC, Fanciulli G, Malandrino P, Ramundo V, Faggiano A, Colao A & NIKE Group. Predictive factors of response to mTOR inhibitors in neuroendocrine tumours. *Endocrine-Related Cancer* 2016 **23** R173–R183. (https://doi.org/10.1530/ERC-15-0413)

13 Qian ZR, Ter-Minassian M, Chan JA, Imamura Y, Hooshmand SM, Kuchiba A, Morikawa T, Brais LK, Daskalova A, Heafield R *et al*. Prognostic significance of MTOR pathway component expression in neuroendocrine tumors. *Journal of Clinical Oncology* 2013 **31** 3418–3425. (https://doi.org/10.1200/JCO.2012.46.6946)

14 Jiao Y, Shi C, Edil BH, de Wilde RF, Klimstra DS, Maitra A, Schulick RD, Tang LH, Wolfgang CL, Choti MA *et al*. DAXX/ATRX, MEN1, and mTOR pathway genes are frequently altered in pancreatic neuroendocrine tumors. *Science* 2011 **331** 1199–1203. (https://doi.org/10.1126/science.1200609)

15 Gleeson FC, Voss JS, Kipp BR, Kerr SE, Van Arnam JS, Mills JR, Marcou CA, Schneider AR, Tu ZJ, Henry MR *et al*. Assessment of pancreatic neuroendocrine tumor cytologic genotype diversity to guide personalized medicine using a custom gastroenteropancreatic next-generation sequencing panel. *Oncotarget* 2017 **8** 93464–93475. (https://doi.org/10.18632/oncotarget.18750)

16 Perren A, Komminoth P, Saremaslani P, Matter C, Feurer S, Lees JA, Heitz PU & Eng C. Mutation and expression analyses reveal differential subcellular compartmentalization of PTEN in endocrine pancreatic tumors compared to normal islet cells. *American Journal of Pathology* 2000 **157** 1097–1103. (https://doi.org/10.1016/S0002-9440(10)64624-X)

17 Vijayvergia N, Boland PM, Handorf E, Gustafson KS, Gong Y, Cooper HS, Sheriff F, Astsaturov I, Cohen SJ & Engstrom PF. Molecular profiling of neuroendocrine malignancies to identify prognostic and therapeutic markers: a Fox Chase Cancer Center Pilot Study. *British Journal of Cancer* 2016 **115** 564–570. (https://doi.org/10.1038/bjc.2016.229)

18 Yuan F, Shi M, Ji J, Shi H, Zhou C, Yu Y, Liu B, Zhu Z & Zhang J. KRAS and DAXX/ATRX gene mutations are correlated with the clinicopathological features, advanced diseases, and poor prognosis in Chinese patients with pancreatic neuroendocrine tumors. *International Journal of Biological Sciences* 2014 **10** 957–965. (https://doi.org/10.7150/ijbs.9773)

19 Chan DL, Clarke SJ, Diakos CI, Roach PJ, Bailey DL, Singh S & Pavlakis N. Prognostic and predictive biomarkers in neuroendocrine tumours. *Critical Reviews in Oncology/Hematology* 2017 **113** 268–282. (https://doi.org/10.1016/j.critrevonc.2017.03.017)

20 Falconi M, Eriksson B, Kaltsas G, Bartsch DK, Capdevila J, Caplin M, Kos-Kudla B, Kwekkeboom D, Rindi G, Kloppel G *et al*. Enets consensus guidelines update for the management of patients with functional pancreatic neuroendocrine tumors and non-functional pancreatic neuroendocrine tumors. *Neuroendocrinology* 2016 **103** 153–171. (https://doi.org/10.1159/000443171)

21 Mazziotti G, Mosca A, Frara S, Vitale G & Giustina A. Somatostatin analogs in the treatment of neuroendocrine tumors: current and emerging aspects. *Expert Opinion on Pharmacotherapy* 2017 **18** 1679–1689. (https://doi.org/10.1080/14656566.2017.1391217)

22 Janson ET, Westlin JE, Eriksson B, Ahlstrom H, Nilsson S & Oberg K. [111In-DTPA-D-Phe1]octreotide scintigraphy in patients with carcinoid tumours: the predictive value for somatostatin analogue treatment. *European Journal of Endocrinology* 1994 **131** 577–581. (https://doi.org/10.1530/eje.0.1310577)

23 Cives M, Kunz PL, Morse B, Coppola D, Schell MJ, Campos T, Nguyen PT, Nandoskar P, Khandelwal V & Strosberg JR. Phase II clinical trial of pasireotide long-acting repeatable in patients with metastatic neuroendocrine tumors. *Endocrine-Related Cancer* 2015 **22** 1–9. (https://doi.org/10.1530/ERC-14-0360)

24 Volante M, Brizzi MP, Faggiano A, La Rosa S, Rapa I, Ferrero A, Mansueto G, Righi L, Garancini S, Capella C *et al*. Somatostatin receptor type 2A immunohistochemistry in neuroendocrine tumors: a proposal of scoring system correlated with somatostatin receptor scintigraphy. *Modern Pathology* 2007 **20** 1172–1182. (https://doi.org/10.1038/modpathol.3800954)

25 Caplin ME, Pavel M & Ruszniewski P. Lanreotide in metastatic enteropancreatic neuroendocrine tumors. *New England Journal of Medicine* 2014 **371** 1556–1557. (https://doi.org/10.1056/NEJMc1409757)

26 Rinke A, Muller HH, Schade-Brittinger C, Klose KJ, Barth P, Wied M, Mayer C, Aminossadati B, Pape UF, Blaker M *et al*. Placebo-controlled, double-blind, prospective, randomized study on the effect of octreotide LAR in the control of tumor growth in patients with metastatic neuroendocrine midgut tumors: a report from the PROMID Study Group. *Journal of Clinical Oncology* 2009 **27** 4656–4663. (https://doi.org/10.1200/JCO.2009.22.8510)

27 Bodei L, Mueller-Brand J, Baum RP, Pavel ME, Horsch D, O'Dorisio MS, O'Dorisio TM, Howe JR, Cremonesi M, Kwekkeboom DJ *et al*. The joint IAEA, EANM, and SNMMI practical guidance on peptide receptor radionuclide therapy (PRRNT) in

neuroendocrine tumours. *European Journal of Nuclear Medicine and Molecular Imaging* 2013 **40** 800–816. (https://doi.org/10.1007/s00259-012-2330-6)

28 Di Nicolantonio F, Arena S, Tabernero J, Grosso S, Molinari F, Macarulla T, Russo M, Cancelliere C, Zecchin D, Mazzucchelli L *et al*. Deregulation of the PI3K and KRAS signaling pathways in human cancer cells determines their response to everolimus. *Journal of Clinical Investigation* 2010 **120** 2858–2866. (https://doi.org/10.1172/JCI37539)

29 Chang TM, Shan YS, Chu PY, Jiang SS, Hung WC, Chen YL, Tu HC, Lin HY, Tsai HJ & Chen LT. The regulatory role of aberrant phosphatase and tensin homologue and liver kinase B1 on AKT/mTOR/c-Myc axis in pancreatic neuroendocrine tumors. *Oncotarget* 2017 **8** 98068–98083. (https://doi.org/10.18632/oncotarget.20956)

30 Gagliano T, Bellio M, Gentilin E, Mole D, Tagliati F, Schiavon M, Cavallesco NG, Andriolo LG, Ambrosio MR, Rea F *et al*. mTOR, p70s6K, AKT, and ERK1/2 levels predict sensitivity to mTOR and PI3K/mTOR inhibitors in human bronchial carcinoids. *Endocrine-Related Cancer* 2013 **20** 463–475. (https://doi.org/10.1530/ERC-13-0042)

31 Serra S, Zheng L, Hassan M, Phan AT, Woodhouse LJ, Yao JC, Ezzat S & Asa SL. The FGFR4-G388R single-nucleotide polymorphism alters pancreatic neuroendocrine tumor progression and response to mTOR inhibition therapy. *Cancer Research* 2012 **72** 5683–5691. (https://doi.org/10.1158/0008-5472.CAN-12-2102)

32 Villaume K, Blanc M, Gouysse G, Walter T, Couderc C, Nejjari M, Vercherat C, Cordier-Bussat M, Roche C & Scoazec JY. VEGF secretion by neuroendocrine tumor cells is inhibited by octreotide and by inhibitors of the PI3K/AKT/mTOR pathway. *Neuroendocrinology* 2010 **91** 268–278. (https://doi.org/10.1159/000289569)

33 van Asselt SJ, Oosting SF, Brouwers AH, Bongaerts AH, de Jong JR, Lub-de Hooge MN, Oude Munnink TH, Fiebrich HB, Sluiter WJ, Links TP *et al*. Everolimus reduces (89)Zr-bevacizumab tumor uptake in patients with neuroendocrine tumors. *Journal of Nuclear Medicine* 2014 **55** 1087–1092. (https://doi.org/10.2967/jnumed.113.129056)

34 Pellat A, Dreyer C, Couffignal C, Walter T, Lombard-Bohas C, Niccoli P, Seitz JF, Hentic O, Andre T, Coriat R *et al*. Clinical and biomarker evaluations of sunitinib in patients with grade 3 digestive neuroendocrine neoplasms. *Neuroendocrinology* 2018 **107** 24–31. (https://doi.org/10.1159/000487237)

35 Zurita AJ, Khajavi M, Wu HK, Tye L, Huang X, Kulke MH, Lenz HJ, Meropol NJ, Carley W, DePrimo SE *et al*. Circulating cytokines and monocyte subpopulations as biomarkers of outcome and biological activity in sunitinib-treated patients with advanced neuroendocrine tumours. *British Journal of Cancer* 2015 **112** 1199–1205. (https://doi.org/10.1038/bjc.2015.73)

36 Grande E, Casanovas O, Earl J, Castellano DE, Garcia-Carbonero R, Teule A, Duran I, Fuster J, Sevilla I, Escudero P *et al*. sVEGFR2 and circulating tumor cells to predict for the efficacy of pazopanib in neuroendocrine tumors (NETs): PAZONET subgroup analysis. *Journal of Clinical Oncology* 2013 **31** 4140–4147.

37 Yao JC, Phan AT, Hess K, Fogelman D, Jacobs C, Dagohoy C, Leary C, Xie K & Ng CS. Perfusion computed tomography as functional biomarker in randomized run-in study of bevacizumab and everolimus in well-differentiated neuroendocrine tumors. *Pancreas* 2015 **44** 190–197. (https://doi.org/10.1097/MPA.0000000000000255)

38 Childs A, Kirkwood A, Edeline J, Luong TV, Watkins J, Lamarca A, Alrifai D, Nsiah-Sarbeng P, Gillmore R, Mayer A *et al*. Ki-67 index and response to chemotherapy in patients with neuroendocrine tumours. *Endocrine-Related Cancer* 2016 **23** 563–570. (https://doi.org/10.1530/ERC-16-0099)

39 Krug S, Boch M, Daniel H, Nimphius W, Muller D, Michl P, Rinke A & Gress TM. Streptozocin-based chemotherapy in patients with advanced neuroendocrine neoplasms – predictive and prognostic markers for treatment stratification. *PLoS ONE* 2015 **10** e0143822. (https://doi.org/10.1371/journal.pone.0143822)

40 Kulke MH, Hornick JL, Frauenhoffer C, Hooshmand S, Ryan DP, Enzinger PC, Meyerhardt JA, Clark JW, Stuart K, Fuchs CS *et al*. O6-methylguanine DNA methyltransferase deficiency and response to temozolomide-based therapy in patients with neuroendocrine tumors. *Clinical Cancer Research* 2009 **15** 338–345. (https://doi.org/10.1158/1078-0432.CCR-08-1476)

41 Campana D, Walter T, Pusceddu S, Gelsomino F, Graillot E, Prinzi N, Spallanzani A, Fiorentino M, Barritault M, Dall'Olio F *et al*. Correlation between MGMT promoter methylation and response to temozolomide-based therapy in neuroendocrine neoplasms: an observational retrospective multicenter study. *Endocrine* 2018 **60** 490–498. (https://doi.org/10.1007/s12020-017-1474-3)

42 Fishbein L, Ben-Maimon S, Keefe S, Cengel K, Pryma DA, Loaiza-Bonilla A, Fraker DL, Nathanson KL & Cohen DL. SDHB mutation carriers with malignant pheochromocytoma respond better to CVD. *Endocrine-Related Cancer* 2017 **24** L51–L55. (https://doi.org/10.1530/ERC-17-0086)

43 Walenkamp A, Crespo G, Fierro Maya F, Fossmark R, Igaz P, Rinke A, Tamagno G, Vitale G, Oberg K & Meyer T. Hallmarks of gastrointestinal neuroendocrine tumours: implications for treatment. *Endocrine-Related Cancer* 2014 **21** R445–R460. (https://doi.org/10.1530/ERC-14-0106)

44 Khan MS, Kirkwood A, Tsigani T, Garcia-Hernandez J, Hartley JA, Caplin ME & Meyer T. Circulating tumor cells as prognostic markers in neuroendocrine tumors. *Journal of Clinical Oncology* 2013 **31** 365–372. (https://doi.org/10.1200/JCO.2012.44.2905)

45 Khan MS, Kirkwood AA, Tsigani T, Lowe H, Goldstein R, Hartley JA, Caplin ME & Meyer T. Early changes in circulating tumor cells are associated with response and survival following treatment of metastatic neuroendocrine neoplasms. *Clinical Cancer Research* 2016 **22** 79–85. (https://doi.org/10.1158/1078-0432.CCR-15-1008)

46 Childs A, Vesely C, Ensell L, Lowe H, Luong TV, Caplin ME, Toumpanakis C, Thirlwell C, Hartley JA & Meyer T. Expression of somatostatin receptors 2 and 5 in circulating tumour cells from patients with neuroendocrine tumours. *British Journal of Cancer* 2016 **115** 1540–1547. (https://doi.org/10.1038/bjc.2016.377)

47 Carter L, Rothwell DG, Mesquita B, Smowton C, Leong HS, Fernandez-Gutierrez F, Li Y, Burt DJ, Antonello J, Morrow CJ *et al*. Molecular analysis of circulating tumor cells identifies distinct copy-number profiles in patients with chemosensitive and chemorefractory small-cell lung cancer. *Nature Medicine* 2017 **23** 114–119. (https://doi.org/10.1038/nm.4239)

48 Wang VE, Young L, Ali S, Miller VA, Urisman A, Wolfe J, Bivona TG, Damato B, Fogh S & Bergsland EK. A case of metastatic atypical neuroendocrine tumor with ALK translocation and diffuse brain metastases. *Oncologist* 2017 **22** 768–773. (https://doi.org/10.1634/theoncologist.2017-0054)

49 Sharabi A, Kim SS, Kato S, Sanders PD, Patel SP, Sanghvi P, Weihe E & Kurzrock R. Exceptional response to nivolumab and stereotactic body radiation therapy (SBRT) in neuroendocrine cervical carcinoma with high tumor mutational burden: management considerations from the Center for Personalized Cancer Therapy at UC San Diego Moores Cancer Center. *Oncologist* 2017 **22** 631–637. (https://doi.org/10.1634/theoncologist.2016-0517)

50 Allin DM, Shaikh R, Carter P, Thway K, Sharabiani MTA, Gonzales-de-Castro D, O'Leary B, Garcia-Murillas I, Bhide S, Hubank M *et al*. Circulating tumour DNA is a potential biomarker for disease progression and response to targeted therapy in advanced thyroid cancer. *European Journal of Cancer* 2018 **103** 165–175. (https://doi.org/10.1016/j.ejca.2018.08.013)

51 Zatelli MC, Grossrubatscher EM, Guadagno E, Sciammarella C, Faggiano A & Colao A. Circulating tumor cells and miRNAs as prognostic markers in neuroendocrine neoplasms. *Endocrine-Related Cancer* 2017 **24** R223–R237. (https://doi.org/10.1530/ERC-17-0091)

52 Cwikla JB, Bodei L, Kolasinska-Cwikla A, Sankowski A, Modlin IM & Kidd M. Circulating transcript analysis (NETest) in GEP-NETs

treated With somatostatin analogs defines therapy. *Journal of Clinical Endocrinology and Metabolism* 2015 **100** E1437–E1445. (https://doi.org/10.1210/jc.2015-2792)
53 Modlin IM, Kidd M, Malczewska A, Drozdov I, Bodei L, Matar S & Chung KM. The NETest: the clinical utility of multigene blood analysis in the diagnosis and management of neuroendocrine tumors. *Endocrinology and Metabolism Clinics of North America* 2018 **47** 485–504. (https://doi.org/10.1016/j.ecl.2018.05.002)
54 Alvarez MJ, Subramaniam PS, Tang LH, Grunn A, Aburi M, Rieckhof G, Komissarova EV, Hagan EA, Bodei L, Clemons PA *et al*. A precision oncology approach to the pharmacological targeting of mechanistic dependencies in neuroendocrine tumors. *Nature Genetics* 2018 **50** 979–989. (https://doi.org/10.1038/s41588-018-0138-4)
55 Pfragner R, Behmel A, Hoger H, Beham A, Ingolic E, Stelzer I, Svejda B, Moser VA, Obenauf AC, Siegl V *et al*. Establishment and characterization of three novel cell lines – P-STS, L-STS, H-STS – derived from a human metastatic midgut carcinoid. *Anticancer Research* 2009 **29** 1951–1961.
56 McMillin DW, Delmore J, Weisberg E, Negri JM, Geer DC, Klippel S, Mitsiades N, Schlossman RL, Munshi NC, Kung AL *et al*. Tumor cell-specific bioluminescence platform to identify stroma-induced changes to anticancer drug activity. *Nature Medicine* 2010 **16** 483–489. (https://doi.org/10.1038/nm.2112)
57 Mitra A, Mishra L & Li S. Technologies for deriving primary tumor cells for use in personalized cancer therapy. *Trends in Biotechnology* 2013 **31** 347–354. (https://doi.org/10.1016/j.tibtech.2013.03.006)
58 Majumder B, Baraneedharan U, Thiyagarajan S, Radhakrishnan P, Narasimhan H, Dhandapani M, Brijwani N, Pinto DD, Prasath A, Shanthappa BU *et al*. Predicting clinical response to anticancer drugs using an ex vivo platform that captures tumour heterogeneity. *Nature Communications* 2015 **6** 6169. (https://doi.org/10.1038/ncomms7169)
59 Gao H, Korn JM, Ferretti S, Monahan JE, Wang Y, Singh M, Zhang C, Schnell C, Yang G, Zhang Y *et al*. High-throughput screening using patient-derived tumor xenografts to predict clinical trial drug response. *Nature Medicine* 2015 **21** 1318–1325. (https://doi.org/10.1038/nm.3954)
60 Hidalgo M, Amant F, Biankin AV, Budinska E, Byrne AT, Caldas C, Clarke RB, de Jong S, Jonkers J, Maelandsmo GM *et al*. Patient-derived xenograft models: an emerging platform for translational cancer research. *Cancer Discovery* 2014 **4** 998–1013. (https://doi.org/10.1158/2159-8290.CD-14-0001)
61 Bertotti A, Migliardi G, Galimi F, Sassi F, Torti D, Isella C, Cora D, Di Nicolantonio F, Buscarino M, Petti C *et al*. A molecularly annotated platform of patient-derived xenografts ('xenopatients') identifies HER2 as an effective therapeutic target in cetuximab-resistant colorectal cancer. *Cancer Discovery* 2011 **1** 508–523. (https://doi.org/10.1158/2159-8290.CD-11-0109)
62 Byrne AT, Alferez DG, Amant F, Annibali D, Arribas J, Biankin AV, Bruna A, Budinska E, Caldas C, Chang DK *et al*. Interrogating open issues in cancer precision medicine with patient-derived xenografts. *Nature Reviews: Cancer* 2017 **17** 254–268. (https://doi.org/10.1038/nrc.2016.140)
63 Grozinsky-Glasberg S, Shimon I & Rubinfeld H. The role of cell lines in the study of neuroendocrine tumors. *Neuroendocrinology* 2012 **96** 173–187. (https://doi.org/10.1159/000338793)
64 Hofving T, Arvidsson Y, Almobarak B, Inge L, Pfragner R, Persson M, Stenman G, Kristiansson E, Johanson V & Nilsson O. The neuroendocrine phenotype, genomic profile and therapeutic sensitivity of GEPNET cell lines. *Endocrine-Related Cancer* 2018 **25** 367–380. (https://doi.org/10.1530/ERC-17-0445)
65 Date S & Sato T. Mini-gut organoids: reconstitution of the stem cell niche. *Annual Review of Cell and Developmental Biology* 2015 **31** 269–289. (https://doi.org/10.1146/annurev-cellbio-100814-125218)
66 Aboulkheyr Es H, Montazeri L, Aref AR, Vosough M & Baharvand H. Personalized cancer medicine: an organoid approach. *Trends in Biotechnology* 2018 **36** 358–371. (https://doi.org/10.1016/j.tibtech.2017.12.005)
67 Lin H, Jiang X, Zhu H, Jiang W, Dong X, Qiao H, Sun X & Jiang H. 2ME2 inhibits the activated hypoxia-inducible pathways by cabozantinib and enhances its efficacy against medullary thyroid carcinoma. *Tumour Biology* 2016 **37** 381–391. (https://doi.org/10.1007/s13277-015-3816-1)
68 Saunders LR, Bankovich AJ, Anderson WC, Aujay MA, Bheddah S, Black K, Desai R, Escarpe PA, Hampl J, Laysang A *et al*. A DLL3-targeted antibody-drug conjugate eradicates high-grade pulmonary neuroendocrine tumor-initiating cells in vivo. *Science Translational Medicine* 2015 **7** 302ra136. (https://doi.org/10.1126/scitranslmed.aac9459)
69 Jiang J, Wang DD, Yang M, Chen D, Pang L, Guo S, Cai J, Wery JP, Li L, Li HQ *et al*. Comprehensive characterization of chemotherapeutic efficacy on metastases in the established gastric neuroendocrine cancer patient derived xenograft model. *Oncotarget* 2015 **6** 15639–15651. (https://doi.org/10.18632/oncotarget.3712)
70 Clermont PL, Lin D, Crea F, Wu R, Xue H, Wang Y, Thu KL, Lam WL, Collins CC, Wang Y *et al*. Polycomb-mediated silencing in neuroendocrine prostate cancer. *Clinical Epigenetics* 2015 **7** 40. (https://doi.org/10.1186/s13148-015-0074-4)
71 Chamberlain CE, German MS, Yang K, Wang J, VanBrocklin H, Regan M, Shokat KM, Ducker GS, Kim GE, Hann B *et al*. A patient-derived xenograft model of pancreatic neuroendocrine tumors identifies Sapanisertib as a possible new treatment for everolimus-resistant tumors. *Molecular Cancer Therapeutics* 2018 **17** 2702–2709. (https://doi.org/10.1158/1535-7163.MCT-17-1204)
72 Morton CL & Houghton PJ. Establishment of human tumor xenografts in immunodeficient mice. *Nature Protocols* 2007 **2** 247–250. (https://doi.org/10.1038/nprot.2007.25)
73 Gaudenzi G, Albertelli M, Dicitore A, Wurth R, Gatto F, Barbieri F, Cotelli F, Florio T, Ferone D, Persani L *et al*. Patient-derived xenograft in zebrafish embryos: a new platform for translational research in neuroendocrine tumors. *Endocrine* 2017 **57** 214–219. (https://doi.org/10.1007/s12020-016-1048-9)
74 Fior R, Povoa V, Mendes RV, Carvalho T, Gomes A, Figueiredo N & Ferreira MG. Single-cell functional and chemosensitive profiling of combinatorial colorectal therapy in zebrafish xenografts. *PNAS* 2017 **114** E8234–E8243. (https://doi.org/10.1073/pnas.1618389114)
75 Lawson ND & Weinstein BM. In vivo imaging of embryonic vascular development using transgenic zebrafish. *Developmental Biology* 2002 **248** 307–318. (https://doi.org/10.1006/dbio.2002.0711)
76 Vitale G, Gaudenzi G, Dicitore A, Cotelli F, Ferone D & Persani L. Zebrafish as an innovative model for neuroendocrine tumors. *Endocrine-Related Cancer* 2014 **21** R67–R83. (https://doi.org/10.1530/ERC-13-0388)

Received 8 January 2019
Revised version received 6 April 2019
Accepted 2 May 2019

International Journal of
Molecular Sciences

MDPI

Article

Vandetanib versus Cabozantinib in Medullary Thyroid Carcinoma: A Focus on Anti-Angiogenic Effects in Zebrafish Model

Silvia Carra [1], Germano Gaudenzi [2], Alessandra Dicitore [2], Davide Saronni [3], Maria Celeste Cantone [3], Alice Plebani [2], Anna Ghilardi [4], Maria Orietta Borghi [5,6], Leo J. Hofland [7], Luca Persani [1,3] and Giovanni Vitale [2,3,*]

1 Laboratory of Endocrine and Metabolic Research, Istituto Auxologico Italiano, IRCCS, 20095 Cusano Milanino, MI, Italy; carra-silvia@libero.it (S.C.); luca.persani@unimi.it (L.P.)
2 Laboratory of Geriatric and Oncologic Neuroendocrinology Research, Istituto Auxologico Italiano, IRCCS, 20095 Cusano Milanino, MI, Italy; germano.gaudenzi@gmail.com (G.G.); alessandra.dicitore@libero.it (A.D.); plebanialice94@gmail.com (A.P.)
3 Department of Medical Biotechnology and Translational Medicine, University of Milan, 20122 Milan, Italy; davide.saronni1@gmail.com (D.S.); celeste.cantone@gmail.com (M.C.C.)
4 Department of Biosciences, University of Milan, 20133 Milan, Italy; anna.ghilardi@unimi.it
5 Experimental Laboratory of Immuno-Rheumatology, Istituto Auxologico Italiano, IRCCS, 20095 Cusano Milanino, MI, Italy; maria.borghi@unimi.it
6 Department of Clinical Sciences and Community Health, University of Milan, 20122 Milan, Italy
7 Division of Endocrinology, Department of Internal Medicine, Erasmus MC, 3015 GD Rotterdam, The Netherlands; l.hofland@erasmusmc.nl
* Correspondence: giovanni.vitale@unimi.it; Tel.: +39-02-619-112-023

Citation: Carra, S.; Gaudenzi, G.; Dicitore, A.; Saronni, D.; Cantone, M.C.; Plebani, A.; Ghilardi, A.; Borghi, M.O.; Hofland, L.J.; Persani, L.; et al. Vandetanib versus Cabozantinib in Medullary Thyroid Carcinoma: A Focus on Anti-Angiogenic Effects in Zebrafish Model. *Int. J. Mol. Sci.* **2021**, *22*, 3031. https://doi.org/10.3390/ijms22063031

Received: 29 January 2021
Accepted: 12 March 2021
Published: 16 March 2021

Abstract: Medullary thyroid carcinoma (MTC) is a tumor deriving from the thyroid C cells. Vandetanib (VAN) and cabozantinib (CAB) are two tyrosine kinase inhibitors targeting REarranged during Transfection (RET) and other kinase receptors and are approved for the treatment of advanced MTC. We aim to compare the in vitro and in vivo anti-tumor activity of VAN and CAB in MTC. The effects of VAN and CAB on viability, cell cycle, and apoptosis of TT and MZ-CRC-1 cells are evaluated in vitro using an MTT assay, DNA flow cytometry with propidium iodide, and Annexin V-FITC/propidium iodide staining, respectively. In vivo, the anti-angiogenic potential of VAN and CAB is evaluated in *Tg(fli1a:EGFP)^{y1}* transgenic fluorescent zebrafish embryos by analyzing the effects on the physiological development of the sub-intestinal vein plexus and the tumor-induced angiogenesis after TT and MZ-CRC-1 xenotransplantation. VAN and CAB exert comparable effects on TT and MZ-CRC-1 viability inhibition and cell cycle perturbation, and stimulated apoptosis with a prominent effect by VAN in MZ-CRC-1 and CAB in TT cells. Regarding zebrafish, both drugs inhibit angiogenesis in a dose-dependent manner, in particular CAB shows a more potent anti-angiogenic activity than VAN. To conclude, although VAN and CAB show comparable antiproliferative effects in MTC, the anti-angiogenic activity of CAB appears to be more relevant.

Keywords: medullary thyroid carcinoma (MTC); zebrafish; tumor xenograft; tyrosine kinase inhibitors (TKIs); angiogenesis; cabozantinib; vandetanib

1. Introduction

Medullary thyroid carcinoma (MTC) is a rare neuroendocrine tumor, that arises from calcitonin-producing parafollicular C cells of the thyroid gland [1,2]. Although the majority of MTCs are sporadic, in 25% of patients this malignancy occurs in a hereditary form as the dominant component of the Multiple Endocrine Neoplasia (MEN) type 2 syndromes, MEN2A and MEN2B, or familial MTC [3,4]. Alterations in the *REarranged during Transfection* (*RET*) proto-oncogene represent the most crucial events that lead to the development of MTC. *RET* encodes a transmembrane receptor of the tyrosine kinase family [5–9]. The

clinical course of patients with MTC is variable, ranging from mild to extremely aggressive. Occurring at diagnosis, about half of the patients present with an advanced stage (III or IV) [3,10]. Surgery is the only curative treatment for MTC since other therapies, including radiotherapy and chemotherapy, have not demonstrated an improvement in long-term survival [3,11].

Although genetic alterations of *RET* are considered the main event involved in the pathogenesis of the vast majority of MTC cases, other kinase receptors may play an important role in the development and progression of this malignancy. Overexpression of epidermal growth factor receptor (EGFR), vascular endothelial growth factor receptors (VEGFRs), fibroblast growth factor receptor 4 (FGFR-4), and tyrosine kinase receptor for the hepatocyte growth factor (encoded by the *MET* proto-oncogene) often has been reported in MTCs [12]. The increased understanding in the molecular pathogenesis of MTC has led to the testing of several tyrosine kinase inhibitors (TKIs) specific for RET and other potential targets involved in angiogenesis [13,14]. Indeed, MTC is highly vascularized, and the impairment of tumor-induced angiogenesis represents an effective therapeutic approach [15–17].

Vandetanib (VAN) and Cabozantinib (CAB) are TKIs currently used for treating unresectable, progressive, and symptomatic MTCs. These drugs increase progression-free survival [18–20]. VAN (ZD6474) targets RET, VEGFR-2 and -3, FGFR, and EGFR [14,21,22]. CAB (XL184) is a small molecule targeting RET, VEGFR-2 and MET [23,24]. A head-to-head comparison in the same clinical trial between VAN and CAB has not been published yet. Two different phase III trials, ZETA and EXAM, evaluated the anti-tumor activity of VAN and CAB, respectively, versus a placebo [25,26]. However, several differences in study-design and enrolled populations make it difficult to make a direct comparison between these two drugs [27–29]. More recently, a retrospective multicenter study collected clinical data from a cohort of 48 patients with metastatic or locally advanced MTC who received treatment with VAN and/or CAB. Median progression-free survival for VAN and CAB were 17 and four months, respectively. However, the poorer prognosis of patients treated with CAB might be due to the high number of patients receiving CAB as second-line treatment after VAN treatment failure, when the course of the disease was more aggressive [30].

Lacking clinical trials directly comparing VAN versus CAB in patients with MTC, there are only a few in vitro studies evaluating the cell survival and anti-proliferative effects of these compounds in MTC cell lines [31,32]. Presently, comparative studies in vitro and/or in vivo on the effects of VAN and CAB on tumor-induced angiogenesis in MTC have not been published.

The zebrafish (*Danio rerio*) is a powerful animal model that has become an important preclinical tool particularly suitable for analyzing different aspects of tumor growth and progression, such as cell–stromal interactions, tumor-induced angiogenesis, and metastasis formation by performing xenotransplantation of human or mouse cancer cells in several sites of embryos [33]. Taking this context, we have recently developed an in vivo platform, based on xenotransplantation of neuroendocrine tumor cells in *Tg(fli1a:EGFP)*^{y} transgenic fluorescent zebrafish embryos expressing EGFP (Enhanced Green Fluorescent Protein) under the control of the endothelial-specific gene promoter *fli1a* [34–36]. The implantation of MTC cell lines allows us to follow in vivo tumor-induced angiogenesis. Moreover, taking advantage of the permeability of zebrafish embryos to small molecules dissolved in their culture media, it is easy to study the anti-angiogenic activity of TKIs.

The aim of the present study is to compare in vitro and in vivo the anti-tumor activity of VAN and CAB in MTC, with a particular focus on angiogenesis through this innovative zebrafish model.

2. Results

2.1. Effects of Vandetanib (VAN) and Cabozantinib (CAB) on Cell Viability in Human Medullary Thyroid Carcinoma (MTC) Cell Lines

Following six days of incubation, both vandetanib (VAN) and cabozantinib (CAB) significantly decreased the viability of TT (Figure 1a) (VAN, IC_{50}: 1.5×10^{-7} M, maximal inhibition: −92.7%; CAB, IC_{50}: 1.7×10^{-7} M, maximal inhibition: −91.2%) and MZ-CRC-1 (Figure 1b) (VAN, IC_{50}: 1×10^{-7} M, maximal inhibition: −83.7%; CAB, IC_{50}: 1.5×10^{-7} M, maximal inhibition: −74.9%) cell lines. Considering these results for further in vitro experiments, we selected the IC_{50} concentrations of VAN and CAB in MTC cells after six days of incubation.

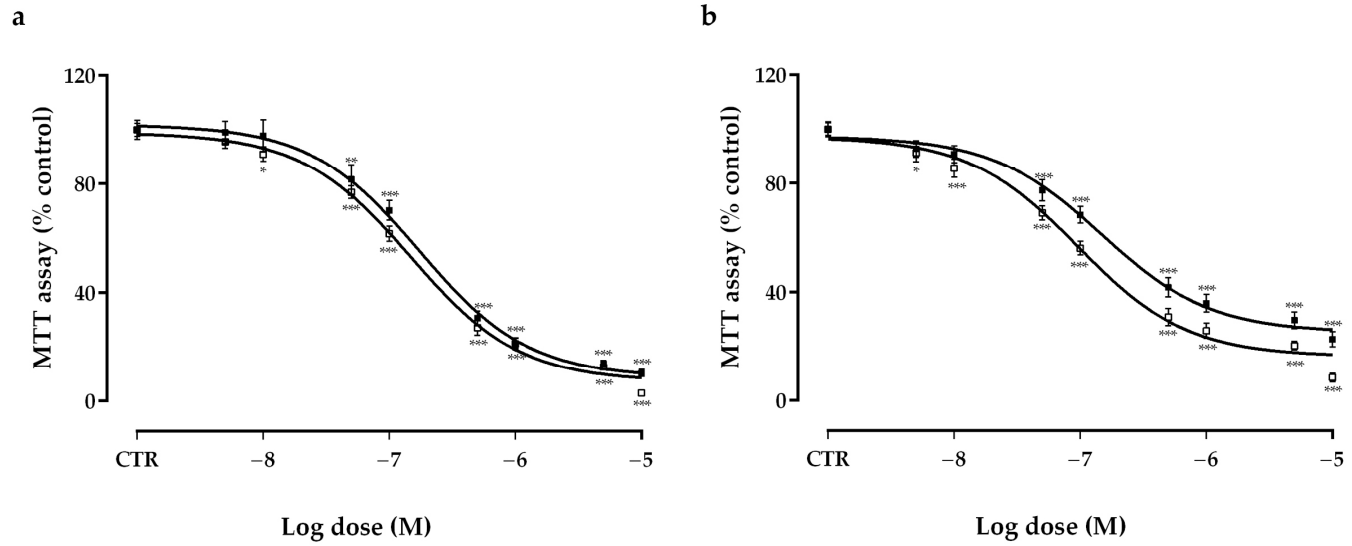

Figure 1. Effects of vandetanib (VAN) (□) and cabozantinib (CAB) (■) on cell viability in TT (**a**) and MZ-CRC-1 (**b**) cell lines measured using an MTT assay. Cells were incubated for six days with vehicle (control), or with the drug at different concentrations, as described in the Material and Methods. Dose response curves were expressed as a nonlinear regression (curve fit) of log (concentration drug) versus the percentage of the control. Values represent the mean ± S.E.M. of at least three independent experiments in six replicates. Control (CTR) values have been set to 100%. * $p < 0.05$; ** $p < 0.01$; *** $p < 0.001$.

2.2. Effects of Vandetanib (VAN) and Cabozantinib (CAB) on Cell Cycle

Both drugs decreased significantly the fraction of TT cells in the S and G_2/M phases after six days of incubation, with a more prominent effect after cabozantinib (CAB) (−59.5% and −22.3% versus the untreated control, $p < 0.001$ and $p < 0.01$, respectively) compared to vandetanib (VAN) (−31.4% and −12.5% versus the untreated control, $p < 0.001$ and $p < 0.05$, respectively) (Figure 2c,d); together with a concomitant accumulation of cells in G_0/G_1 (VAN: +29.3%, CAB: +20.1%, $p < 0.05$) (Figure 2b) and sub-G1 phase (VAN: +141%, CAB: +176%, $p < 0.001$) (Figure 2a). Regarding MZ-CRC-1 cells, VAN exerted a more potent effect in decreasing cells in S (−61.7%, versus the untreated control $p < 0.001$) and G_2/M (−26.5%, versus the untreated control $p < 0.05$) phases (Figure 2g,h) compared to CAB, which significantly decreased the number of cells in the S phase (−34.2% versus the untreated control, $p < 0.01$) (Figure 2g). Similarly, both drugs increased the proportion of MZ-CRC-1 cells in the G_0/G_1 phase (VAN: +11.8%, versus the untreated control, $p < 0.01$; CAB: +9.6% versus the untreated control, $p < 0.01$) and the sub-G1 phase (VAN: +98%, $p < 0.05$; CAB: +91%, $p < 0.01$) (Figure 2e,f).

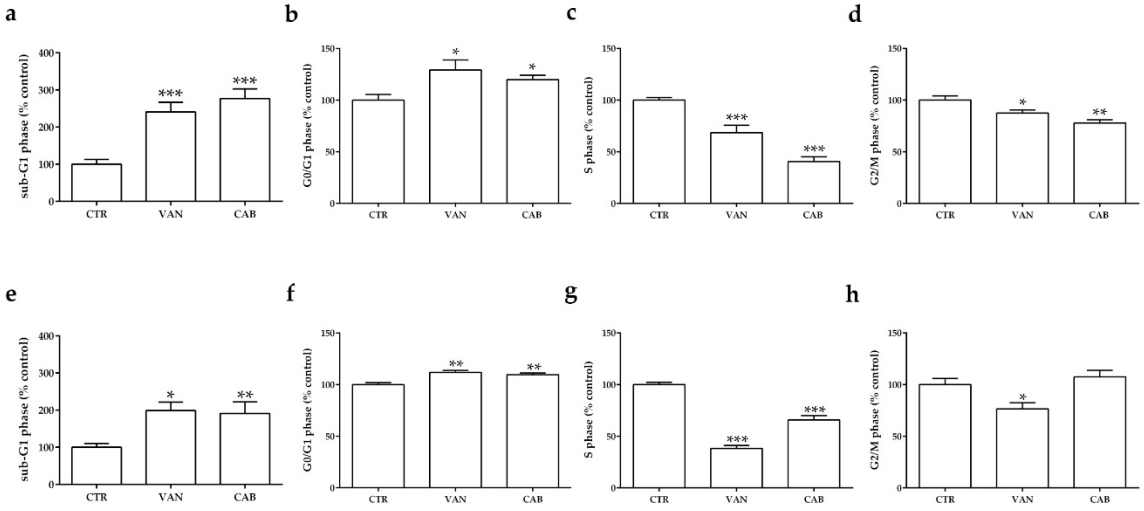

Figure 2. Effects of vandetanib (VAN) and cabozantinib (CAB) on the cell cycle in medullary thyroid carcinoma (MTC) cell lines. Cell cycle analysis after six days of incubation with VAN and CAB in TT (**a**–**d**) and MZ-CRC-1 cell lines (**e**–**h**). Cells were detected using FACS analysis after staining with propidium iodide. Control (CTR) values have been set to 100%. Cell cycle distribution is expressed as the percentage of cells in the G_0/G_1, S, and G_2/M phases compared to the untreated CTR. Values represent the mean ± S.E.M. of at least three independent experiments. * $p < 0.05$; ** $p < 0.01$; *** $p < 0.001$.

2.3. Effects of Vandetanib (VAN) and Cabozantinib (CAB) on Apoptosis

Following six days of incubation, both drugs significantly increased the fraction of medullary thyroid carcinoma (MTC) cells in apoptosis. Cabozantinib (CAB) showed a more potent increase in the number of TT cells in early apoptosis (+1750% versus the untreated control, $p < 0.001$) and late apoptosis (+316% versus the untreated control, $p < 0.001$) compared to vandetanib (VAN) (+805% and +215% versus the untreated control, $p < 0.001$ and $p < 0.01$, respectively) (Figure 3a,b). There was no statistically significant change in the number of necrotic treated TT cells compared to the untreated control (Figure 3c). Regarding MZ-CRC-1, VAN markedly increased the fraction of cells in early apoptosis (+488%, versus the untreated control, $p < 0.05$), late apoptosis (+106% versus the untreated control, $p < 0.05$) and necrosis (+117% versus the untreated control, $p < 0.01$). A lower pro-apoptotic activity was observed with CAB, which increased the fraction of MZ-CRC-1 cells in early apoptosis (+396% versus the untreated control, $p < 0.05$), late apoptosis (+77% versus the untreated control, $p < 0.05$) and necrosis (+85% versus the untreated control, $p < 0.01$, respectively) (Figure 3d–f).

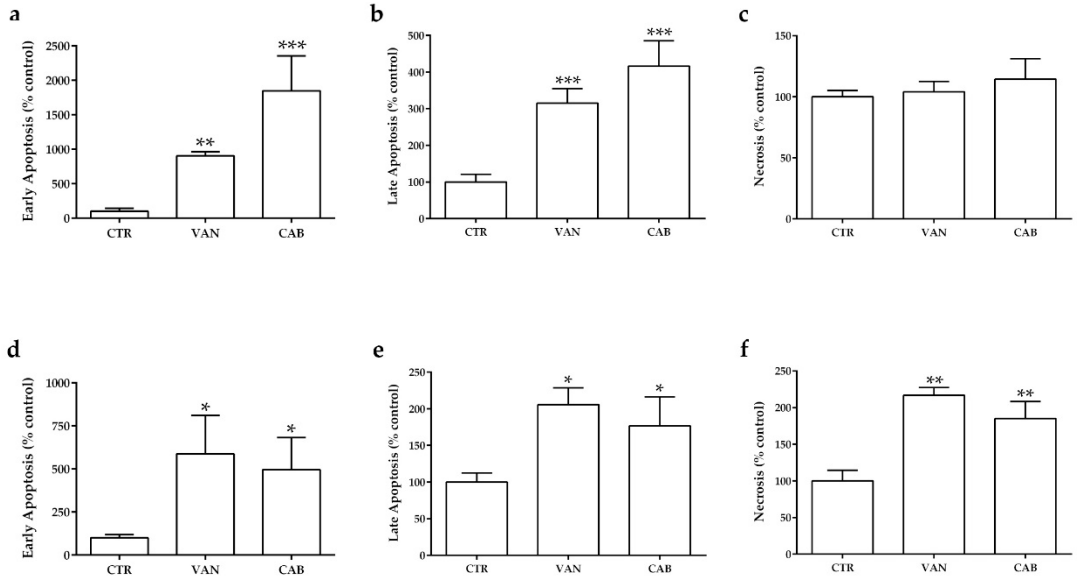

Figure 3. Effects of vandetanib (VAN) and cabozantinib (CAB) on apoptosis in medullary thyroid carcinoma (MTC) cell lines. Cell death analysis after six days of incubation with VAN and CAB in TT (**a**–**c**) and MZ-CRC-1 cell lines (**d**–**f**) through flow cytometry with Annexin V and propidium iodine. The proportions of cells in early apoptosis (**a**,**d**), late apoptosis (**b**,**e**) and necrosis (**c**,**f**) were expressed as the percentage compared with the untreated control (CTR) and represent the mean ± S.E.M. of at least three independent experiments. * $p < 0.05$; ** $p < 0.01$; *** $p < 0.001$.

2.4. Effects of Vandetanib (VAN) and Cabozantinib (CAB) on Physiological Angiogenesis in Zebrafish Embryos

To test the anti-angiogenic potential of vandetanib (VAN) and cabozantinib (CAB) on the physiological angiogenesis of transgenic fluorescent zebrafish *Tg(fli1a:EGFP)*^{y1}, we treated embryos with different concentrations of these tyrosine kinase inhibitors (TKIs) dissolved in the culture media. Following 24 h of treatment, we analyzed the development of the SIV (sub-intestinal vein) plexus, in particular we counted the number of vertical vessels comprising the SIV basket. Occurring at 72 h post fertilization (hpf) in the control embryos treated with vehicle dimethyl sulfoxide (DMSO), SIV developed as a basket-like structure over the yolk, blood vessels were lined in an orderly vertical pattern, and the integrity appeared to be well maintained (Figure 4a). Embryos treated with increasing concentrations of VAN and CAB showed a dose-dependent reduction in the number of vertical vessels and their size appeared narrower than those observed in the controls (Figure 4b–e). CAB displayed a more potent anti-angiogenic effect than VAN (Figure 4b–e). Occurring at 5×10^{-6} M, the highest tested dose for CAB, we observed a complete inhibition of the SIV vessel formation in embryos (Figure 4c,e) while, at this concentration, VAN (Figure 4b,d) only moderately reduced the number of vertical vessels in embryos compared to the control (Figure 4a).

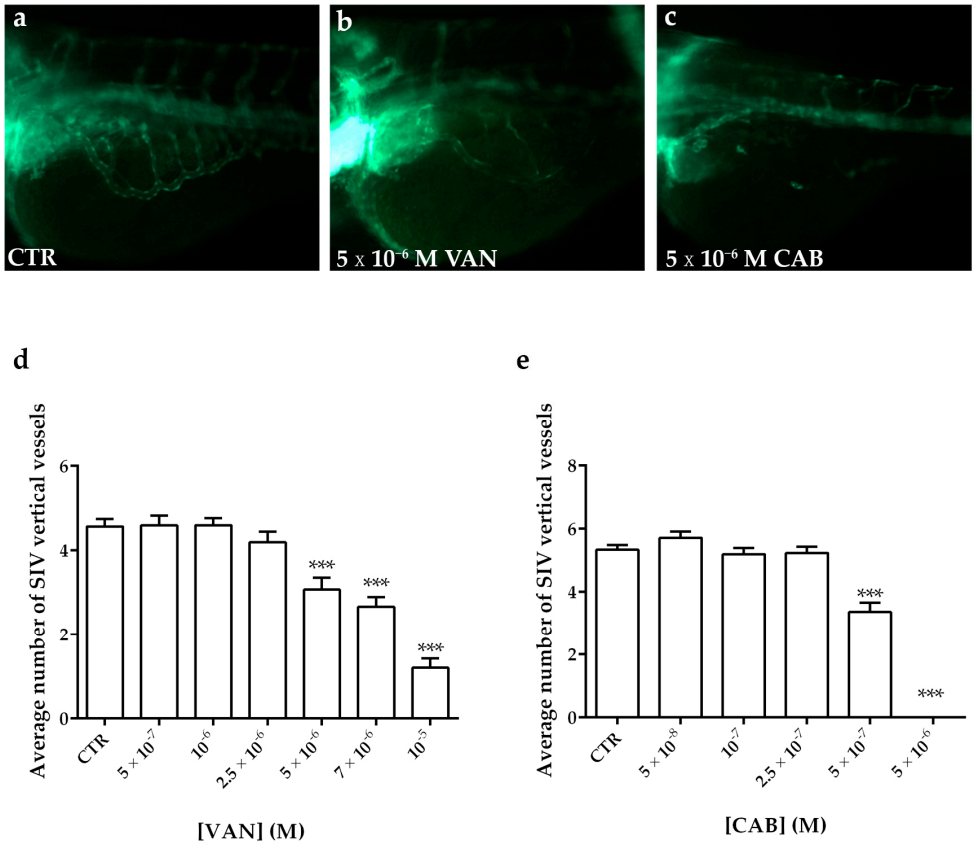

Figure 4. Anti-angiogenic effect of vandetanib (VAN) and cabozantinib (CAB) on the physiological development of the zebrafish sub-intestinal vein (SIV) plexus. Representative fluorescence images of the SIV basket of 72 hpf *Tg(fli1a:EGFP)*^{y1} zebrafish embryos treated for 24 h with dimethyl sulfoxide (DMSO) (**a**), 5 × 10^{-6} M VAN (**b**) and CAB (**c**). Following 24 h of VAN (**d**) and CAB (**e**) treatments at different concentrations, the number of vertical vessels comprising the SIV basket was counted and compared with that of the control (CTR) embryos. Graphed values represent the mean ± S.E.M. *** $p < 0.001$ versus the CTR. Embryos are shown anterior to the left.

2.5. Effects of Vandetanib (VAN) and Cabozantinib (CAB) on Tumor-Induced Angiogenesis in Zebrafish Embryos

We analyzed the anti-angiogenic potential of vandetanib (VAN) and cabozantinib (CAB) on TT and MZ-CRC-1 cell lines implanted in 48 hpf *Tg(fli1a:EGFP)*^{y1} zebrafish embryos, taking advantage of the zebrafish medullary thyroid carcinoma (MTC) xenograft platform. Red dye-loaded MTC cells were grafted into the subperidermal space (between the periderm and the yolk syncytial layer) close to the sub-intestinal vein (SIV) plexus of 48 hpf embryos. Following only 24 h, grafted embryos showed vessel structures that sprouted from the SIV plexus toward the tumor mass (Figure 5).

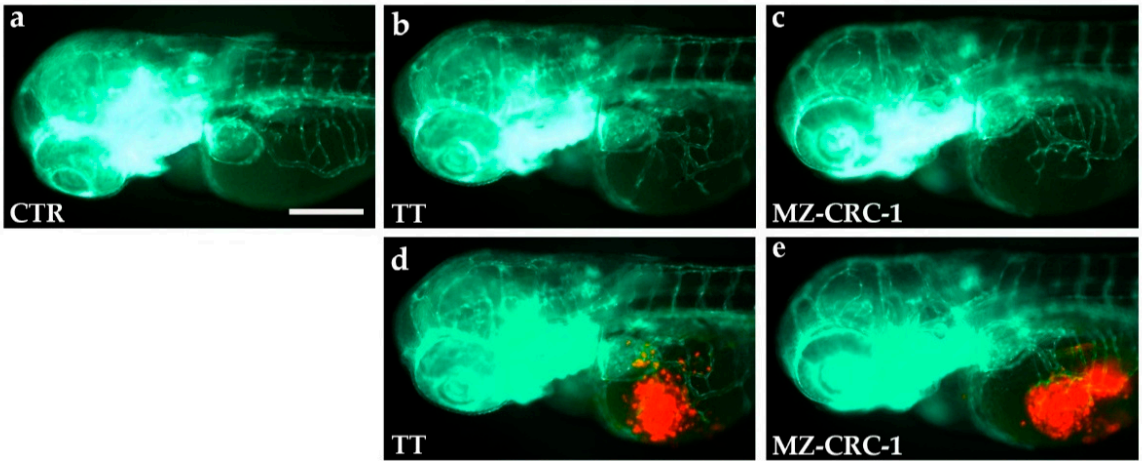

Figure 5. TT and MZ-CRC-1 implanted cells stimulate angiogenesis in zebrafish embryos after only 24 h post-injection. Representative fluorescence images of 72 hpf *Tg(fli1a:EGFP)*^{y1} zebrafish control embryos (**a**) and embryos implanted at 48 hpf with TT (**b**,**d**) and MZ-CRC-1 cells (**c**,**e**). The red channel, corresponding to TT or MZ-CRC-1 cells, was omitted in panels b and c to highlight the tumor-induced microvascular network. Compared to the control, grafted embryos showed vessels in green that sprout from the sub-intestinal vein (SIV) toward the xenograft of both cell lines. Embryos are shown anterior to the left. Scale bar: 100 μm.

Following the tumor cell implantation, injected embryos were treated with different concentrations of VAN and CAB. Following 24 h of treatment, the quantification of the tumor-induced vessel length revealed a reduction in vascular sprouts starting from the SIV plexus in a dose-dependent manner for both drugs, compared to dimethyl sulfoxide (DMSO)-treated embryos (Figures 6 and 7). Particularly, CAB resulted in being more potent in inhibiting tumor-induced angiogenesis. Regarding both cell lines, the IC_{50} of CAB (4.6×10^{-7} M and 5.7×10^{-7} M in embryos xenotransplanted with TT and MZ-CRC-1, respectively) was significantly lower ($p < 0.0001$) than the VAN IC_{50} (2.5×10^{-6} M and 2.8×10^{-6} M in embryos xenotransplanted with TT and MZ-CRC-1, respectively) after 24 h of treatment. Moreover, CAB exerted a maximal anti-angiogenic effect (E_{max}) that was significantly higher than VAN ($p < 0.005$) in zebrafish embryos injected with both cell lines (Figures 6g,h and 7g,h).

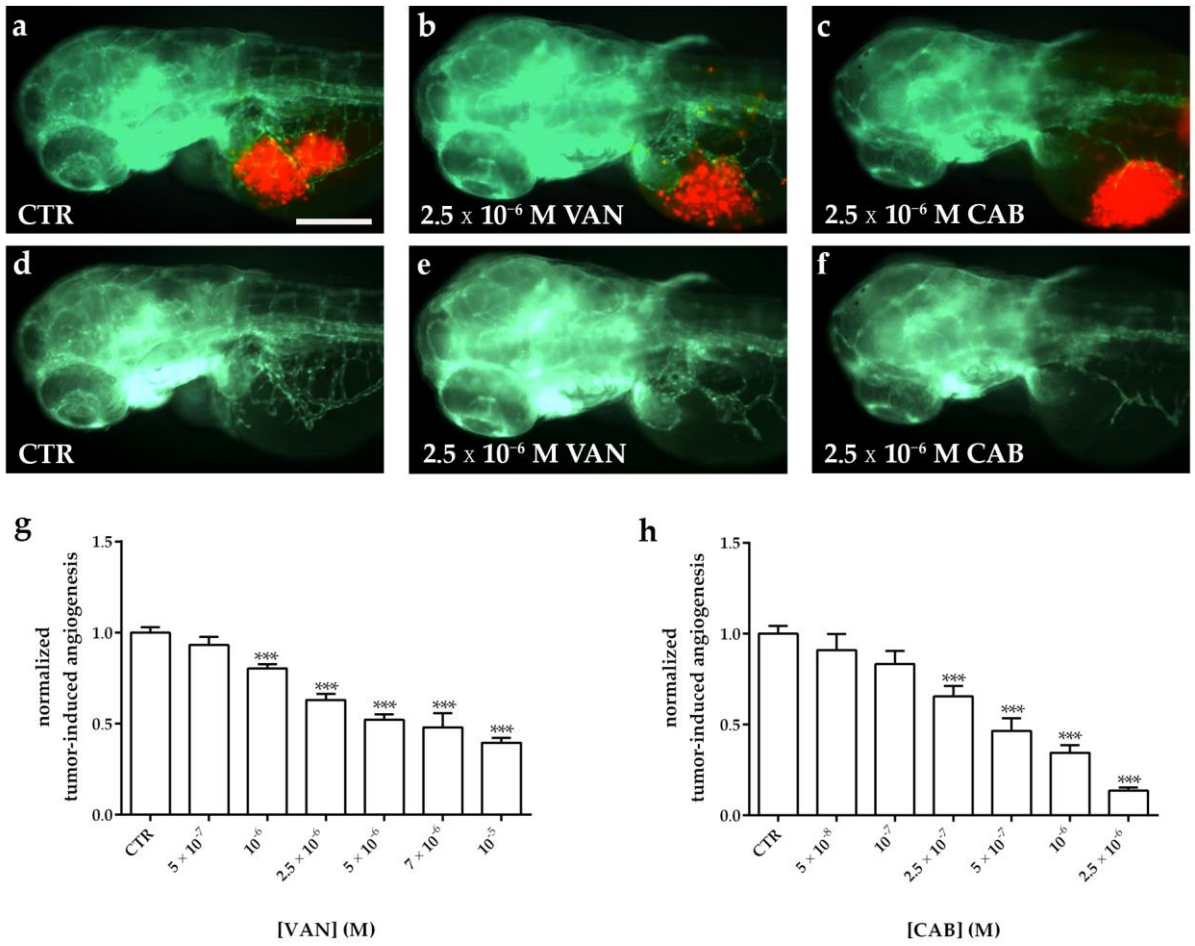

Figure 6. Effect of vandetanib (VAN) and cabozantinib (CAB) treatments on tumor-induced angiogenesis after TT cell xenograft in zebrafish embryos. Representative fluorescence images of 72 hpf *Tg(fli1a:EGFP)*^{y1} zebrafish embryos implanted at 48 hpf with TT cells and subsequently treated for 24 h with dimethyl sulfoxide (DMSO) (**a**,**d**), VAN (**b**,**e**) and CAB (**c**,**f**). The red channel, corresponding to TT cells, was omitted in panels d, e, and f to highlight the tumor-induced microvascular network. Grafted larvae showed vessels in green that sprout from the sub-intestinal vein (SIV) toward the xenograft. Quantification of tumor-induced angiogenesis in TT-injected *Tg(fli1a:EGFP)*^{y1} embryos after 24 h of VAN (**g**) and CAB (**h**) treatments at different concentrations. Control (CTR) values have been set to 1.0. Graphed values represent the mean ± S.E.M. *** $p < 0.001$ versus CTR. Embryos are shown anterior to the left. Scale bar: 100 µm.

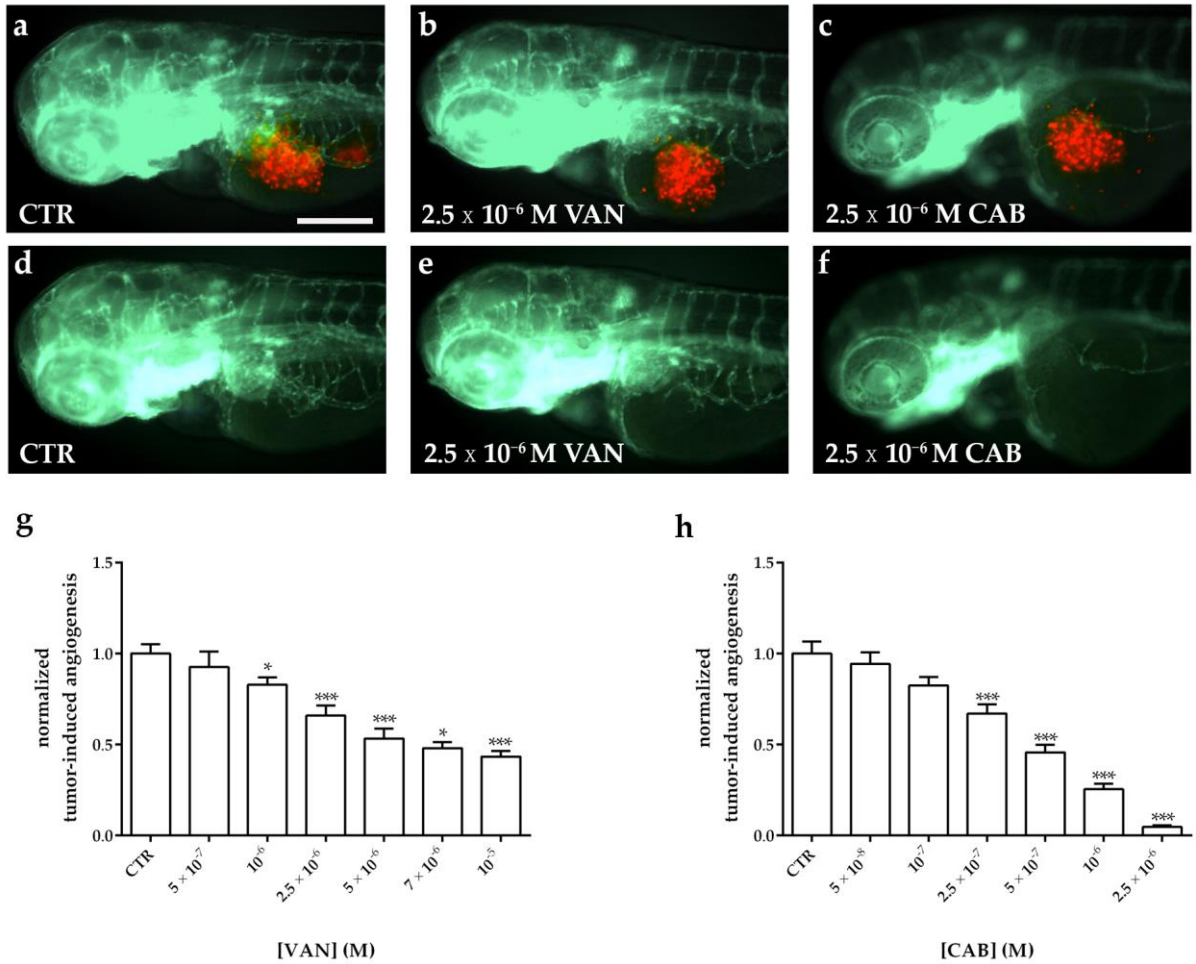

Figure 7. Effect of vandetanib (VAN) and cabozantinib (CAB) treatments on tumor-induced angiogenesis after MZ-CRC-1 cell xenograft in zebrafish embryos. Representative fluorescence images of 72 hpf *Tg(fli1a:EGFP)*^{y1} zebrafish embryos implanted at 48 hpf with MZ-CRC-1 cells and subsequently treated for 24 h with dimethyl sulfoxide (DMSO) (**a**,**d**), VAN (**b**,**e**) and CAB (**c**,**f**). The red channel, corresponding to MZ-CRC-1 cells, was omitted in panels d, e, and f to highlight the tumor-induced microvascular network. Grafted larvae showed vessels in green that sprout from the sub-intestinal vein (SIV) toward the xenograft. Quantification of tumor-induced angiogenesis in MZ-CRC-1-injected *Tg(fli1a:EGFP)*^{y1} embryos after 24 h of VAN (**g**) and CAB (**h**) treatments at different concentrations. Control (CTR) values have been set to 1.0. Graphed values represent the mean ± S.E.M. * $p < 0.05$ versus the CTR; *** $p < 0.001$ versus the CTR. Embryos are shown anterior to the left. Scale bar: 100 μm.

3. Discussion

During the present preclinical study, we provide new findings about the anti-angiogenic effects of vandetanib (VAN) and cabozantinib (CAB), two tyrosine kinase inhibitors (TKIs) approved for the treatment of unresectable, progressive, and symptomatic medullary thyroid carcinomas (MTCs).

First, we perform an in vitro head-to-head comparison of these two drugs in the same experimental conditions using two human MTC cell lines to evaluate their anti-tumor activity and related mechanisms. Considering the literature, the anti-proliferative effects of VAN and CAB have been separately analyzed in several in vitro studies [37–44]. However, only a few in vitro studies have compared in the same experimental conditions the anti-tumor activity of VAN and CAB in MTC cell lines. Verbeek and colleagues reported a certain specificity of VAN and CAB for different *REarranged during Transfection* (*RET)* mutations in vitro, that differentially characterized human MTC cell lines, TT, and MZ-CRC-1. VAN inhibited cell proliferation at the lowest concentration in MZ-CRC-1 (IC_{50}: 2.6×10^{-7} M), while CAB exerted the most effective inhibition in TT cells (IC_{50}:

4×10^{-8} M) [31]. Regarding another in vitro head-to-head study, MTC cells were exposed to increasing doses of these two drugs for 48 h and then recovered in a drug-free fresh culture medium for 48 h before measuring their viability using an MTT assay. During these experimental conditions, VAN and CAB exerted a similar cell growth inhibition in both TT and MZ-CRC-1 cells [32]. Following six days of incubation with VAN or CAB, we found comparable inhibition of cell viability in both MTC cell lines. It is well known that these two TKIs are multitarget agents, therefore the anti-proliferative effects that we reported in our long-term treatment may be mediated by the simultaneous inhibition of multiple targets, in addition to REarranged during Transfection (RET) inhibition.

These anti-proliferative activities were modulated by the cell cycle arrest and/or induction of apoptosis. It already has been demonstrated that VAN is mainly cytostatic in MTC cells [42,45] with a lock in the G_0/G_1 phase and no increase in apoptosis [41]. Conversely, CAB exerted a different modulation of cell cycle phases and had a pro-apoptotic effect in MTC cells [44,46]. During the head-to-head study by Starenki et al., after four days of incubation with VAN and CAB, both drugs (10^{-6} M) increased the sub-G1 phase in TT cells, whereas in the MZ-CRC-1 cell line they (5×10^{-7} M) decreased the S phase with a concomitant increase in the G_0/G_1 phase [32]. Regarding both MTC cell lines, we found that VAN and CAB induced a significant decrease in cells in the S and G_2/M phases and an accumulation of cells in the G_0/G_1 phase after six days of incubation. Moreover, an increased sub-G1 phase after exposure with both drugs was predictive of a potential pro-apoptotic activity, which was confirmed through FACS analysis with Annexin/Propidium iodide (PI) staining of MTC cell lines.

Angiogenesis inhibition is another relevant anti-tumor mechanism of VAN and CAB. Indeed, both drugs inhibit the activity of various tyrosine kinases, which are implicated in angiogenesis. Currently, direct comparative studies in vitro and/or in vivo on the effects of VAN and CAB on tumor-induced angiogenesis in MTC have not been published.

Concerning different cell lines (such as PC3, MDA-MB-231, BaF3 and HUVEC), it has been demonstrated that CAB is a potent inhibitor of several tyrosine kinases involved in angiogenesis (MET, VEGFR-2, RET, KIT, AXL, TIE-2 and FLT-3). CAB exerted an anti-angiogenic effect in vitro, as shown by the inhibition of endothelial cell tube formation in HMVEC. To analyze in vivo the effect of CAB on tumor-induced vasculature, anti-angiogenic-sensitive human breast cancer MDA-MB-231 cells expressing *MET* and *VEGF* were implanted in mice. The drug administration increased hypoxia and cell death in tumor cells as well as in the endothelial cells of tumor-induced vasculature [23]. A recent work evaluated the anti-angiogenic effect of VAN and CAB on the stability of the vascular network using a microfabricated platform consisting of a micro-physiological system that incorporates human tumor cells in a 3D extracellular matrix, supported by perfused human microvessels, to create vascularized microtumors. Through this platform, the anti-angiogenic effects of several TKIs have been tested. Interestingly, CAB had more effective results than VAN, probably due to its activity against TIE-2, as well as to VEGFR-2 [47].

However, angiogenic assays consisting of in vitro cell-based models, in contrast to in vivo models, cannot simulate the biological complexity associated with blood vessels growing in their natural environment. Considering this context, zebrafish represents an ideal platform to analyze in vivo the angiogenesis process in physiological and pathological conditions. Several anti-angiogenic agents have been successfully tested in zebrafish [48]. Zebrafish embryos are permeable to small molecules, which can be dissolved in their culture medium; moreover, it is well known that some aspects of the physiological development of the sub-intestinal vein (SIV) and intersomitic and retinal vessels can simulate tumor-induced angiogenesis and be an important platform to test and quantify the effect of anti-angiogenic compounds [49]. Moreover, a zebrafish tumor-xenograft is a suitable platform to study neovascularization occurring with cancer progression in live animals. The implanted cells are able to form masses and recruit zebrafish endothelial cells that can infiltrate the tumor mass and lead to the formation of new vessels which express known endothelial markers, such as *VE-cadherin*, *fli1*, and *vegfr2* [50–52]. Noteworthy, the rapidity

of this procedure and the response to angiogenesis inhibitors (24–48 h post treatment) makes this model a promising platform to perform preclinical drug screening [53].

Two different studies evaluated the anti-angiogenic effects of VAN and CAB in zebrafish separately [54,55]. Beedie and colleagues performed a dose response study with the aim of identifying potential risks of fetal toxicity in drugs that target the developing blood vessels of zebrafish and chicken embryos. Different TKIs were tested and VAN was identified among the less potent compounds, but it was still able to induce defects in vivo [54]. Recently, Wu and colleagues compared the anti-angiogenic and the anti-cancer potential of CAB and other drugs in a gastric cancer xenograft zebrafish model. Xenografted embryos treated with 5×10^{-7} M CAB showed a reduction of 15% in tumor-induced angiogenesis compared to the controls [55]. During a multiple screening, testing the effects of different anti-angiogenic compounds, zebrafish embryos were treated with different doses of VAN and CAB. The ability of anti-angiogenic agents to inhibit SIV physiological development after a 72 h treatment was evaluated, determining the anti-angiogenic efficacy for each compound. A more prominent effect of CAB at lower doses with respect to VAN (CAB: $EC_{50} = 10^{-7}$ M and VAN: $EC_{50} = 10^{-5}$ M) has been observed in this study [56].

Here, we compared in vivo the effect of VAN and CAB on physiological angiogenesis as well as on MTC tumor-induced angiogenesis, a first to our knowledge, taking advantage of a zebrafish xenograft model after the implantation of TT and MZ-CRC-1 cell lines. Analyzing their effects on the physiological angiogenic development, we found that both drugs inhibited SIV development in a dose-dependent manner. Following 24 h of incubation, CAB completely inhibited SIV development at lower concentrations compared to VAN. Regarding tumor-induced angiogenesis, *Tg(fli1a:EGFP)*^{y1} zebrafish embryos were used as recipients for the xenotransplantation of MTC cell lines. Only 24 h after the implantation, grafted cells affected the physiological angiogenesis of the SIV plexus, leading to the formation of endothelial sprouts starting from the SIV toward the tumor mass. In our MTC xenograft model, both drugs showed tumor-induced angiogenesis inhibition in a dose-dependent manner. CAB had a stronger inhibitory effect on angiogenesis than VAN in embryos injected with both MTC cell lines.

In conclusion, through an innovative zebrafish model we found that the anti-angiogenic activity of CAB resulted in being more potent than that of VAN in MTC. Zebrafish have proven to be a powerful, reliable, and effective platform for the testing of anti-angiogenic compounds. Later, this zebrafish MTC xenograft model coupled with drug screening, may be a useful pre-clinical tool to enhance the understanding of molecular interactions between anti-angiogenic agents and different biological pathways involved in MTC progression.

4. Materials and Methods

4.1. Reagents and Cell Culture

Vandetanib (VAN), and cabozantinib (CAB) were provided by Cayman Chemicals (Ann Arbor, MI, USA). Stock solutions (4 mM) were made in 100% dimethyl sulfoxide (DMSO) and diluted with culture media before use. Two human medullary thyroid carcinoma (MTC) cell lines, TT and MZ-CRC-1, were kindly provided by Prof. Lips (Utrecht, the Netherland). Cells were maintained at 37 °C in 5% CO_2 and cultured in T75 flasks filled with 10 mL of F-12K Kaighn's modification medium (Gibco™ Thermo Fisher Scientific, Waltham, MA, USA). Media was supplemented with 10% heat-activated fetal bovine serum (FBS) (Invitrogen™ Thermo Fisher Scientific, Waltham, MA, USA) and 10^5 U·L^{-1} penicillin/streptomycin (EuroClone™, Milan, Italy). Cells were harvested by trypsinization (Trypsin 0.05% and EDTA 0.02%) (Sigma-Aldrich ® Merck KGaA, Darmstadt, Germany), resuspended in complete medium, then counted through an optical microscope using a standard haemocytometer before plating. Cells used in all experiments were below 5 passages. All in vitro experiments were monitored for up to 6 days of drug incubation. We performed long-term treatments due to the slow doubling time (about 4 days) of the MTC cell lines.

4.2. Assessment of Cell Viability

Medullary thyroid carcinoma (MTC) cell lines were seeded in 96 well plates at their optimal culture concentration (TT: 20×10^3 cells/well; MZ-CRC-1: 20×10^3 cells/well). The following day, the cell culture medium was replaced with a medium containing vandetanib (VAN) and cabozantinib (CAB) for 3 days at different concentrations (from 5×10^{-9} to 10^{-5} M). Then, the medium was replaced with a new one containing drugs at the same differing concentrations for a further 3 days. A culture media containing an equivalent dimethyl sulfoxide (DMSO) concentration of the highest treatment dose served as the vehicle control. Following six days, an MTT assay (3-(4,5-dimethylthiazol-2-yl)-2,5-diphenyltetrazolium bromide) was performed, as previously described [57]. Considering these results, the IC_{50} were statistically calculated for each cell line using the Prism 5.0-GraphPad (GraphPad Software Inc., La Jolla, CA, USA).

4.3. Cell Cycle and Apoptosis Evaluation

Cell lines were seeded in 6-well plates in duplicates (MZ-CRC-1 and TT 3×10^5 cells/well). The following day, the cell culture medium was replaced with a medium containing an equivalent dimethyl sulfoxide (DMSO) concentration (control), vandetanib (VAN), or cabozantinib (CAB) at their EC_{50} for 3 days. Then, the medium was replaced with a new one containing the vehicle or drugs with the same concentrations for a further 3 days, at the end of which the cells were harvested by gentle trypsinization, washed with cold PBS (calcium- and magnesium-free), and collected by centrifugation at $1200 \times g$ for 5 min. A propidium iodide (PI) (Sigma-Aldrich® Merck KGaA, Darmstadt, Germany) solution (50 µg/mL PI, 0.05% Triton X-100 and 0.6 µg/mL RNase A in 0.1% sodium citrate) was added to stain the pellets at 4 °C for 30 min. To evaluate the cell-cycle PI for each tube, 10,000 cells were immediately measured and fluorescence was collected as FL1-A with a FACScalibur flow cytometer (Becton Dickinson, Erembodegem, Belgium) using Cell Quest Pro Software and data analyzed, as previously reported [57]. Cell cycle distribution was expressed as the percentage of cells in the G_0/G_1, S, and G_2/M phases compared to the control. Regarding apoptosis, cells were resuspended in 100 µL of 1X binding buffer (BB: 1.4M NaCl, 0.1M HEPES/NaOH, pH 7.4, 25 mM CaCl2). Following incubation with 5 µL of Annexin V-FITC (BD Pharmingen, San Diego, CA, USA) and 10 µL PI (50 µg/mL in PBS) for 15 min at room temperature in the dark for each sample, 400 µL of 1X BB was added and stained cells were analyzed using FACScalibur on 10,000 events and analyzed, as previously described [57].

4.4. Zebrafish Line and Maintenance

Embryo and adult zebrafish (*Danio rerio*) were raised and maintained according to Italian (D.Lgs 26/2014) and European laws (2010/63/EU and 86/609/EEC). Embryos were staged according to morphological criteria [58]. Starting from 24 hpf, embryos were cultured in fish water (0.1 g/L NaHCO3, 0.1 g/L Instant Ocean, 0.192 g/L $CaSO_4 \bullet 2H_2O$) containing 0.003% PTU (1-phenyl-2-thiourea; Sigma-Aldrich ® Merck KGaA, Darmstadt, Germany) to prevent pigmentation, and 0.01% methylene blue to prevent fungal growth. All experiments were performed on *Tg(fli1a:EGFP)^{y1}* transgenic fluorescent zebrafish embryos [59].

4.5. In Vivo Subintestinal Angiogenesis Assay on Zebrafish Embryos

Occurring at 48 hpf, transgenic embryos were treated for 24 h with different concentrations of vandetanib (VAN) and cabozantinib (CAB). Stock solutions of VAN and CAB, prepared in dimethyl sulfoxide (DMSO), were diluted in fish water to concentrations ranging from 5×10^{-7} up to 1×10^{-5} M, and from 5×10^{-8} up to 5×10^{-6} M for VAN and CAB, respectively. As a control, some embryos were incubated with a fish medium containing the same concentration of DMSO used for the drug treated embryos. Occurring at 72 hpf, sub-intestinal vein (SIV) plexus images were taken with a Leica M205 FA stereomicroscope equipped with a Leica DFC 450 C digital camera using the LAS software (Leica

Microsystems, Wetzlar, Germany). Vertical vessels that composed the SIV basket were counted in the controls and in the treated embryos to analyze physiological angiogenesis.

4.6. In Vivo Zebrafish Assay for Tumor-Induced Angiogenesis

Forty-eight hours post-fertilization, zebrafish *Tg(fli1a:EGFP)^{y1}* embryos were anesthetized with 0.016% tricaine (Ethyl 3-aminobenzoate methanesulfonate salt, Sigma-Aldrich® Merck KGaA, Darmstadt, Germany) and implanted with TT and MZ-CRC-1 cells, as previously described [34,60,61]. Briefly, TT and MZ-CRC-1 cells were labeled with a red fluorescent viable dye (CellTrackerTM CM-DiI, Invitrogen™ Thermo Fisher Scientific, Waltham, MA, USA), resuspended with PBS, and grafted into the sub-peridermal space of *Tg(fli1a: EGFP)^{y1}* embryos, close to the sub-intestinal vein (SIV) plexus. As a control of the implantation, we considered embryos injected with only PBS. This transplantable platform was used to test CAB and VAN effects on tumor-induced angiogenesis. Following the implantation, zebrafish embryos were treated for 24 h with these two drugs and directly dissolved into fish water. The drug concentrations ranged from 5×10^{-7} up to 1×10^{-5} M, and from 5×10^{-8} up to 2.5×10^{-6} M for VAN and CAB, respectively. The untreated controls were considered to be the injected embryos incubated in the fish water and the vehicle in which the experimental substance was dissolved (dimethyl sulfoxide (DMSO)). Assays were performed 3 times, considering about 20 embryos in each experimental group. All images were taken at 24 h post-injection with a Leica M205 FA stereomicroscope equipped with a Leica DFC 450 C digital camera using the LAS software (Leica Microsystems, Wetzlar, Germany). To measure the arbitrary unit of tumor-induced angiogenesis, we calculated the total cumulative length of the vessels sprouting from the SIV plexus and the common cardinal vein in each embryo using Fiji software.

4.7. Statistical Analysis

All experiments were performed at least three times. Statistical differences among groups were first evaluated using a *t*-test or ANOVA test together with the standard post hoc test (Newman–Keuls). A p value < 0.05 was considered significant. Statistical comparison of the $\log IC_{50}$ and maximal anti-angiogenic effect (E_{max}) values were performed with the extra sum-of-squares F test approach (cutoff at $p = 0.05$). The values reported in the figures represent the mean ± standard error of the mean (S.E.M). Regarding statistical analysis, graphpad prism 5.0 was used (GraphPad Software Inc., La Jolla, CA, USA).

Author Contributions: Conceptualization, S.C., G.G. and G.V.; methodology, S.C., G.G., A.D. and G.V.; validation, G.V. and L.P.; formal analysis, S.C., G.G., A.D.; investigation, S.C., G.G., A.D., D.S., M.C.C., A.P., A.G. and M.O.B.; resources, L.J.H., L.P. and G.V.; writing—original draft preparation, S.C. and A.D.; writing—review and editing, S.C., G.G., A.D., L.J.H., L.P. and G.V.; supervision, G.V.; project administration, G.V.; funding acquisition, G.V. All authors have read and agreed to the published version of the manuscript.

Funding: The study was partially supported by the Italian Ministry of Health (IRCCS funding Ricerca Corrente, ZEBRANET, code: 05C402_2014) and Italian Ministry of Education, University and Research (PRIN 2017Z3N3YC).

Institutional Review Board Statement: The study was conducted according to the guidelines of the Declaration of Helsinki, and approved by the Ethics Committee of Istituto Auxologico Italiano (protocol code: 2017_03_28_19, date of approval: 28 March 2017).

Conflicts of Interest: The authors declare no conflict of interest. The funders had no role in the design of the study; in the collection, analyses, or interpretation of data; in the writing of the manuscript, or in the decision to publish the results.

Abbreviations

MTC	medullary thyroid carcinoma
MEN	multiple endocrine neoplasia
RET	REarranged during Transfection
EGFR	epidermal growth factor receptor
VEGFRs	vascular endothelial growth factor receptors
FGFR	fibroblast growth factor receptor
TKIs	tyrosine kinase inhibitors
VAN	vandetanib
CAB	cabozantinib
EGFP	enhanced green fluorescent protein
SIV	Sub-intestinal vein

References

1. Fagin, J.A.; Wells, S.A., Jr. Biologic and Clinical Perspectives on Thyroid Cancer. *N. Engl. J. Med.* **2016**, *375*, 2307. [CrossRef]
2. Cancela-Nieto, M.G.; Sanchez-Sobrino, P.; Velogarcia, A. Procalcitonin as a marker of medullary thyroid carcinoma. *Minerva Endocrinol.* **2020**. [CrossRef]
3. Fialkowski, E.A.; Moley, J.F. Current approaches to medullary thyroid carcinoma, sporadic and familial. *J. Surg. Oncol.* **2006**, *94*, 737–747. [CrossRef] [PubMed]
4. Raue, F.; Frank-Raue, K. Update on Multiple Endocrine Neoplasia Type 2: Focus on Medullary Thyroid Carcinoma. *J. Endocr. Soc.* **2018**, *2*, 933–943. [CrossRef] [PubMed]
5. Mulligan, L.M.; Kwok, J.B.; Healey, C.S.; Elsdon, M.J.; Eng, C.; Gardner, E.; Love, D.R.; Mole, S.E.; Moore, J.K.; Papi, L.; et al. Germ-line mutations of the RET proto-oncogene in multiple endocrine neoplasia type 2A. *Nature* **1993**, *363*, 458–460. [CrossRef]
6. Carlson, K.M.; Dou, S.; Chi, D.; Scavarda, N.; Toshima, K.; Jackson, C.E.; Wells, S.A., Jr.; Goodfellow, P.J.; Donis-Keller, H. Single missense mutation in the tyrosine kinase catalytic domain of the RET protooncogene is associated with multiple endocrine neoplasia type 2B. *Proc. Natl. Acad. Sci. USA* **1994**, *91*, 1579–1583. [CrossRef] [PubMed]
7. Hofstra, R.M.; Landsvater, R.M.; Ceccherini, I.; Stulp, R.P.; Stelwagen, T.; Luo, Y.; Pasini, B.; Hoppener, J.W.; van Amstel, H.K.; Romeo, G.; et al. A mutation in the RET proto-oncogene associated with multiple endocrine neoplasia type 2B and sporadic medullary thyroid carcinoma. *Nature* **1994**, *367*, 375–376. [CrossRef]
8. Marsh, D.J.; Learoyd, D.L.; Andrew, S.D.; Krishnan, L.; Pojer, R.; Richardson, A.L.; Delbridge, L.; Eng, C.; Robinson, B.G. Somatic mutations in the RET proto-oncogene in sporadic medullary thyroid carcinoma. *Clin. Endocrinol.* **1996**, *44*, 249–257. [CrossRef]
9. Wells, S.A., Jr.; Pacini, F.; Robinson, B.G.; Santoro, M. Multiple endocrine neoplasia type 2 and familial medullary thyroid carcinoma: An update. *J. Clin. Endocrinol. Metab.* **2013**, *98*, 3149–3164. [CrossRef]
10. Wells, S.A., Jr.; Asa, S.L.; Dralle, H.; Elisei, R.; Evans, D.B.; Gagel, R.F.; Lee, N.; Machens, A.; Moley, J.F.; Pacini, F.; et al. Revised American Thyroid Association guidelines for the management of medullary thyroid carcinoma. *Thyroid* **2015**, *25*, 567–610. [CrossRef]
11. Vitale, G.; Caraglia, M.; Ciccarelli, A.; Lupoli, G.; Abbruzzese, A.; Tagliaferri, P.; Lupoli, G. Current approaches and perspectives in the therapy of medullary thyroid carcinoma. *Cancer* **2001**, *91*, 1797–1808. [CrossRef]
12. Giunti, S.; Antonelli, A.; Amorosi, A.; Santarpia, L. Cellular signaling pathway alterations and potential targeted therapies for medullary thyroid carcinoma. *Int. J. Endocrinol.* **2013**, *2013*, 803171. [CrossRef]
13. Fischer, P.M. Approved and Experimental Small-Molecule Oncology Kinase Inhibitor Drugs: A Mid-2016 Overview. *Med. Res. Rev.* **2017**, *37*, 314–367. [CrossRef] [PubMed]
14. Viola, D.; Elisei, R. Management of Medullary Thyroid Cancer. *Endocrinol Metab Clin North Am* **2019**, *48*, 285–301. [CrossRef] [PubMed]
15. Rodriguez-Antona, C.; Munoz-Repeto, I.; Inglada-Perez, L.; de Cubas, A.A.; Mancikova, V.; Canamero, M.; Maliszewska, A.; Gomez, A.; Leton, R.; Leandro-Garcia, L.J.; et al. Influence of RET mutations on the expression of tyrosine kinases in medullary thyroid carcinoma. *Endocr. Relat. Cancer* **2013**, *20*, 611–619. [CrossRef]
16. Rodriguez-Antona, C.; Pallares, J.; Montero-Conde, C.; Inglada-Perez, L.; Castelblanco, E.; Landa, I.; Leskela, S.; Leandro-Garcia, L.J.; Lopez-Jimenez, E.; Leton, R.; et al. Overexpression and activation of EGFR and VEGFR2 in medullary thyroid carcinomas is related to metastasis. *Endocr. Relat. Cancer* **2010**, *17*, 7–16. [CrossRef] [PubMed]
17. Verrienti, A.; Tallini, G.; Colato, C.; Boichard, A.; Checquolo, S.; Pecce, V.; Sponziello, M.; Rosignolo, F.; de Biase, D.; Rhoden, K.; et al. RET mutation and increased angiogenesis in medullary thyroid carcinomas. *Endocr. Relat. Cancer* **2016**, *23*, 665–676. [CrossRef]
18. Sherman, S.I. Targeted therapy of thyroid cancer. *Biochem. Pharmacol.* **2010**, *80*, 592–601. [CrossRef]
19. Liu, X.; Shen, T.; Mooers, B.H.M.; Hilberg, F.; Wu, J. Drug resistance profiles of mutations in the RET kinase domain. *Br. J. Pharmacol.* **2018**, *175*, 3504–3515. [CrossRef]

20. Milling, R.V.; Grimm, D.; Kruger, M.; Grosse, J.; Kopp, S.; Bauer, J.; Infanger, M.; Wehland, M. Pazopanib, Cabozantinib, and Vandetanib in the Treatment of Progressive Medullary Thyroid Cancer with a Special Focus on the Adverse Effects on Hypertension. *Int. J. Mol. Sci.* **2018**, *19*, 3258. [CrossRef]
21. Wedge, S.R.; Ogilvie, D.J.; Dukes, M.; Kendrew, J.; Chester, R.; Jackson, J.A.; Boffey, S.J.; Valentine, P.J.; Curwen, J.O.; Musgrove, H.L.; et al. ZD6474 inhibits vascular endothelial growth factor signaling, angiogenesis, and tumor growth following oral administration. *Cancer Res.* **2002**, *62*, 4645–4655.
22. Carlomagno, F.; Vitagliano, D.; Guida, T.; Ciardiello, F.; Tortora, G.; Vecchio, G.; Ryan, A.J.; Fontanini, G.; Fusco, A.; Santoro, M. ZD6474, an orally available inhibitor of KDR tyrosine kinase activity, efficiently blocks oncogenic RET kinases. *Cancer Res.* **2002**, *62*, 7284–7290. [PubMed]
23. Yakes, F.M.; Chen, J.; Tan, J.; Yamaguchi, K.; Shi, Y.; Yu, P.; Qian, F.; Chu, F.; Bentzien, F.; Cancilla, B.; et al. Cabozantinib (XL184), a novel MET and VEGFR2 inhibitor, simultaneously suppresses metastasis, angiogenesis, and tumor growth. *Mol. Cancer Ther.* **2011**, *10*, 2298–2308. [CrossRef] [PubMed]
24. Elisei, R.; Schlumberger, M.J.; Muller, S.P.; Schoffski, P.; Brose, M.S.; Shah, M.H.; Licitra, L.; Jarzab, B.; Medvedev, V.; Kreissl, M.C.; et al. Cabozantinib in progressive medullary thyroid cancer. *J. Clin. Oncol.* **2013**, *31*, 3639–3646. [CrossRef] [PubMed]
25. Wells, S.A., Jr.; Robinson, B.G.; Gagel, R.F.; Dralle, H.; Fagin, J.A.; Santoro, M.; Baudin, E.; Elisei, R.; Jarzab, B.; Vasselli, J.R.; et al. Vandetanib in patients with locally advanced or metastatic medullary thyroid cancer: A randomized, double-blind phase III trial. *J. Clin. Oncol.* **2012**, *30*, 134–141. [CrossRef] [PubMed]
26. Schoffski, P.; Elisei, R.; Müller, S.; Brose, M.S.; Shah, M.H.; Licitra, L.F.; Jarzab, B.; Medvedev, V.; Kreissl, M.; Niederle, B.; et al. An international, double-blind, randomized, placebo-controlled phase III trial (EXAM) of cabozantinib (XL184) in medullary thyroid carcinoma (MTC) patients (pts) with documented RECIST progression at baseline. *J. Clin. Oncol.* **2012**, *30* (Suppl. 15), 5508. [CrossRef]
27. Spitzweg, C.; Morris, J.C.; Bible, K.C. New drugs for medullary thyroid cancer: New promises? *Endocr. Relat. Cancer* **2016**, *23*, R287–R297. [CrossRef]
28. Priya, S.R.; Dravid, C.S.; Digumarti, R.; Dandekar, M. Targeted Therapy for Medullary Thyroid Cancer: A Review. *Front. Oncol.* **2017**, *7*, 238. [CrossRef]
29. Tappenden, P.; Carroll, C.; Hamilton, J.; Kaltenthaler, E.; Wong, R.; Wadsley, J.; Moss, L.; Balasubramanian, S. Cabozantinib and vandetanib for unresectable locally advanced or metastatic medullary thyroid cancer: A systematic review and economic model. *Health Technol. Assess.* **2019**, *23*, 1–144. [CrossRef] [PubMed]
30. Koehler, V.F.; Adam, P.; Frank-Raue, K.; Raue, F.; Berg, E.; Hoster, E.; Allelein, S.; Schott, M.; Kroiss, M.; Spitzweg, C. Real-World Efficacy and Safety of Cabozantinib and Vandetanib in Advanced Medullary Thyroid Cancer. *Thyroid* **2020**. [CrossRef]
31. Verbeek, H.H.; Alves, M.M.; de Groot, J.W.; Osinga, J.; Plukker, J.T.; Links, T.P.; Hofstra, R.M. The effects of four different tyrosine kinase inhibitors on medullary and papillary thyroid cancer cells. *J. Clin. Endocrinol. Metab.* **2011**, *96*, E991–995. [CrossRef]
32. Starenki, D.; Hong, S.K.; Wu, P.K.; Park, J.I. Vandetanib and cabozantinib potentiate mitochondria-targeted agents to suppress medullary thyroid carcinoma cells. *Cancer Biol. Ther.* **2017**, *18*, 473–483. [CrossRef]
33. Wertman, J.; Veinotte, C.J.; Dellaire, G.; Berman, J.N. The Zebrafish Xenograft Platform: Evolution of a Novel Cancer Model and Preclinical Screening Tool. *Adv. Exp. Med. Biol.* **2016**, *916*, 289–314. [CrossRef] [PubMed]
34. Vitale, G.; Gaudenzi, G.; Dicitore, A.; Cotelli, F.; Ferone, D.; Persani, L. Zebrafish as an innovative model for neuroendocrine tumors. *Endocr. Relat. Cancer* **2014**, *21*, R67–83. [CrossRef]
35. Vitale, G.; Gaudenzi, G.; Circelli, L.; Manzoni, M.F.; Bassi, A.; Fioritti, N.; Faggiano, A.; Colao, A.; Group, N. Animal models of medullary thyroid cancer: State of the art and view to the future. *Endocr. Relat. Cancer* **2017**, *24*, R1–R12. [CrossRef] [PubMed]
36. Carra, S.; Gaudenzi, G. New perspectives in neuroendocrine neoplasms research from tumor xenografts in zebrafish embryos. *Minerva Endocrinol.* **2020**, *45*, 393–394. [CrossRef] [PubMed]
37. O'Brien, S.; Golubovskaya, V.M.; Conroy, J.; Liu, S.; Wang, D.; Liu, B.; Cance, W.G. FAK inhibition with small molecule inhibitor Y15 decreases viability, clonogenicity, and cell attachment in thyroid cancer cell lines and synergizes with targeted therapeutics. *Oncotarget* **2014**, *5*, 7945–7959. [CrossRef]
38. Mancikova, V.; Montero-Conde, C.; Perales-Paton, J.; Fernandez, A.; Santacana, M.; Jodkowska, K.; Inglada-Perez, L.; Castelblanco, E.; Borrego, S.; Encinas, M.; et al. Multilayer OMIC Data in Medullary Thyroid Carcinoma Identifies the STAT3 Pathway as a Potential Therapeutic Target in RET(M918T) Tumors. *Clin Cancer Res.* **2017**, *23*, 1334–1345. [CrossRef]
39. Bentzien, F.; Zuzow, M.; Heald, N.; Gibson, A.; Shi, Y.; Goon, L.; Yu, P.; Engst, S.; Zhang, W.; Huang, D.; et al. In vitro and in vivo activity of cabozantinib (XL184), an inhibitor of RET, MET, and VEGFR2, in a model of medullary thyroid cancer. *Thyroid* **2013**, *23*, 1569–1577. [CrossRef]
40. Broutin, S.; Commo, F.; De Koning, L.; Marty-Prouvost, B.; Lacroix, L.; Talbot, M.; Caillou, B.; Dubois, T.; Ryan, A.J.; Dupuy, C.; et al. Changes in signaling pathways induced by vandetanib in a human medullary thyroid carcinoma model, as analyzed by reverse phase protein array. *Thyroid* **2014**, *24*, 43–51. [CrossRef]
41. Walter, M.A.; Benz, M.R.; Hildebrandt, I.J.; Laing, R.E.; Hartung, V.; Damoiseaux, R.D.; Bockisch, A.; Phelps, M.E.; Czernin, J.; Weber, W.A. Metabolic imaging allows early prediction of response to vandetanib. *J. Nucl. Med.* **2011**, *52*, 231–240. [CrossRef]
42. Vitagliano, D.; De Falco, V.; Tamburrino, A.; Coluzzi, S.; Troncone, G.; Chiappetta, G.; Ciardiello, F.; Tortora, G.; Fagin, J.A.; Ryan, A.J.; et al. The tyrosine kinase inhibitor ZD6474 blocks proliferation of RET mutant medullary thyroid carcinoma cells. *Endocr. Relat. Cancer* **2011**, *18*, 1–11. [CrossRef] [PubMed]

43. Lassalle, S.; Zangari, J.; Popa, A.; Ilie, M.; Hofman, V.; Long, E.; Patey, M.; Tissier, F.; Belleannee, G.; Trouette, H.; et al. MicroRNA-375/SEC23A as biomarkers of the in vitro efficacy of vandetanib. *Oncotarget* **2016**, *7*, 30461–30478. [CrossRef]
44. Bertazza, L.; Sensi, F.; Cavedon, E.; Watutantrige-Fernando, S.; Censi, S.; Manso, J.; Vianello, F.; Casal Ide, E.; Iacobone, M.; Pezzani, R.; et al. EF24 (a Curcumin Analog) and ZSTK474 Emphasize the Effect of Cabozantinib in Medullary Thyroid Cancer. *Endocrinology* **2018**, *159*, 2348–2360. [CrossRef] [PubMed]
45. Starenki, D.; Park, J.I. Mitochondria-targeted nitroxide, Mito-CP, suppresses medullary thyroid carcinoma cell survival in vitro and in vivo. *J. Clin. Endocrinol. Metab.* **2013**, *98*, 1529–1540. [CrossRef]
46. Yoon, H.; Kwak, Y.; Choi, S.; Cho, H.; Kim, N.D.; Sim, T. A Pyrazolo[3,4-d]pyrimidin-4-amine Derivative Containing an Isoxazole Moiety Is a Selective and Potent Inhibitor of RET Gatekeeper Mutants. *J. Med. Chem.* **2016**, *59*, 358–373. [CrossRef] [PubMed]
47. Sobrino, A.; Phan, D.T.; Datta, R.; Wang, X.; Hachey, S.J.; Romero-Lopez, M.; Gratton, E.; Lee, A.P.; George, S.C.; Hughes, C.C. 3D microtumors in vitro supported by perfused vascular networks. *Sci. Rep.* **2016**, *6*, 31589. [CrossRef]
48. Santoro, M.M. Antiangiogenic cancer drug using the zebrafish model. *Arterioscler. Thromb. Vasc. Biol.* **2014**, *34*, 1846–1853. [CrossRef]
49. Zhang, J.; Gao, B.; Zhang, W.; Qian, Z.; Xiang, Y. Monitoring antiangiogenesis of bevacizumab in zebrafish. *Drug Des. Dev. Ther.* **2018**, *12*, 2423–2430. [CrossRef]
50. Nicoli, S.; Ribatti, D.; Cotelli, F.; Presta, M. Mammalian tumor xenografts induce neovascularization in zebrafish embryos. *Cancer Res.* **2007**, *67*, 2927–2931. [CrossRef]
51. Konantz, M.; Balci, T.B.; Hartwig, U.F.; Dellaire, G.; Andre, M.C.; Berman, J.N.; Lengerke, C. Zebrafish xenografts as a tool for in vivo studies on human cancer. *Ann. N. Y. Acad. Sci.* **2012**, *1266*, 124–137. [CrossRef]
52. Tobia, C.; Gariano, G.; De Sena, G.; Presta, M. Zebrafish embryo as a tool to study tumor/endothelial cell cross-talk. *Biochim. Biophys. Acta* **2013**, *1832*, 1371–1377. [CrossRef]
53. Hasan, J.; Shnyder, S.D.; Bibby, M.; Double, J.A.; Bicknel, R.; Jayson, G.C. Quantitative angiogenesis assays in vivo—A review. *Angiogenesis* **2004**, *7*, 1–16. [CrossRef] [PubMed]
54. Beedie, S.L.; Mahony, C.; Walker, H.M.; Chau, C.H.; Figg, W.D.; Vargesson, N. Shared mechanism of teratogenicity of anti-angiogenic drugs identified in the chicken embryo model. *Sci. Rep.* **2016**, *6*, 30038. [CrossRef]
55. Wu, J.Q.; Fan, R.Y.; Zhang, S.R.; Li, C.Y.; Shen, L.Z.; Wei, P.; He, Z.H.; He, M.F. A systematical comparison of anti-angiogenesis and anti-cancer efficacy of ramucirumab, apatinib, regorafenib and cabozantinib in zebrafish model. *Life Sci.* **2020**, *247*, 117402. [CrossRef]
56. Chimote, G.; Sreenivasan, J.; Pawar, N.; Subramanian, J.; Sivaramakrishnan, H.; Sharma, S. Comparison of effects of anti-angiogenic agents in the zebrafish efficacy-toxicity model for translational anti-angiogenic drug discovery. *Drug Des. Dev. Ther.* **2014**, *8*, 1107–1123. [CrossRef] [PubMed]
57. Dicitore, A.; Castiglioni, S.; Saronni, D.; Gentilini, D.; Borghi, M.O.; Stabile, S.; Vignali, M.; Di Blasio, A.M.; Persani, L.; Vitale, G. Effects of human recombinant type I IFNs (IFN-alpha2b and IFN-beta1a) on growth and migration of primary endometrial stromal cells from women with deeply infiltrating endometriosis: A preliminary study. *Eur. J. Obstet. Gynecol. Reprod. Biol.* **2018**, *230*, 192–198. [CrossRef] [PubMed]
58. Kimmel, C.B.; Ballard, W.W.; Kimmel, S.R.; Ullmann, B.; Schilling, T.F. Stages of embryonic development of the zebrafish. *Dev. Dyn.* **1995**, *203*, 253–310. [CrossRef]
59. Lawson, N.D.; Weinstein, B.M. In vivo imaging of embryonic vascular development using transgenic zebrafish. *Dev. Biol.* **2002**, *248*, 307–318. [CrossRef]
60. Gaudenzi, G.; Albertelli, M.; Dicitore, A.; Wurth, R.; Gatto, F.; Barbieri, F.; Cotelli, F.; Florio, T.; Ferone, D.; Persani, L.; et al. Patient-derived xenograft in zebrafish embryos: A new platform for translational research in neuroendocrine tumors. *Endocrine* **2017**, *57*, 214–219. [CrossRef] [PubMed]
61. Cirello, V.; Gaudenzi, G.; Grassi, E.S.; Colombo, C.; Vicentini, L.; Ferrero, S.; Persani, L.; Vitale, G.; Fugazzola, L. Tumor and normal thyroid spheroids: From tissues to zebrafish. *Minerva Endocrinol.* **2018**, *43*, 1–10. [CrossRef] [PubMed]

frontiers in Endocrinology

MINI REVIEW
published: 14 April 2021
doi: 10.3389/fendo.2021.665631

Role of FGF System in Neuroendocrine Neoplasms: Potential Therapeutic Applications

Giovanni Vitale[1,2], Alessia Cozzolino[3], Pasqualino Malandrino[4], Roberto Minotta[5], Giulia Puliani[3,6], Davide Saronni[2], Antongiulio Faggiano[7] and Annamaria Colao[5] on behalf of NIKE*

[1] Laboratory of Geriatric and Oncologic Neuroendocrinology Research, Istituto Auxologico Italiano, IRCCS, Cusano Milanino, Italy, [2] Department of Medical Biotechnology and Translational Medicine, University of Milan, Milan, Italy, [3] Department of Experimental Medicine, Sapienza University of Rome, Rome, Italy, [4] Endocrinology, Department of Clinical and Experimental Medicine, Garibaldi-Nesima Medical Center, University of Catania, Catania, Italy, [5] Department of Clinical Medicine and Surgery, Federico II University of Naples, Naples, Italy, [6] Oncological Endocrinology Unit, IRCCS Regina Elena National Cancer Institute, Rome, Italy, [7] Department of Clinical and Molecular Medicine, Sapienza University of Rome, Rome, Italy

OPEN ACCESS

Edited by:
Michele Caraglia, University of Campania Luigi Vanvitelli, Italy

Reviewed by:
Davide Gentilini, University of Pavia, Italy
Boccellino Mariarosaria, University of Campania Luigi Vanvitelli, Italy

***Correspondence:**
Giovanni Vitale
giovanni.vitale@unimi.it;
g.vitale@auxologico.it

Specialty section:
This article was submitted to Cancer Endocrinology, a section of the journal Frontiers in Endocrinology

Received: *08 February 2021*
Accepted: *22 March 2021*
Published: *14 April 2021*

Citation:
Vitale G, Cozzolino A, Malandrino P, Minotta R, Puliani G, Saronni D, Faggiano A, and Colao A (2021) Role of FGF System in Neuroendocrine Neoplasms: Potential Therapeutic Applications. Front. Endocrinol. 12:665631. doi: 10.3389/fendo.2021.665631

Neuroendocrine neoplasms (NENs) are a heterogeneous group of tumors originating from neuroendocrine cells dispersed in different organs. Receptor tyrosine kinases are a subclass of tyrosine kinases with a relevant role in several cellular processes including proliferation, differentiation, motility and metabolism. Dysregulation of these receptors is involved in neoplastic development and progression for several tumors, including NENs. In this review, we provide an overview concerning the role of the fibroblast growth factor (FGF)/fibroblast growth factor receptor (FGFR) system in the development and progression of NENs, the occurrence of fibrotic complications and the onset of drug-resistance. Although no specific FGFR kinase inhibitors have been evaluated in NENs, several clinical trials on multitarget tyrosine kinase inhibitors, acting also on FGF system, showed promising anti-tumor activity with an acceptable and manageable safety profile in patients with advanced NENs. Future studies will need to confirm these issues, particularly with the development of new tyrosine kinase inhibitors highly selective for FGFR.

Keywords: neuroendocrine neoplasms, FGFR (fibroblast growth factor receptor), FGF (fibroblast growth factor), VEGF - vascular endothelial growth factor, VEGFR - vascular endothelial growth factor receptor

INTRODUCTION

Neuroendocrine neoplasms (NENs) are a heterogeneous group of tumors originating from neuroendocrine cells dispersed in different organs (1–5).

Receptor tyrosine kinases are a subclass of tyrosine kinases with a relevant role in several cellular processes including proliferation, differentiation, motility and metabolism. Dysregulation of these receptors plays a relevant role in neoplastic development and progression for several tumors, including NENs (6, 7).

In this review, we provide an overview concerning the role of the fibroblast growth factor (FGF)/fibroblast growth factor receptor (FGFR) system in NENs.

FGF SYSTEM IN HEALTH AND CANCER

FGFs and related receptors are members of a large family with a wide range of effects. This system is involved in organogenesis (during development), homeostasis and repair of adult tissues. Moreover, FGF family promotes angiogenesis, growth, differentiation and migration of cells mainly through the activation of RAS-MAPK, PI3K-AKT and PLCγ pathways, with a relevant role in the development and progression of several tumors (8). These effects are mediated by the interaction of FGFs with four tyrosine kinase receptors: FGFR1, FGFR2, FGFR3 and FGFR4, which are composed by an extracellular domain, a transmembrane domain and an intracellular domain. The binding of ligands induces conformational changes that lead to a dimerization of these receptors. This event activates the intracellular tyrosine kinase domain, which in turn triggers the signalling cascade (8). FGFs, based on their biochemical functions, sequence similarity and evolutionary relationships, are classified into different subfamilies: FGF1, FGF4, FGF7, FGF8, FGF9, FGF15/19 and FGF11.

FGF1 and FGF2 are members of the FGF1 subfamily. FGF1 is the only FGF that can activate all FGFRs splice variants. It is involved in cell cycle regulation, cell differentiation, survival and apoptosis. FGF1 plays a central role in neuroprotection and axon regeneration and appears to improve functional recovery after spinal cord injury (9). FGF2 has known angiogenic properties (10, 11). The FGF4 subfamily (FGF4, 5,6) can activate FGFR1-3 (IIIc) and FGFR4. These molecules are fundamental in embryonic development and muscle regeneration (8, 9). FGF7 subfamily (FGF3, 7, 10, 22) preferentially activates FGFR2(IIIb), although FGF3 and FGF10 can also interact with FGFR1(IIIb). FGF3 is involved in the neural development, while FGF7 is required for lung, kidney and neuronal synapses development. The development of epithelial components, such as limb and lungs, and mammary gland requires epithelial-mesenchymal interactions granted by FGF10. Finally, FGF22 regulates the circuit remodeling in the injured spinal cord (12–15). FGF8 subfamily members (FGF8, 17 and 18) activate FGFR4 and FGFR1-3(IIIc). They are involved in the skeletal and brain development and in odontogenesis (8, 14, 16–18). The FGF9 subfamily (FGF9, 16, 20) interacts with FGFR1-3(IIIc), FGFR3 (IIIb) and FGFR4. These proteins are involved in a proper heart, kidney and skeletal development (8, 14, 19, 20). The FGF15/19 subfamily comprises FGF15/19, 21 and 23. FGF15/19 bind FGFR1-3(IIIc) and FGFR4. FGF21 can activate FGFR1(IIIc) and 3(IIIc), as well as FGF23, which can also interact with FGFR4. This subfamily acts as hormones and regulates hepatocyte and adipocyte metabolism (8, 14). FGF11 subfamily members (FGF11, 12, 13, 14) are known as intracellular FGFs. These peptides are not secreted and interact with the cytosolic carboxy terminal tail of voltage gated sodium channels. They cover an important role in the development of the nervous system (8, 21).

A deregulation of the FGF/FGFR system can be involved in cancer development and progression through modulation of cell proliferation, migration and angiogenesis (22).

Besides its role in physiological angiogenesis, FGF2 is implied in tumor-induced angiogenesis and metastatic process and appears to direct tumor-associated macrophages toward a pro-tumorigenic state (23–25). FGF4 promotes cancer cell proliferation, invasion and migration by causing a switch of the receptor FGFR2-IIIb, a splice variant expressed in epithelial cells, into FGFR2-IIIc, expressed in mesenchymal cells and able to induce epithelial-mesenchymal transition (26). FGF5 can promote osteosarcoma proliferation by activating the MAPK signaling pathway (27) and the FGF5/FGFR1 axis contributes to melanoma progression (28). FGF6 can stimulate proliferation of prostate cancer cells through the activation of FGFR4 (29). Among the FGF7 subfamily, FGF3 and FGF7 have been reported to be highly expressed in breast cancer (30, 31) and gastric adenocarcinoma (32), respectively. In addition, the FGF10/FGFR-IIb signaling appears to have a role in breast and pancreatic tumors (15, 33). Although the mechanism is unclear, Jarosz et al. observed a potential role of FGF22 in skin tumorigenesis (34). In a recent study, FGF22 and its receptor FGFR-IIb appear to be associated with the development of lung adenocarcinoma through the MAPK and Rap I signaling pathways (35). A deregulation of FGF18, caused by an altered expression of its negative regulator miR-590-5p, is able to stimulate proliferation and epithelial-mesenchymal transition, with enhanced invasion abilities, in gastric cancer cells (36). In HER^+ breast cancer cell lines, overexpression of FGF18 stimulates the expression of genes involved in migration and cancer metastasis through Akt/GSK3β pathway (37). By the interaction with FGFR2 and FGFR3 and the activation of the ERK/Akt pathway, FGF18 is able to induce proliferation and invasion in endometrial carcinoma (38).

The FGF/FGFR pathway has also a key role in the onset of drug-resistance (39). FGF/FGFR pathway is the first compensatory mechanism in tumors resistant to drugs targeting the vascular endothelial growth factor (VEGF) system (40–42). Indeed, VEGF-dependent vessels are suppressed during prolonged anti-VEGF therapy, while the expression of FGF2 is increased, leading to a novel angiogenesis dependent on FGF2 signaling pathway. This condition drives the tumor toward drug-resistance (42). Boichuk et al. (43) showed that FGF signaling is activated in gastrointestinal stromal tumors after the acquisition of imatinib resistance. Interestingly, the use of a potent FGF inhibitor markedly reduced cell growth in resistant cells compared to imatinib-sensitive cells. This effect increased when the two molecules were combined in resistant cells, showing also that the FGF-inhibitor can restore sensitivity to imatinib.

FGF SYSTEM IN NEUROENDOCRINE NEOPLASMS

The role of the FGF/FGFR system has been analyzed also in NENs and several lines of evidence support its function in the modulation of tumor fibrosis, proliferation, angiogenesis and drug resistance, through a dynamic cross talk between NEN cells, fibroblasts, endothelial cells and inflammatory cells (44).

Bordi et al. identified FGF2 by immunohistochemistry in endocrine cells of the gastric oxyntic mucosa and mRNA of FGF2 in enterochromaffin-like carcinoid tumors (45). Immunohistochemical studies demonstrated the staining for FGF-2 in 100% of NEN cells from the midgut and the pancreas, while FGF2 receptors were observed only in the stromal component (46). La Rosa et al. found cytoplasmic immunoreactivity for FGF1 in 26 (43%) out of 60 GEP-NENs and FGFR1-4 were found in 68-88% of tumors with tumor microenvironment components also expressing FGFRs (47). The authors observed also that normal endocrine cells of the gut rarely expressed FGFRs thus hypothesizing that in normal mucosa the FGF/FGFR system has not an autocrine role on modulating endocrine cells functions. Therefore, *de novo* expression of FGFRs by NEN cells may play a role in the autocrine/paracrine signaling responsible of tumorigenesis, stromal fibrosis and tumor-induced angiogenesis.

NEN are often characterized by the development of fibrosis, local or distant. The best-known fibrotic complications are carcinoid heart disease, which develops in about 20% of patients with carcinoid syndrome (48), and mesenteric fibrosis, which affects up to 40-50% of small bowel NENs (49, 50). Less known complications are represented by retroperitoneal fibrosis (50), scleroderma (51), infiltration of the pleura (52) or alveoli (53) and fibrosis of the bladder (54). Although the pathogenesis of fibrotic complications is unclear, serotonin, with a relevant mitogenic power on fibroblasts, mesangial cells, smooth muscle cells, endothelial cells and NEN cells, may have a role in these events (55). The FGF system appears to be also implicated in the mechanism of gastrointestinal NEN fibrosis (56). In fact, Bordi (45) showed that among the 10 patients suffering from type 3 gastric NEN and with positive immunohistochemistry for FGF2, some had diffuse stromal fibrosis. Another study (57), which analyzed a pool of 41 gastrointestinal NENs, showed a positive correlation between FGF1 and the amount of fibrous stroma in tumors. The FGF is responsible of cell proliferation and stroma formation and its action is potentiated by serotonin (58). Moreover, FGF may activate also the expression of the connective tissue growth factor genes that regulate myofibroblast differentiation, collagen synthesis and fibroblast proliferation (59).

The mRNA expression of FGF receptor was found more frequently in functioning NENs (including gastrinomas and insulinomas) than in functionally inactive NENs (53.6% vs. 22.2%) (60). Although this difference was not statistically significant (p=0.10), speculating on the association between FGFR expression and hormone production may be not totally irrational, but further evidence is required to corroborate these findings.

The FGFR4-G388R single-nucleotide polymorphism was investigated in 71 patients with pancreatic NEN (61). The authors observed that FGFR4-R388 allele was independently associated with liver metastases. To further analyze the impact of the FGFR4 SNP, the same authors transfected BON1 cells with either FGFR4-G388 or FGFR4-R388 and injected them in SCID mice. They found that xenografts expressing FGFR4-R388 displayed a more aggressive biological behavior and were resistant to everolimus treatment. This latter aspect was investigated also among 17 patients previously treated with everolimus in a clinical trial. Patients harboring FGFR4-R388 allele achieved a worse tumor response (9% vs. 25%) and a reduced median PFS (4.8 vs. 16.6 months) and OS (9.3vs 40 months) compared to patients homozygous for FGFR4-G388. Although decreased drug response was related to persistently high mTOR and STAT3 phosphorylation despite of everolimus treatment, these data were not confirmed by Cros et al., who reported no modification of the mTOR pathway in patients with pancreatic or ileal NENs harboring FGFR4-R388 allele (62). This apparent inconsistency corroborates the need for further studies validating the identification of molecular parameters useful to predict drug efficacy and resistance (63).

The FGF/FGFR system collaborates with the VEGF signaling pathway in the initiation and maintenance of tumor angiogenesis. These mechanisms have been demonstrated in allograft transplantation experiments and in mouse model of pancreatic NEN (the Rip1Tag2 transgenic mice), where interfering with the FGF function by a soluble form of the FGFR2 IIIb significantly inhibited tumor-induced angiogenesis and tumor growth (64). The FGF system acts as a second proangiogenic circuit, indeed VEGF is the main regulator of angiogenesis but, as reported by Casanovas et al., experiments in the Rip1Tag2 model of pancreatic islet carcinoma documented that initial inhibition of the angiogenesis achieved by VEGF signaling blockade was restored by the upregulation of the FGF system (65). Therefore, blocking both VEGF and FGF signaling pathways may reveal synergic antiangiogenic effects and inhibit tumor progression secondary to compensatory feedback loops driving tumor revascularization. For instance, Allen et al. investigated the effect of brivanib, a selective inhibitor targeting both VEGF and FGF receptors, in a mouse model of pancreatic NEN. Brivanib was effective not only as first-line therapy, but also as second-line treatment after failure of two agents inhibiting VEGF receptors (DC101 and sorafenib) (66).

FGFRs AS THERAPEUTIC TARGET IN NENs

In the last few years, the therapeutic approach for NENs has changed following the approval of several innovative targeted treatments such as tyrosine kinase inhibitors (TKIs). Although no specific FGFR kinase inhibitors have been evaluated in NENs, several clinical trials on multitarget TKIs, acting also on FGF, are ongoing and few published studies have demonstrated their efficacy in NENs (44). The interest in FGF pathway inhibitors relies also in the possibility to overcome resistance to VEGF inhibition that may arise after long term use of these drugs or could be intrinsic in tumor expressing FGF2 (67–69). The results of clinical trials in NENs evaluating multitarget TKI, acting also on FGF, are described below (**Table 1**).

Surufatinib is a potent TKI targeting VEGF receptors (VEGFR) 1, 2, and 3, FGFR1, and CSF-1R. In preliminary phase I and Ib/II studies surufatinib showed encouraging anti-tumor activity in advanced NENs (81, 82).

TABLE 1 | Clinical trials evaluating the effects of multitarget tyrosine kinase inhibitors, acting also on FGFR, in patients with NENs.

Ref	Therapy and dose	Molecular target	Study design (Trial name)	Tumors	Number of patients (placebo)	Median follow- up (placebo)	Primary outcome	Results	Main AE (%)
(70)	Surufatinib 300 mg/day	VEGFR 1,2,3 FGFR1 CSF-1R	Randomised, double-blind, placebo-controlled, phase 3 (SANET-EP)	Advanced extrapancreatic NETs (G1-G2)	129 (69)	13.8 months (16.6 months)	PFS	Median PFS: 9.2 months (surufatinib) vs. 3.8 months (placebo)	Hypertension (36%); proteinuria (19%)
(71)	Surufatinib 300 mg/day	VEGFR 1,2,3 FGFR1 CSF-1R	Randomised, double-blind, placebo-controlled, phase 3 (SANET-P)	Advanced pancreatic NETs (G1-G2)	113 (59)	19.3 months (11.1 months)	PFS	Median PFS: 10.9 months (surufatinib) vs. 3.7 months (placebo)	Hypertension (38%); proteinuria (10%); hypertriglyceridemia (7%)
(72)	Surufatinib 300 mg/day	VEGFR 1,2,3 FGFR1 CSF-1R	Dose escalation/expansion study	Heavily pre-treated progressive NETs	32	19 weeks	ORR	9.4%	Hypertension, fatigue, diarrhea
(73)	Surufatinib 300 mg/day	VEGFR 1,2,3 FGFR1 CSF-1R	Phase 2, open label, two stage design study	Advanced MTC	27	–	ORR	22.2%	hypertension (20.3%), proteinuria (11.9%), hypertriglyceridemia (5.1%)*
(74)	Lenvatinib 24 mg/day	VEGFR 1-3 FGFR1-4	Prospective multicohort phase 2 (TALENT)	Advanced pancreatic and gastrointestinal NETs (G1-G2)	111	19 months	ORR	42.3% pancreatic 16.3% gastrointestinal	Hypertension (22%); fatigue (11%); diarrhea (11%)
(75)	Lenvatinib 24 mg/day	VEGFR 1-3 FGFR1-4	Phase 2, multicenter, open-label, single-arm clinical trial	Unresectable or metastatic progressive MTC	59	–	ORR	36% (all PR)	Diarrhea (14%); hypertension (7%); decreased appetite (7%)
(76)	Lenvatinib 24 mg/day	VEGFR 1-3 FGFR1-4	Nonrandomized, open-label, multicenter, phase 2 study	Progressive MTC	9	9.6 months	Safety	100% of patients ≥1 AE; 1.7% of patients AE leading to discontinuation	Decreased appetite (100%); hypertension (89%); palmar-plantar erythrodysesthesia (89%)
(77)	Lenvatinib 24 mg/day	VEGFR 1-3 FGFR1-4	Prospective, post-marketing observational study	UnresectableMTC	28	12 months	Safety	100% pts ≥1 AE	Hypertension; proteinuria; palmar-plantar erythrodysesthesia
(78)	Nintedanib	VEGFR 1,2,3 FGFR2	Multicenter phase 2 study	Advanced progressing carcinoid on stable dose SSA for ≥3 months	30	16 weeks	PFS	PFS at 16 weeks 86.7% in 26 pts	Diarrhea (18%); increase in GGT (18%); lymphopenia (18%)
(79)	Anlotinib 12 mg/day	VEGFR 2-3 FGFR1-4	Single-arm phase 2 study	Advanced or metastatic MTC	58	9.8 months	PFS	PFS at 48 weeks 84.5%	Hand-foot syndrome (79.3%); hypertriglyceridemia (46.5%); elevated cholesterol levels (43.1%)
(80)	Anlotinib 12 mg/day	VEGFR 2-3 FGFR1-4	Multicenter, randomized, double-blind, placebo-controlled phase IIB trial (ALTER01031)	Advanced or metastatic MTC	62 (29)	–	PFS	Median PFS: 20.67 months (anlotinib) vs 11.07 months (placebo)	Hand-foot syndrome; hypertension; hypertriglyceridemia

AE, adverse events; FGFR, fibroblast growth factor receptor; MTC, medullary thyroid carcinoma; NET, neuroendocrine tumor; ORR, overall response rate; PFS, progression free survival; pts, patients; SSA, somatostatin analogs; VEGFR, Vascular Endothelial Growth Factor Receptor.

**data reported for the overall population (differentiated thyroid cancer and MTC).*

Two randomized phase III placebo controlled trials evaluated safety and efficacy of surufatinib in patients with well differentiated NENs of extra-pancreatic (SANET-ep) and pancreatic (SANET-p) origin (70, 71).

In SANET-ep study (70) 198 patients were randomly assigned to surufatinib 300 mg/day (n=129) or placebo (n=69). Median progression-free survival (PFS) was 9.2 months in the surufatinib group versus 3.8 months in the placebo group. The overall response rate (ORR) was 10% in the surufatinib group versus zero in the placebo group. The most common treatment-related adverse events (AE) of grade ≥ 3 were hypertension (36% surufatinib vs 13% placebo) and proteinuria (19% vs. 0%). In SANET-p study (71) 113 patients were randomly assigned to surufatinib (300 mg/day) and 59 to placebo. The median PFS was 10.9 months for surufatinib versus 3.7 months for placebo; ORR was 19% in the surufatinib group and 2% in the placebo group. The most common AE of grade ≥ 3 were hypertension (38% surufatinib *vs.* 7% placebo), proteinuria (10% *vs.* 2%) and hypertriglyceridemia (7% *vs.* none).

Another study evaluated the effect of surufatinib dose escalation/expansion in 32 patients with heavily pre-treated progressive NENs, 16 patients with pancreatic NENs and 16 with extra-pancreatic NENs. Nineteen patients remained on active treatment (13 extra-pancreatic and 6 pancreatic), 9 patients discontinued due to disease progression, 2 withdrew consent and 2 discontinued due to AE. An ORR of 9.4% was observed (72).

An open label phase II study evaluated efficacy and tolerability of surufatinib (300 mg/day) in 27 patients with progressive medullary thyroid cancer (MTC). Objective response was observed in 22.2% of patients with MTC, and the majority (88.9%) achieved disease control. The therapy was well tolerated (73).

Therefore, surufatinib demonstrated promising anti-tumor activity with an acceptable and manageable safety profile in advanced NENs.

Lenvatinib is a potent VEGFR1-3 and FGFR1-4 inhibitor. The TALENT trial, a prospective phase II study, evaluated efficacy, safety and tolerability of lenvatinib (24 mg once daily) in G1/G2 advanced pancreatic (n=55) and gastrointestinal (n=56) NENs resistant to previous targeted agents. The ORR was 29% (42.3% for pancreatic NENs and 16.3% for gastrointestinal NENs). PFS and overall survival (OS) for pancreatic NENs were 15.5 months and 29.2 months, while for gastrointestinal NENs were 15.4 months and not reached, respectively. The most frequent grade 3/4 AE were hypertension (22%), fatigue (11%) and diarrhea (11%) (74). Thus, lenvatinib showed a promising PFS and OS in a pretreated population.

A phase II, multicenter, open-label, single-arm clinical trial evaluated efficacy and tolerability of lenvatinib (24-mg daily, 28-day cycles) in 59 patients with MTC. ORR was 36%, all PR. Disease control rate (DCR) was 80%, 44% had SD. Median time to response was 3.5 months. Median PFS was 9.0 months. Grade 3/4 AE included diarrhea (14%), hypertension (7%), decreased appetite (7%), fatigue, dysphagia and increased alanine aminotransferase levels (5% each) (75).

Another phase II study evaluated lenvatinib treatment in 9 patients with MTC. The most frequently reported AE were decreased appetite (100%), hypertension (89%), palmar-plantar erythrodysesthesia (89%), diarrhea (89%), fatigue (78%) and proteinuria (67%). Median PFS was 9.2 months. Median OS was 12.1 months. ORR was 22% and DCR was 100% (76).

Recently, a prospective, post-marketing observational study evaluated, in daily clinical practice, the safety and effectiveness of lenvatinib in 28 patients with MTC. Hypertension, proteinuria and palmar-plantar erythrodysesthesia syndrome were the most frequently reported AE. The 12-months OS rate was 83%. ORR was 45% (77).

Nintedanib is a dual inhibitor of VEGFR1, -2, and -3 as well as FGFR2 and showed both antiangiogenic and antitumor activity in the RIP1-Tag2 transgenic mouse model of tumorigenesis for pancreatic NEN (44). A multicenter phase II study evaluated efficacy, safety and tolerability of nintedanib in 30 patients with unresectable/metastatic carcinoids on stable dose of SSA for ≥3 months. PFS at 16 weeks was 86.7% in 26 patients. PR was observed in 4%, SD in 83%, disease progression in 8% of patients. Quality of life was maintained or improved in at least 50% of subjects. The most common grade 3 AE were hypertension and decreased appetite (78).

A prospective randomized double-blind phase II study evaluated the efficacy and tolerability of nintedanib in progressing MTC after prior TKI treatment. The study was stopped due to slow accrual with 32/67 patients enrolled, without reaching the targeted statistical power. The most common AE were diarrhea (18%), nausea (9%), GGT increase (18%) and lymphopenia (18%) (83).

Anlotinib is a novel TKI targeting VEGFR2-3 and FGFR1-4 with high affinity. Anlotinib has previously shown promising antitumor activity on MTC in preclinical models and a phase I study (84). A phase II clinical trial showed a relevant antitumor activity of anlotinib (12 mg once daily, two weeks on/one week off) in 58 patients with advanced MTC. PFS rates at 24, 36, and 48 weeks were 92.2%, 87.8% and 84.5%, respectively. Significant decreases in serum calcitonin (≥50%) occurred in 57.5% of patients. The most common AE included hand-foot syndrome (79.3%), hypertriglyceridemia (46.5%), hypercholesterolemia (43.1%), fatigue (41.4%), proteinuria (39.7%), hypertension (39.7%), sore throat (37.9%), diarrhea (34.5%) and anorexia (34.5%) (79).

These data have been confirmed in a phase IIb study (ALTER01031), enrolling a larger cohort of patients (80). Ninety-one patients with advanced MTC were randomized: 62 to anlotinib arm and 29 to placebo arm (12 mg/die from day 1 to 14 of a 21-day cycle). Median PFS was 20.7 months in anlotinib arm vs. 11.1 months in placebo arm. The most common AE after anlotinib arm were hand-foot syndrome, hypertension, hypertriglyceridemia and diarrhea (80).

Several clinical trials on the use of multi target TKI, with an action also on FGFR, in patients with NENs are currently ongoing. **Table 2** reports the main characteristics of trials registered on clinicaltrials.gov.

TABLE 2 | Ongoing clinical trials evaluating the effects of multitarget tyrosine kinase inhibitors, acting also on FGFR, in patients with NENs.

Identifier	Therapy	Molecular target	Study design	Tumors	Estimated sample size	Primary outcome	Start date	Estimated Completion Date
NCT02399215	Nindetanib	FGFR VEGFR PDGFR	Multicenter open label phase II study	Well or moderately differentiated (G1, G2) NEN not pancreatic	30	PFS	May 2015	October 2020
NCT04207463	Anlotinib + AK105 *(anti PD1)*	FGFR VEGFR PDGFR c-kit	Multicenter multi-cohort open label phase II study	G1 or G2 GEP NET (cohort 5)	150 (all cohorts)	ORR	June 2020	December 2020
NCT02259725	Regorafenib	FGFR VEGFR1-3 TIE2 KIT RET RAF-1 BRAF BRAFV600E PDGFR	Multicenter multi-cohort open-label phase II study	Carcinoid (cohort A) or pancreatic islet cell tumors (cohort B)	48	PFS	August 2016	August 2021
NCT03950609	Lenvatinib + Everolimus *(mTOR inhibitor)*	FGFR1-4 VEGFR1-3	Single center open-label phase II study	Unresectable well differentiated carcinoid tumors	32	ORR	July 2019	May 2021
NCT03475953	Regorafenib + Avelumab *(anti PD-L1)*	FGFR VEGFR1-3 TIE2 KIT RET RAF-1 BRAF BRAFV600E PDGFR	Multicenter, open label phase I/II study	G2 or G3 GEP NEN (cohort G)	362	ORR (Phase 2)	May 2018	November 2020
NCT02657551	Regorafenib	FGFR VEGFR1-3 TIE2 KIT RET RAF-1 BRAF BRAFV600E PDGFR	Open-label phase II study	Metastatic medullary thyroid cancer	33	PFS	January 2016	October 2022
NCT03008369	Lenvatinib	FGFR1-4VEGFR1-3	Open-label phase II study	Metastatic PPGLs	25	TRR	May 2017	December 2020

FGFR, fibroblast growth factor receptor; GEP, gastro-entero-pancreatic; NA, not available; NEN, neuroendocrine neoplasm; NET, neuroendocrine tumor; ORR, objective response rate; PD1, Programmed cell death protein 1; PDGFR, Platelet-derived growth factor receptor; PD-L1, Programmed cell death ligand 1; PFS, progression free survival; PPGL, Pheochromocytoma and Paraganglioma; pts, patients; TRR, tumor response rate (complete response and partial response); VEGFR, Vascular Endothelial Growth Factor Receptor.

CONCLUSIONS AND FUTURE PERSPECTIVES

In the last years there is mounting evidence supporting the role of FGF/FGFR system in the development and progression of NENs and probably in the occurrence of fibrotic complications (mesenteric and/or retroperitoneal fibrosis). In addition, the FGF/FGFR pathway could also have a key role in the onset of drug-resistance. Indeed, FGF/FGFR pathway is a main compensatory mechanism in anti-VEGF-therapy-resistant tumors.

Currently no specific FGFR kinase inhibitors have been evaluated in patients affected by advanced NENs. Although recent clinical trials have reported a significant antitumor activity and manageable safety profile of several multitarget TKIs, which are able to block many molecular pathways including FGFR, it is not possible to isolate the efficacy of FGFR inhibition alone. Future studies should better confirm these issues and clarify the role of FGF/FGFR pathway in promoting drug-resistance in NENs. The development of new TKIs, highly selective for FGFR and with less toxicity, may open an innovative therapeutic strategy to be integrated into a personalized approach for this heterogeneous class of tumors. In addition, recent preclinical studies showed a potent inhibition in tumor growth both in hepatocellular carcinoma (85) and in ovarian cancer (86), through the simultaneous blockade of mTOR and FGFR pathways. Considering the pivotal role of deregulated mTOR signaling activation in the proliferation of NENs, particularly in pancreatic tumors, combining mTOR inhibitors and TKIs targeting FGFRs could represent a future therapeutic approach in NENs.

AUTHOR CONTRIBUTIONS

GV, AlC, PM, RM, GP, and DS conceptualized and wrote the manuscript. AF and AnC contributed to draft the manuscript. All authors contributed to the article and approved the submitted version.

FUNDING

This work was supported by the Italian Ministry of Education, University and Research (MIUR): PRIN 2017Z3N3YC.

ACKNOWLEDGMENTS

This review is part of the 'Neuroendocrine Tumors Innovation Knowledge and Education' project led by Prof. Annamaria Colao and Prof. Antongiulio Faggiano, which aims at increasing the knowledge on NET. We would like to acknowledge all the Collaborators of the "NIKE" project: Manuela Albertelli - Genova; Barbara Altieri – Wurzburg; Luigi Barrea – Napoli; Filomena Bottiglieri – Napoli; Severo Campione – Napoli; Federica Campolo – Roma, Roberta Centello – Roma; Alessia Cozzolino – Roma; Federica De Cicco – Napoli; Sergio Di Molfetta - Bari; Valentina Di Vito – Roma; Alessandra Dicitore – Milano; Andrea Dotto – Genova; Giuseppe Fanciulli – Sassari; Tiziana Feola - Roma; Diego Ferone - Genova; Francesco Ferraù - Messina; Marco Gallo – Alessandria; Elisa Giannetta - Roma; Federica Grillo - Genova; Erika Maria Grossrubatscher – Milano; Elia Guadagno - Napoli; Valentina Guarnotta - Palermo; Andrea M. Isidori - Roma; Andrea Lania - Milano; Andrea Lenzi - Roma; Fabio Lo Calzo – Avellino; Pasqualino Malandrino - Catania; Erika Messina – Messina; Roberto Minotta – Napoli; Roberta Modica - Napoli; Giovanna Muscogiuri – Napoli; Riccardo Pofi - Roma; Giulia Puliani - Roma; Alberto Ragni – Torino; Paola Razzore – Torino; Laura Rizza - Roma; Manila Rubino - Milano; Rosaria Maria Ruggeri – Messina; Davide Saronni – Milano; Emilia Sbardella – Roma; Concetta Sciammarella – Verona; Francesca Sciarra – Roma; Franz Sesti – Roma; Maria Grazia Tarsitano – Roma; Mary Anna Venneri - Roma; Giovanni Vitale – Milano; Isabella Zanata - Ferrara.

REFERENCES

1. La Rosa S, Uccella S. Classification of neuroendocrine neoplasms: lights and shadows. *Rev Endocr Metab Disord* (2020). doi: 10.1007/s11154-020-09612-2
2. Barriuso J, Lamarca A. Clinical and Translational Research Challenges in Neuroendocrine Tumours. *Curr Med Chem* (2020) 27:4823–39. doi: 10.2174/0929867327666200207120725
3. Alexandraki KI, Tsoli M, Kyriakopoulos G, Angelousi A, Nikolopoulos G, Kolomodi D, et al. Current concepts in the diagnosis and management of neuroendocrine neoplasms of unknown primary origin. *Minerva Endocrinol* (2019) 44:378–86. doi: 10.23736/S0391-1977.19.03012-8
4. Fuentes-Fayos AC, García-Martínez A, Herrera-Martínez AD, Jiménez-Vacas JM, Vázquez-Borrego MC, Castaño JP, et al. Molecular determinants of the response to medical treatment of growth hormone secreting pituitary neuroendocrine tumors. *Minerva Endocrinol* (2019) 44:109–28. doi: 10.23736/S0391-1977.19.02970-5
5. Tamagno G, Bennett A, Ivanovski I. Lights and darks of neuroendocrine tumors of the appendix. *Minerva Endocrinol* (2020) 45:381–92. doi: 10.23736/S0391-1977.20.03206-X
6. Kiesewetter B, Raderer M. How I treat neuroendocrine tumours. *ESMO Open* (2020) 5:e000811. doi: 10.1136/esmoopen-2020-000811
7. Walenkamp A, Crespo G, Fierro Maya F, Fossmark R, Igaz P, Rinke A, et al. Hallmarks of gastrointestinal neuroendocrine tumours: implications for treatment. *Endocr Relat Cancer* (2014) 21:R445–60. doi: 10.1530/ERC-14-0106
8. Ornitz DM, Itoh N. The Fibroblast Growth Factor signaling pathway. *Wiley Interdiscip Rev Dev Biol* (2015) 4(3):215–66. doi: 10.1002/wdev.176
9. Li J, Wang Q, Cai H, He Z, Wang H, Chen J, et al. FGF1 improves functional recovery through inducing PRDX1 to regulate autophagy and anti-ROS after spinal cord injury. *J Cell Mol Med* (2018) 22(5):2727–38. doi: 10.1111/jcmm.13566
10. Presta M, Andrés G, Leali D, Dell'Era P, Ronca R. Inflammatory cells and chemokines sustain FGF2-induced angiogenesis. *Eur Cytokine Netw* (2009) 20 (2):39–50. doi: 10.1684/ecn.2009.0155
11. Carmeliet P, Jain RK. Molecular mechanisms and clinical applications of angiogenesis. *Nature* (2011) 473(7347):298–307. doi: 10.1038/nature10144
12. Jacobi A, Loy K, Schmalz AM, Hellsten M, Umemori H, Kerschensteiner M, et al. FGF22 signaling regulates synapse formation during post-injury remodeling of the spinal cord. *EMBO J* (2015) 34(9):1231–43. doi: 10.15252/embj.201490578
13. Anderson MJ, Schimmang T, Lewandoski M. An FGF3-BMP Signaling Axis Regulates Caudal Neural Tube Closure, Neural Crest Specification and Anterior-Posterior Axis Extension. *PloS Genet* (2016) 12(5):e1006018. doi: 10.1371/journal.pgen.1006018
14. Xie Y, Su N, Yang J, Tan Q, Huang S, Jin M, et al. FGF/FGFR signaling in health and disease. *Signal Transduct Target Ther* (2020) 5(1):181. doi: 10.1038/s41392-020-00222-7
15. Rivetti S, Chen C, Chen C, Bellusci S. Fgf10/Fgfr2b Signaling in Mammary Gland Development, Homeostasis, and Cancer. *Front Cell Dev Biol* (2020) 8:415. doi: 10.3389/fcell.2020.00415

16. Chan WK, Price DJ, Pratt T. FGF8 morphogen gradients are differentially regulated by heparan sulphotransferases Hs2st and Hs6st1 in the developing brain. *Biol Open* (2017) 6(12):1933–42. doi: 10.1242/bio.028605
17. Hao Y, Tang S, Yuan Y, Liu R, Chen Q. Roles of FGF8 subfamily in embryogenesis and oral–maxillofacial diseases (Review). *Int J Oncol* (2019) 54(3):797–806. doi: 10.3892/ijo.2019.4677
18. Boylan M, Anderson MJ, Ornitz DM, Lewandoski M. The Fgf8 subfamily (Fgf8, Fgf17 and Fgf18) is required for closure of the embryonic ventral body wall. *Development* (2020) 147(21):dev189506. doi: 10.1242/dev.189506
19. Charoenlarp P, Rajendran AK, Iseki S. Role of fibroblast growth factors in bone regeneration. *Inflammation Regen* (2017) 37:10. doi: 10.1186/s41232-017-0043-8
20. Wang S, Li Y, Jiang C, Tian H. Fibroblast growth factor 9 subfamily and the heart. *Appl Microbiol Biotechnol* (2018) 102(2):605–13. doi: 10.1007/s00253-017-8652-3
21. Zhang X, Bao L, Yang L, Wu Q, Li S. Roles of intracellular fibroblast growth factors in neural development and functions. *Sci China Life Sci* (2012) 55 (12):1038–44. doi: 10.1007/s11427-012-4412-x
22. Tanner Y, Grose RP. Dysregulated FGF signalling in neoplastic disorders. *Semin Cell Dev Biol* (2016) 53:126–35. doi: 10.1016/j.semcdb.2015.10.012
23. Cao Y, Cao R. Hedlund EM. R Regulation of tumor angiogenesis and metastasis by FGF and PDGF signaling pathways. *J Mol Med (Berl)* (2008) 86(7):785–9. doi: 10.1007/s00109-008-0337-z
24. Hosaka K, Yang Y, Seki T, Du Q, Jing X, He X, et al. Therapeutic paradigm of dual targeting VEGF and PDGF for effectively treating FGF-2 off-target tumors. *Nat Commun* (2020) 11(1):3704. doi: 10.1038/s41467-020-17525-6
25. Im JH, Buzzelli JN, Jones K, Franchini F, Gordon-Weeks A, Markelc B, et al. FGF2 alters macrophage polarization, tumour immunity and growth and can be targeted during radiotherapy. *Nat Commun* (2020) 11(1):4064. doi: 10.1038/s41467-020-17914-x
26. Qi L, Song W, Li L, Cao L, Yu Y, Song C, et al. FGF4 induces epithelial-mesenchymal transition by inducing store-operated calcium entry in lung adenocarcinoma. *Oncotarget* (2016) 7(45):74015–30. doi: 10.18632/oncotarget.12187
27. Han D, Wang M, Yu Z, Yin L, Liu C, Wang J, et al. FGF5 promotes osteosarcoma cells proliferation via activating MAPK signaling pathway. *Cancer Manag Res* (2019) 11:6457–66. doi: 10.2147/CMAR.S200234
28. Ghassemi S, Vejdovszky K, Sahin E, Ratzinger L, Schelch K, Mohr T, et al. FGF5 is expressed in melanoma and enhances malignancy in vitro and in vivo. *Oncotarget* (2017) 8(50):87750–62. doi: 10.18632/oncotarget.21184
29. Ropiquet F, Giri D, Kwabi-Addo B, Mansukhani A, Ittmann M. Increased expression of fibroblast growth factor 6 in human prostatic intraepithelial neoplasia and prostate cancer. *Cancer Res* (2000) 60(15):4245–50.
30. Roy D, Calaf GM. Allelic loss at chromosome 11q13 alters FGF3 gene expression in a human breast cancer progression model. *Oncol Rep* (2014) 32(6):2445–52. doi: 10.3892/or.2014.3502
31. Parish A, Schwaederle M, Daniels G, Piccioni D, Fanta P. Schwab Ret al. Fibroblast growth factor family aberrations in cancers: clinical and molecular characteristics. *Cell Cycle* (2015) 14(13):2121–8. doi: 10.1080/15384101.2015.1041691
32. Huang T, Wang L, Liu D, Li P, Xiong H, Zhuang L, et al. FGF7/FGFR2 signal promotes invasion and migration in human gastric cancer through upregulation of thrombospondin-1. *Int J Oncol* (2017) 50(5):1501–12. doi: 10.3892/ijo.2017.3927
33. Ndlovu R, Deng LC, Wu J, Li XK, Zhang JS. Fibroblast Growth Factor 10 in Pancreas Development and Pancreatic Cancer. *Front Genet* (2018) 9:482. doi: 10.3389/fgene.2018.00482
34. Jarosz M, Robbez-Masson L, Chioni AM, Cross B, Rosewell I, Grose R. Fibroblast growth factor 22 is not essential for skin development and repair but plays a role in tumorigenesis. *PloS One* (2012) 7(6):e39436. doi: 10.1371/journal.pone.0039436
35. Liu HY, Zhao H, Li WX. Integrated Analysis of Transcriptome and Prognosis Data Identifies FGF22 as a Prognostic Marker of Lung Adenocarcinoma. *Technol Cancer Res Treat* (2019) 18:1533033819827317. doi: 10.1177/1533033819827317
36. Zhang J, Zhou Y, Huang T, Wu F, Pan Y, Dong Y, et al. FGF18, a prominent player in FGF signaling, promotes gastric tumorigenesis through autocrine manner and is negatively regulated by miR-590-5p. *Oncogene* (2019) 38 (1):33–46. doi: 10.1038/s41388-018-0430-x
37. Song N, Zhong J, Hu Q, Gu T, Yang B, Zhang J, et al. FGF18 Enhances Migration and the Epithelial-Mesenchymal Transition in Breast Cancer by Regulating Akt/GSK3β/B-Catenin Signaling. *Cell Physiol Biochem* (2018) 49 (3):1019–32. doi: 10.1159/000493286
38. Wu J, Tao X, Zhang H, Yi XH, Yu YH. Estrogen-Induced Stromal FGF18 Promotes Proliferation and Invasion of Endometrial Carcinoma Cells Through ERK and Akt Signaling. *Cancer Manag Res* (2020) 12:6767–77. doi: 10.2147/CMAR.S254242
39. Zhou Y, Wu C, Lu G, Hu Z, Chen Q, Du X. FGF/FGFR signaling pathway involved resistance in various cancer types. *J Cancer* (2020) 11(8):2000–7. doi: 10.7150/jca.40531
40. Ellis LM, Hicklin DJ. Pathways mediating resistance to vascular endothelial growth factor-targeted therapy. *Clin Cancer Res* (2008) 14(20):6371–5. doi: 10.1158/1078-0432.CCR-07-5287
41. Zhao Y, Adjei AA. Targeting Angiogenesis in Cancer Therapy: Moving Beyond Vascular Endothelial Growth Factor. *Oncologist* (2015) 20(6):660–73. doi: 10.1634/theoncologist.2014-0465
42. Ichikawa K, Watanabe Miyano S, Minoshima Y, Matsui J, Funahashi Y. Activated FGF2 signaling pathway in tumor vasculature is essential for acquired resistance to anti-VEGF therapy. *Sci Rep* (2020) 10(1):2939. doi: 10.1038/s41598-020-59853-z
43. Boichuk S, Galembikova A, Dunaev P, Micheeva E, Valeeva E, Novikova M, et al. Targeting of FGF-Signaling Re-Sensitizes Gastrointestinal Stromal Tumors (GIST) to Imatinib In Vitro and In Vivo. *Molecules* (2018) 23 (10):2643. doi: 10.3390/molecules23102643
44. Cives M, Pelle' E, Quaresmini D, Rizzo FM, Tucci M, Silvestris F. The Tumor Microenvironment in Neuroendocrine Tumors: Biology and Therapeutic Implications. *Neuroedocrinology* (2019) 109:83–99. doi: 10.1159/000497355
45. Bordi C, Falchetti A, Buffa R, Azzoni C, D'Adda T, Caruana P, et al. Production of basic fibroblast growth factor by gastric carcinoid tumors and their putative cells of origin. *Hum Pathol* (1994) 25:175–80. doi: 10.1016/0046-8177(94)90275-5
46. Chaudhry A, Funa K, Oberg K. Expression of growth factor peptides and their receptors in neuroendocrine tumors of the digestive system. *Acta Oncol* (1993) 32:107–14. doi: 10.3109/02841869309083898
47. La Rosa S, Uccella S, Erba S, Capella C, Sessa F. Immunohistochemical Detection of Fibroblast Growth Factor Receptors in Normal Endocrine Cells and Related Tumors of the Digestive System. *Appl Immunohistochem Mol Morphol* (2001) 9:319–28. doi: 10.1097/00129039-200112000-00006
48. Bhattacharyya S, Toumpanakis C, Chilkunda D, Caplin ME, Davar J. Risk factors for the development and progression of carcinoid heart disease. *Am J Cardiol* (2011) 107(8):1221–6. doi: 10.1016/j.amjcard.2010.12.025
49. Koumarianou A, Alexandraki KI, Wallin G, Kaltsas G. Pathogenesis and Clinical Management of Mesenteric Fibrosis in Small Intestinal Neuroendocine Neoplasms: A Systematic Review. *J Clin Med* (2020) 9 (6):1777. doi: 10.3390/jcm9061777
50. Daskalakis K, Karakatsanis A, Stålberg P, Norlén O, Hellman P. Clinical signs of fibrosis in small intestinal neuroendocrine tumours. *Br J Surg* (2017) 104:69–75. doi: 10.1002/bjs.10333
51. Ratnavel RC, Burrows NP, Pye RJ. Scleroderma and the carcinoid syndrome. *Clin Exp Dermatol* (1994) 19:83–5. doi: 10.1111/j.1365-2230.1994.tb01126.x
52. Moss SF, Lehner PJ, Gilbey SG, Kennedy A, Hughes JM, Bloom SR, et al. Pleural involvement in the carcinoid syndrome. *Q J Med* (1993) 86:49–53. doi: 10.1093/oxfordjournals.qjmed.a068737
53. Seo JW, Im JG, Kim YW, Kim JH, Sheppard MN. Synchronous double primary lung cancers of squamous and neuroendocrine type associated with cryptogenic fibrosing alveolitis. *Thorax* (1991) 46:857–8. doi: 10.1136/thx.46.11.857
54. Hallen A. FIBROSIS IN THE CARCINOID SYNDROME. *Lancet* (1964) 1:746–7. doi: 10.1016/s0140-6736(64)92853-3
55. Laskaratos F-M, Rombouts K, Caplin M, Toumpanakis C, Thirlwell C, Mandair D. Neuroendocrine tumors and fibrosis: An unsolved mystery? *Cancer* (2017) 123:4770–90. doi: 10.1002/cncr.31079
56. Zuetenhorst JM, Bonfrer JMGM, Korse CM, Bakker R, van Tinteren H, Taal BG. Carcinoid heart disease: the role of urinary 5-hydroxyindoleacetic acid excretion and plasma levels of atrial natriuretic peptide, transforming growth factor-beta and fibroblast growth factor. *Cancer* (2003) 97:1609–15. doi: 10.1002/cncr.11226
57. La Rosa S, Chiaravalli AM, Capella C, Uccella S, Sessa F. Immunohistochemical localization of acidic fibroblast growth factor in

normal human enterochromaffin cells and related gastrointestinal tumours. *Virchows Archiv* (1997) 430:117–24. doi: 10.1007/BF01008032
58. Svejda B, Kidd M, Giovinazzo F, Eltawil K, Gustafsson BI, Pfragner R, et al. The 5-HT(2B) receptor plays a key regulatory role in both neuroendocrine tumor cell proliferation and the modulation of the fibroblast component of the neoplastic microenvironment. *Cancer* (2010) 116:2902–12. doi: 10.1002/cncr.25049
59. Koumarianou A, Alexandraki KI, Wallin G, Kaltsas G, Daskalakis K. Pathogenesis and Clinical Management of Mesenteric Fibrosis in Small Intestinal Neuroendocine Neoplasms: A Systematic Review. *J Clin Med* (2020) 9. doi: 10.3390/jcm9061777
60. Wulbrand U, Wied M, Zöfel P, Göke B, Arnold R, Fehmann H-C. Growth factor receptor expression in human gastroenteropancreatic neuroendocrine tumours. *Eur J Clin Invest* (1998) 28:1038–49. doi: 10.1046/j.1365-2362.1998.00397.x
61. Serra S, Zheng L, Hassan M, Phan AT, Woodhouse LJ, Yao JC, et al. The FGFR4-G388R single-nucleotide polymorphism alters pancreatic neuroendocrine tumor progression and response to mTOR inhibition therapy. *Cancer Res* (2012) 72:5683–91. doi: 10.1158/0008-5472.CAN-12-2102
62. Cros J, Moati E, Raffenne J, Hentic O, Svrcek M, de Mestier L, et al. Gly388Arg FGFR4 Polymorphism Is Not Predictive of Everolimus Efficacy in Well-Differentiated Digestive Neuroendocrine Tumors. *Neuroendocrinology* (2016) 103:495–9. doi: 10.1159/000440724
63. Zatelli MC, Fanciulli G, Malandrino P, Ramundo V, Faggiano A, Colao A, et al. Predictive factors of response to mTOR inhibitors in neuroendocrine tumours. *Endocr Relat Cancer* (2016) 23:R173–83. doi: 10.1530/ERC-15-0413
64. Compagni A, Wilgenbus P, Impagnatiello MA, Cotten M, Christofori G. Fibroblast growth factors are required for efficient tumor angiogenesis. *Cancer Res* (2000) 60:7163–9.
65. Casanovas O, Hicklin DJ, Bergers G, Hanahan D. Drug resistance by evasion of antiangiogenic targeting of VEGF signaling in late-stage pancreatic islet tumors. *Cancer Cell* (2005) 8:299–309. doi: 10.1016/j.ccr.2005.09.005
66. Allen MD, Neumann S, Gershengorn MC. Occupancy of both sites on the thyrotropin (TSH) receptor dimer is necessary for phosphoinositide signaling. *FASEB J* (2011) 25:3687–94. doi: 10.1096/fj.11-188961
67. Turner N, Grose R. Fibroblast growth factor signalling: from development to cancer. *Nat Rev Cancer* (2010) 10(2):116–29. doi: 10.1038/nrc2780
68. Arai H, Battaglin F, Wang J, Lo JH, Soni S, Zhang W, et al. Molecular insight of regorafenib treatment for colorectal cancer. *Cancer Treat Rev* (2019) 81:101912. doi: 10.1016/j.ctrv.2019.101912
69. Kopetz S, Hoff PM, Morris JS, Wolff RA, Eng C, Glover KY, et al. Phase II trial of infusional fluorouracil, irinotecan, and bevacizumab for metastatic colorectal cancer: efficacy and circulating angiogenic biomarkers associated with therapeutic resistance. *J Clin Oncol* (2010) 28(3):453–9. doi: 10.1200/JCO.2009.24.8252
70. Xu J, Shen L, Zhou Z, Li J, Bai C, Chi Y, et al. Surufatinib in advanced extrapancreatic neuroendocrine tumours (SANET-ep): a randomised, double-blind, placebo-controlled, phase 3 study. *Lancet Oncol* (2020) 21(11):1500–12. doi: 10.1016/S1470-2045(20)30496-4
71. Xu J, Shen L, Bai C, Wang W, Li J, Yu X, et al. Surufatinib in advanced pancreatic neuroendocrine tumours (SANET-p): a randomised, double-blind, placebo-controlled, phase 3 study. *Lancet Oncol* (2020) 21(11):1489–99. doi: 10.1016/S1470-2045(20)30493-9
72. Dasari A, Li D, Sung M, Tucci C, Kauh J, Kania M, et al. Efficacy and safety of surufatinib in United States (US) patients (pts) with neuroendocrine tumors (NETs). *J Clin Oncol* (2020) 38(15):4610. doi: 10.1200/JCO.2020.38.15_suppl.4610
73. Chen J, Ji Q, Bai C, Lin Y, Zheng X, Zhang Y, et al. Surufatinib in Chinese Patients with Locally Advanced or Metastatic Differentiated Thyroid Cancer and Medullary Thyroid Cancer: A Multicenter, Open-Label, Phase II Trial. *Thyroid* (2020) 30(9):1245–53. doi: 10.1089/thy.2019.0453
74. Capdevila J, Fazio N, Lopez Lopez C, Teule A, Valle J, Tafuto S, et al. Final results of the TALENT trial (GETNE1509): a prospective multicohort phase II study of lenvatinib in patients (pts) with G1/G2 advanced pancreatic (panNETs) and gastrointestinal (giNETs) neuroendocrine tumors (NETs). *J Clin Oncol* (2019) 37(15):4106. doi: 10.1200/JCO.2019.37.15_suppl.4106
75. Schlumberger M, Jarzab B, Cabanillas ME, Robinson B, Pacini F, Ball DW, et al. A Phase II Trial of the Multitargeted Tyrosine Kinase Inhibitor Lenvatinib (E7080) in Advanced Medullary Thyroid Cancer. *Clin Cancer Res* (2016) 22(1):44–53. doi: 10.1158/1078-0432.CCR-15-1127
76. Takahashi S, Kiyota N, Yamazaki T, Chayahara N, Nakano K, Inagaki L, et al. A Phase II study of the safety and efficacy of lenvatinib in patients with advanced thyroid cancer. *Future Oncol* (2019) 15(7):717–26. doi: 10.2217/fon-2018-0557
77. Takahashi S, Tahara M, Ito K, Tori M, Kiyota N, Yoshida K, et al. Safety and Effectiveness of Lenvatinib in 594 Patients with Unresectable Thyroid Cancer in an All-Case Post-Marketing Observational Study in Japan. *Adv Ther* (2020) 37(9):3850–62. doi: 10.1007/s12325-020-01433-8
78. Iyer R, Konda B, Hall Owen D, Attwood K, Sarker S, Suffren S, et al. Multicenter phase 2 study of nintedanib in patients (pts) with advanced progressing carcinoid tumors. *J Clin Oncol* (2018) 36(15):4105. doi: 10.1200/JCO.2018.36.15_suppl.4105
79. Sun Y, Du F, Gao M, Ji Q, Li Z, Zhang Y, et al. Anlotinib for the Treatment of Patients with Locally Advanced or Metastatic Medullary Thyroid Cancer. *Thyroid* (2018) 28(11):1455–61. doi: 10.1089/thy.2018.0022
80. Li D, Tang P, Chen X, Ge M, Zhang Y, Guo Z, et al. Anlotinib treatment in locally advanced or metastatic medullary thyroid carcinoma: A multicenter, randomized, double-blind, placebo-controlled phase IIB trial. *J Clin Oncol* (2019) 37(15):6019. doi: 10.1200/JCO.2019.37.15_suppl.6019
81. Xu JM, Wang Y, Chen YL, Jia R, Li J, Gong JF, et al. Sulfatinib, a novel kinase inhibitor, in patients with advanced solid tumors: results from a phase I study. *Oncotarget* (2017) 8(26):42076–86. doi: 10.18632/oncotarget.14942
82. Xu J, Li J, Bai C, Xu N, Zhou Z, Li Z, et al. Surufatinib in Advanced Well-Differentiated Neuroendocrine Tumors: A Multicenter, Single-Arm, Open-Label, Phase Ib/II Trial. *Clin Cancer Res* (2019) 25(12):3486–94. doi: 10.1158/1078-0432.CCR-18-2994
83. Newbold K, Schoeffski P, Hasan B, Locati L, Godbert Y, De la Fouchardiere C, et al. Nintedanib (BIBF1120) after first line therapy in progressive medullary thyroid cancer: A multicenter EORTC prospective randomized double-blind phase II study (NCT01788982). *Ann Oncol* (2020) 31(4):S1087–S8. doi: 10.1016/j.annonc.2020.08.1407
84. Sun Y, Niu W, Du F, Du C, Li S, Wang J, et al. Safety, pharmacokinetics, and antitumor properties of anlotinib, an oral multi-target tyrosine kinase inhibitor, in patients with advanced refractory solid tumors. *J Hematol Oncol* (2016) 9(1):105. doi: 10.1186/s13045-016-0332-8
85. Scheller T, Hellerbrand C, Moser C, Schmidt K, Kroemer A, Brunner SM, et al. mTOR inhibition improves fibroblast growth factor receptor targeting in hepatocellular carcinoma. *Br J Cancer* (2015) 112(5):841–50. doi: 10.1038/bjc.2014.638
86. Cai W, Song B, Ai H. Combined inhibition of FGFR and mTOR pathways is effective in suppressing ovarian cancer. *Am J Transl Res* (2019) 11(3):1616–25.

Conflict of Interest: The authors declare that the research was conducted in the absence of any commercial or financial relationships that could be construed as a potential conflict of interest.